Tsunami Evacuation Model for Sumner, Christchurch, New Zealand

A thesis

submitted in partial fulfilment of the requirements

for the degree of

Master of Science in Hazard and Disaster Management

at the

University of Canterbury

by

Lina Le

Department of Geological Sciences

University of Canterbury

New Zealand

2016

Frontispiece

View across Sumner, Christchurch, New Zealand, May 2015.

Abstract

Sumner, a coastal suburb located to the south-east of Christchurch, New Zealand, is highly exposed to a number of tsunami hazards. In tsunami mitigation plans, evacuation plays a crucial role in saving human lives, especially for communities located in low-lying coastal areas.

The aim of this thesis is to enhance the methodological basis for development of tsunami evacuation plans in Sumner. To achieve this, a numerical simulation output of far-field tsunami impacts in Sumner was used to establish the maximum likely inundation extent and flow depth. This, together with population census data and daily activity patterns specified for the study area, established the spatio-temporal basis for characterising population exposure to the tsunamic hazard. A geospatial evacuation analysis method (Least Cost Path Distance), augmented with variable population exposure and distributed travel speeds, was used to characterise spatial variation in evacuation times and the corresponding numbers of evacuees and vehicles. Three ‘extreme’ end-member scenarios were utilised to address possible evacuation methods; all pedestrians evacuated to 20 metres elevation, all pedestrians to bus stops for evacuation using public transport, and all people evacuated using private vehicles.

This thesis has made a methodological contribution to tsunami evacuation simulation by characterising variable spatio-temporal population exposure, and incorporating terrain properties into population and vehicle movements. The methods are equally applicable to other locations, to other hazards, and for both pre- and post-disaster evacuation analyses.

Acknowledgements

I would like to thank many people who have been always supporting, caring, inspiring, and making my last two years in New Zealand so wonderful and rewarding.

I wish to firstly express my gratitude to my supervision team: Dr Matthew Hughes, Dr Thomas Wilson, Professor Tim Davies, and Dr Emily Lane (National Institute of Water and Atmospheric Science), for all your support, guidance and motivation throughout this master project. I would like thank Dr Matthew Hughes for always being inspiring, encouraging and making yourself available for revisions, and to solve my many research issues. I wish to express appreciation for Dr Thomas Wilson for providing me countless guidance and opportunities for me to learn and expand my horizons. Professor Tim Davies has been always providing greatly informative and constructive discussion. Dr Emily Lane has been providing excellent tsunami hazard models and especially valuable revisions on this research methodology, for which I am very appreciative.

I also wish to thank Dr Marion Gadsby (Environment Canterbury) and James Thompson (Canterbury Civil Defence and Emergency Management Group) for providing great research direction for this thesis.

I am indebted to Dr Grant Wilson and Hamish McNair, who greatly contributed to this research. Thanks Grant for all late nights revising my thesis (in general, helping with pretty much everything in my life), and Hamish McNair with his heavily involvement in developing methodology and models of this research.

Thank you to the administrative staff within the Department of Geology in dealing with administrative issues!
I would like to express my sincere gratitude to financial support from the Mason Trust and especially from NZAID who gives me this invaluable chance to come here and study.

I also want to thank my friends at home in Vietnam, and in New Zealand, especially my flatmates in Suva flat who never stop supporting and encouraging me. James Williams and Finn Scheele, thank you both for your collaboration and discussions, and especially for making my master student life much more interesting!

Last but not least, special thanks to my Mum, Dad, Lena, and Kem Kem for all their unconditional love and support over the many years. Thanks Andrew for always here with me through thick and thin, and together with his family making New Zealand is another sweet home for me.

Contents

List of figures

List of tables

Chapter 1

Introduction and tsunami hazard background

Contents

1.1. Context of study

Long-favoured locations for human settlements, coastal regions make up only 4% of the world's land area but have with approximately 10% of the current world population, most of this is contained within densely populated urban centres, whose populations are growing (McGranahan, et al. 2007; Power, 2013; Sinaga, 2011). This means that more people and infrastructure in coastal regions will be exposed to natural hazards such as tsunami (Power, 2013; Sinaga et al., 2011). Even though tsunami are typically a low-probability event they pose a major threat to a number of coastal areas around the world, with potentially catastrophic impacts leading to massive loss of life, and causing significant destruction of coastal infrastructure and major economic losses (Charvet et al., 2014; Horspool & Fraser, 2015; Papathoma & Dominey-Howes, 2003; Power, 2013). The human toll in large tsunami events can be especially devastating to the fabric of communities and wider societies (e.g. December 2004 Boxing Day tsunami, July 2006 Java tsunami, 2011 Great East Japan Earthquake and Tsunami). Although severe impacts to the built environment (structures and infrastructure lifelines) can seldom be avoided in large tsunami events, with sufficient information and warning times coastal populations may be evacuated, thereby minimising loss of life and injuries (Fraser et al, 2012; Ishida & Ando, 2014).

In a tsunami mitigation plan, evacuation plays a crucial part in saving human lives, especially for communities who are living in low-lying coastal areas. The destruction due to tsunami impact varies depending on the source, the distance from the earthquake epicentre, and the intensity of the trigger factors which cause the tsunami. Mostly, coastal areas which are densely populated may suffer severe damages because of high concentration of population, buildings, infrastructure and socio-economic facilities. In these areas, a tsunami can cause a large number of fatalities, significant damages, and cause considerable economic and business losses. The primary strategy for saving lives immediately before tsunami waves arrive is to evacuate people from the hazard zone (Bernard, 2005; Dewi, 2012).

Most of the New Zealand east coast is exposed to tsunami (MCDEM, 2010). Sumner, a coastal suburb located to the South-East of Christchurch which lies on the western edge of the Pacific Ocean, is highly exposed to a number of tsunami hazards (local, regional and far-field tsunami sources). Far-field tsunami hazards sourced from the Peruvian-Chilean subduction zone off the South American coast are the most likely threat for Sumner (Environment Canterbury Regional Council, 2014; Horspool & Fraser, 2015). According to Lane et al. (2014), Sumner would be one of the six areas in Canterbury coast to experience the highest levels of inundation (>2.5 m depth). Sumner's geography poses significant constraints for evacuation planning; it is an isolated location with unfavourable exits which are either along the coast, or uphill roads with narrow widths (4-8 m), and located on very steep slopes.

Sumner is a relatively high socio-economic area (Statistics New Zealand, 2013) and offers lifestyle, entertainment and leisure opportunities close to beaches popular for swimming, surfing and other outdoor activities (Christchurch City Council, 2014). Thus, Sumner services both the local community, day visitors from the wider Christchurch area, and longer-stay tourists, making its commuting patterns and demographic characteristic complex; this hinders the ability to predict/estimate population exposure to tsunami. The most recent, publically available evacuation plan for the Sumner community, developed by New Zealand Police in 2010 (uses a tsunami model scenario generated in 2007 using the scale event of the 1868 South American tsunami, M_w9.1 (Christchurch City Council, 2016a). More recent modelling of a potential M_w 9.485 earthquake from the Peru subduction zone has been used for an updated Christchurch tsunami hazard model (Lane et al., 2014), and this needs to be used to update evacuation impacts assessments and evacuation planning as the new model impacts areas and populations not currently considered.

Consequences from tsunami events depend on the complex interactions among physical processes, the built environment and the actions taken by communities (Horspool & Fraser, 2015). Several studies have shown that factors critical to decreasing the number of casualties lie in the effectiveness of tsunami warning systems and evacuation, which can change population exposure and vulnerability to the hazard (Koshimura et al., 2006; Mas et al., 2013; Power, 2013; Yeh, 2014; Yun & Hamada, 2012, 2014). Therefore, given the high risk from tsunami together with the lack of updated information in the current evacuation plan, an updated evacuation plan is essential for effective and timely response in the event of a tsunami, and the mitigation of tsunami impacts for Sumner.

This thesis presents a credible tsunami evacuation model that uses current tsunami hazard models, the most recent census information to provide an improved understanding of the dynamics of how people in Sumner may respond to tsunami hazards, and to inform managing and mitigating tsunami risk in Sumner. This research has been conducted in parallel with that of (Scheele, 2016) and (Williams, 2016), who have used the (Lane et al., 2014) hazard model to investigate, respectively, impacts on building structures and infrastructure lifelines. Together these studies provide a holistic tsunami impact assessment of Christchurch City.

1.2. Research aim and objectives

The objective of this research is to demonstrate a method for introducing variability in population and vehicle exposure scenarios, for introducing travel speed distributions into a model of pedestrian evacuation, and to evaluate the potential for vehicular evacuation.

The aim of this research is to address three research aims:

- Assess population exposure tsunami hazard in Sumner, including how many people face tsunami risk, where is population distributed at the time of an event, and what are the demographics of the exposed population;
- Identify and assess the most effective evacuation routes, using Least Cost Path Distance (LCD) modelling within geospatial platforms, including assessing the duration for the exposed population to reach safe locations under different scenarios;
- Identify what management options are available for mitigating tsunami risk, as informed by answering the previous aims.

The above aims are addressed by the following research objectives:

- Characterise the spatio-temporal variability of Sumner population exposure to tsunami hazards;
- Develop a credible tsunami evacuation model for Sumner, considering factors that influence evacuation behaviour during a tsunami event (demographic and landscape characteristics);

- Inform emergency management tools which will contribute to community and emergency management tsunami risk reduction plans, for use by local government and other tsunami-threatened coastal areas.

1.3. Conceptual framework

The risk management framework (Figure 1.1) is presented here as the conceptual framework for this study. This framework has been developed to provide a systematic and logical process in which to undertake effective risk management and ultimately risk reduction through: risk identification, risk analysis, risk evaluation, and risk treatment (Standard New Zealand, 2009). The research presented in this thesis focuses on a tsunami evacuation model, which is developed by embedding the whole process of risk assessment within the risk management framework.

The following equation defines terms used in the risk management process (Blong, 2000):

$$\text{Hazard} \times \text{Vulnerability} = \text{Risk}$$

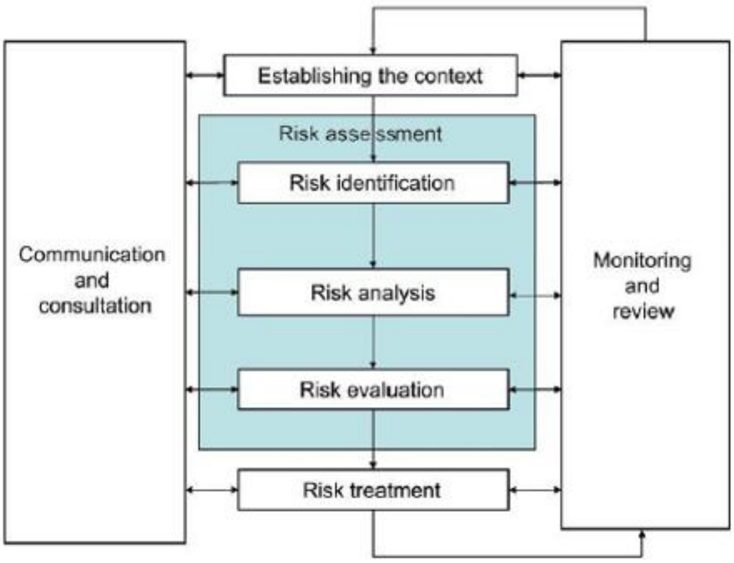

Figure 1.1. Risk management framework (Standards New Zealand, 2009).

Hazard is identified as the interaction between society (population exposure) and an extreme natural event (e.g. tsunami) with the potential to cause loss of life and infrastructure damage. Vulnerability is the degree to which elements (population, in this study) can be impacted (injured or loss of life) due to exposure to the hazard. Risk is the probability that damage to elements will occur as a result of the hazard upon an asset's vulnerability to the hazard.

1.3.1. Risk Identification

After context and objectives are established (Section 1.1 and 1.2), risk identification will be the next step in the risk management process. In the context of this research, this step involves identifying all potential tsunami hazards within a certain area. In addition, the element (e.g. population) at risk from the hazard also needs to be identified. Variability in population exposure (spatially and temporally) to the hazard and their potential vulnerabilities due to their demographic characteristics are very important (Fraser et al., 2014; Wood & Schmidtlein, 2012; Wood et al., 2010). As the only viable mitigation for people in the event of tsunami is evacuation (Fraser et al., 2012; Power, 2013), vulnerabilities in the context of being able to evacuate by foot are assessed, as is the availability of motor vehicles. In addition to determining the ability of populations to evacuate as pedestrians, the potential use of motor vehicles is also assessed. This step is achieved through reviewing literature on the dynamics of population distribution and vehicle use in evacuations, both in normal daily conditions, and in previous disasters, especially tsunami events worldwide (Fraser et al., 2014; Yun & Hamada, 2014).

1.3.2. Risk analysis

The risk analysis stage focuses on developing an understanding of the risks, so they can be compared and ranked (Standard New Zealand, 2009) by determining the vulnerability of the exposed population to tsunami hazards. Vulnerability factors are identified by reviewing literature on previous tsunami and other hazard evacuation research, as well as a range of studies about vulnerable social indices. In addition, vulnerability factors are also achieved by understanding whether landscape characteristics benefit or hinder evacuations in the tsunami event.

1.3.3. Risk evaluation

Risk evaluation compares various risks to determine what actions could be taken to reduce impacts and therefore risk (Power, 2013; Standard New Zealand, 2009). Understanding different levels of risk (acceptable, tolerable, and/or unacceptable) is crucial to the next step of risk treatment. In the context of this thesis, this step involves testing different evacuation scenarios, then identifying areas at high risk based on numbers of people who might not have enough time to evacuate. This step also can identity those factors contributing to increased tsunami risk for the community.

1.3.4. Risk Treatment

Risk treatment is the final step in the risk management process, which is aimed at how to best reduce the vulnerability of exposed assets and/or the hazard. Impacts, and therefore risk, can be reduced through the application of various mitigation strategies, including structural options (harden infrastructure, designate evacuation buildings) and non-structural options (land use planning, relocation of assets, hazard monitoring, societal education) (Horspool & Fraser, 2015; NZEIR, 2015; Palliyaguru et al., 2008; Power, 2013). In the context of this research, this step focusses specifically on the non-structural option of evacuation planning. The results from all of the above steps can be used to provide emergency managers and planners a basis for response and mitigation strategies.

1.4. Tsunami hazard background

Subsection 1.4.1 below presents an overview of tsunami, their generation and impact over the world, in New Zealand and in Sumner specifically, highlighting the need for tsunami risk reduction. Subsection 1.4.2 then discusses international literature on risk reduction strategies and the current approach to risk reduction in New Zealand, providing context to this study's focus on evacuation planning.

1.4.1. Tsunami generation and impacts

1.4.1.1. Global overview

Tsunami are generated when a source event rapidly displaces a sufficiently large volume of water (Fraser, 2014; Power, 2013) (Figure 1.2 and Figure 1.3). The greatest tsunami hazard exists along coastlines adjacent to subduction boundaries, with the highest distribution of tsunami in Pacific Ocean, which accounts for 25.4% of tsunami in the world's oceans and seas (Bryant, 2014; Fraser, 2014).

The principal sources of tsunami generation are submarine seismic sources or coastal earthquakes, underwater landslides, large landslides from coastal or lakeside cliffs, volcanic eruptions and meteor (bolide) splashdown (Power, 2013). Among these sources, the most common is large submarine seismic sources (1,811 events (72%) of 2,501 events) (Fraser, 2014). The highest ratio of tsunami-genic earthquakes to all offshore earthquakes occurs in New Guinea-Solomon Islands region (62%), Alaska-Aleutians region (59%), Japan (56%), Kurile- Kamchatka region (56%), South America (54%) and New Zealand-Tonga region (51 %) (Suppasri et al., 2012).

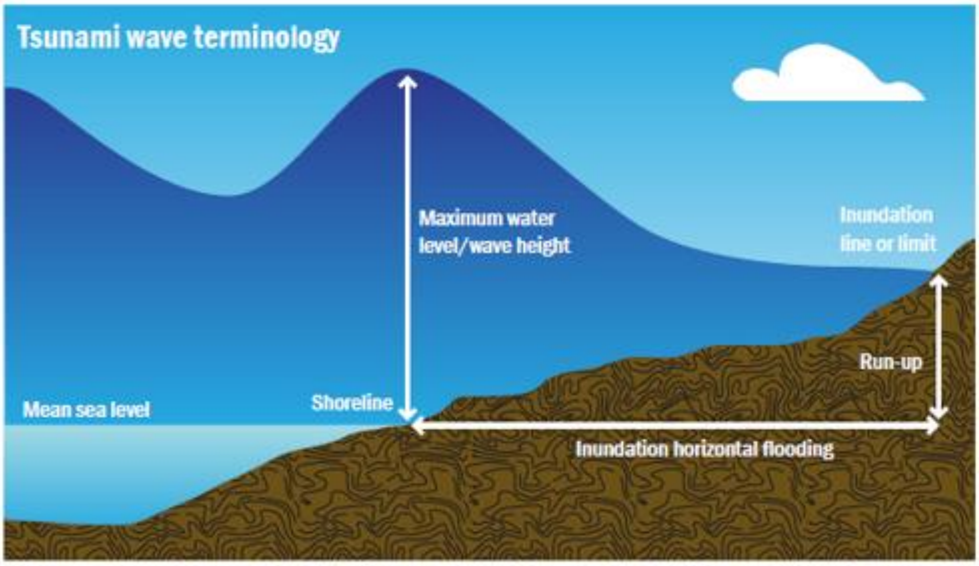

Figure 1.2. Schematic diagram of a tsunami wave approaching the coast (MCDEM, 2010) after Reese et al., 2007).

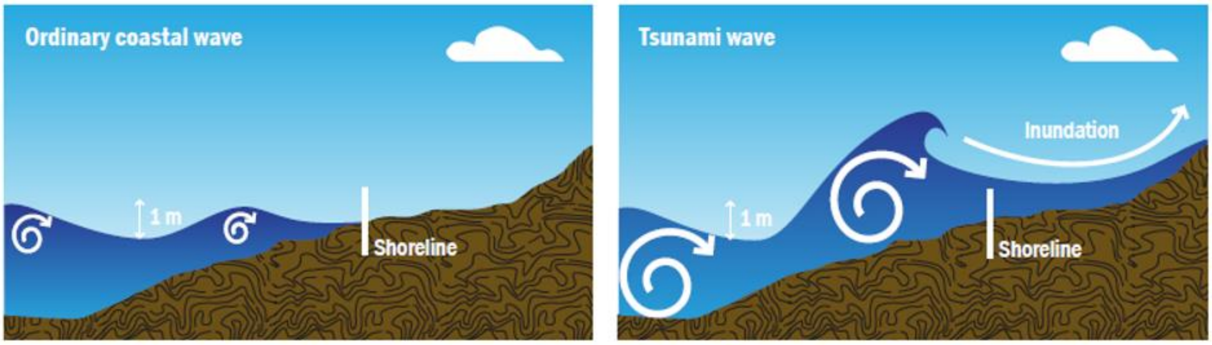

Figure 1.3. In ordinary coastal waves (left), the energy contained is limited to the ocean surface, and rapidly dissipates as the wave breaks. Conversely, the energy in tsunami waves (right) is contained throughout the whole column of water. As the ocean rises, the water is pushed upwards, and the water and energy contained are released further inland, resulting in damage and inundation (from MCDEM, 2010).

Tsunami are generally classified by their travel time from source to impact, and this classification is useful for tsunami research and effective response (Fraser, 2014). In New Zealand, local tsunami (also near-field tsunami), regional-source tsunami, and distant-source tsunami (also far-field tsunami) are defined as the sources which have < 1 hour, 1-3 hours, and > 3 hours of travel time, respectively (MCDEM, 2010).

Tsunami are destructive natural phenomena, potentially causing extremely destruction and disruption to the coastal built environment and economic activity, and especially resulting in massive loss of life. Table 1.1 presents historical tsunami and recorded casualties.

The most common cause of death in tsunami is drowning, which is likely to be influenced by injuries sustained in the water. Mortality rate due to tsunami is highly variable and dependent on both hazard factors and human factors (Fraser, 2014; Power, 2013). Hazard factors include: flow depth and velocity; inundation extent; wave arrival time after the source event; time of tsunami occurrence; and presence of debris. Human factors include: timing and efficacy of official or natural warnings; coastal population density; cultural, social, economic and demographic vulnerability; preparedness levels; and availability of evacuation routes and refuges (Fraser, 2014).

Various formulas have been proposed for mortality as a function of flow depth, for coastal floods, river floods and tsunami (Fraser et al., 2013; Fritz & Borrero, 2006; Hayashi & Koshimura, 2013; Jonkman et al., 2008; Kawata, 2001; Oya et al., 2006; Reese et al., 2007;

Rossetto et al., 2007; Yeh, 2010). These estimates demonstrate the importance of early and efficient evacuation to avoid contact with tsunami flow.

Table 1.1. Historical tsunami and recorded casualties. Where numbers are unknown, a question mark is presented.

Date	Location	Deaths	Injuries	Reference
May 27, 1293	Sagami Bay (Japan)	23,024	?	(Bryant, 2014)
September 20, 1498	Nankaido (Japan)	26,000	?	(Bryant, 2014)
October 28, 1707	Nankaido (Japan)	30,000	?	(Bryant, 2014)
October 29, 1746	Lima (Peru)	18,000	?	(Bryant, 2014)
May 1765	Guangzhou, South China Sea	10,000	?	(Bryant, 2014)
April 24, 1771	Ryukyu Archipelago	13,486	?	(Bryant, 2014)
May 22, 1782	Taiwan	50,000	?	(Bryant, 2014)
May 21, 1792	Unzen, Ariake Sea, Japan	14,524	?	(Bryant, 2014)
November 22, 1815	Bali (Indonesia)	10,253	?	(Bryant, 2014)
August 13, 1868	Arica (Chile)	25,674	?	(Bryant, 2014)
August 27, 1883	Krakatau Indonesia	36, 417	?	(Bryant, 2014)
June 15, 1896	Sanriku (Japan)	27, 122	?	(Bryant, 2014)
January 21, 1917	Bali (Indonesia)	15,000	?	(Bryant, 2014)
February 4, 1976	Guatemala	22,778	?	(Bryant, 2014)
August 16, 1976	Moro Gulf (Philippines)	8,000	?	(Bryant, 2014)
July 17, 1998	Ataipe coast, Papua New Guinea	2,200	1000	(Davies, Davies, Perembo, & Lus, 2003)
December 26, 2004	14 countries, mostly in Sumatra in Indonesia (mostly) and Thailand, Sri Lanka, India and the Maldives	Over 200,000	?	(Fritz, Borrero, Synolakis, & Yoo, 2006)
July 17, 2006	Java	733	9299	(Abidin & Kato, 2009)
April 1, 2007	Solomon Islands	52	?	(Fritz, Papantoniou, Biukoto, Albert, & Wei, 2014)
September 29, 2009	American Samoa, Samoa and Tonga	189	?	(Synolakis, Okal, & Bernard, 2005)
February 27, 2010	Chile	521	150	(Elnashai et al., 2010)
October 25, 2010	Sumatra	>500	>11000	(Revi & Singh, 2007)
March 11, 2011	North-Eastern Japan	15,821	5940	(Dunbar, McCullough, Mungov, Varner, & Stroker, 2011)
February 6, 2013	Solomon Islands	10	15	(Newman et al., 2011)
September 16, 2015	Chile	11	?	

Environmental cues or natural phenomena have been observed prior to wave arrival in many previous tsunami. Japanese data from early as 1896 and 1933 include accounts of audible cues such as 'continuous sound like locomotive' and 'thunder-like' sounds (Shuto, 1997). In Thailand, the majority of people surveyed following the 2004 Indian Ocean tsunami reported seeing or hearing something unusual in the sea (Gregg et al., 2007). These phenomena can provide a natural tsunami warning in the cases of distant, regional and local tsunami, as they are due to the mass movement of water occurring sometimes significant distances from the event source. Post-hazard studies conducted after several tsunami events show the importance of natural cues in early and efficient response. In the 2006 Java tsunami event, despite various natural warning signs very few people were alerted to the impending tsunami. Hence, the death toll was significant with average death and injury rates both being about 10% of the people exposed, for water depths of about 3 m (Reese et al., 2007).

Despite the widespread inundation and significant tsunami heights that occurred during the 2011 Great East Japan Tsunami (GEJT) that destroyed many towns and villages along the Japanese coast, the overall survival rate of people living in the inundated areas was 96% (Fraser et al., 2013; Suppasri et al., 2012, 2013); this is in contrast to the high death rates experienced by Indonesian coastal communities following the 2004 Indian Ocean Tsunami. Factors influencing the lower fatality rates in Japan included structural countermeasures (e.g. sea walls) along with rapid dissemination of warning information, disaster education, tsunami awareness, and in particular, evacuation (Mas et al., 2013; Suppasri et al., 2014). However, some coastal Japanese communities did experience significant fatalities. Ishida & Ando (2014) showed that many lives could have been saved if people had taken appropriate action immediately after the strong ground shaking stopped. Because the tsunami arrived at the coast 25-30 minutes after the earthquake shaking stopped, safe refuges at higher elevations could have been reached within 10-20 minutes on foot.

Other examples of note include different events in Chile, in which there were higher fatalities in the February 2010 earthquake and tsunami compared with the event in September 2015. The February 2010 event killed 525 people, including those who died in the tsunami it spawned, while in the 2015, only 11 people have so far been reported killed, which could have been victims of the earthquake itself (Bonnefoy & Lyons, 2015).

In addition to the lower earthquake magnitude in 2015 (M_w 8.3) compared to that of 2010 (M_w 8.8), human factors also played an important role in the smaller death toll. The 2015 event mainly affected a single, less densely populated region (Coquimbo), in contrast to large cities and populous areas that included crowded vacation resorts (mostly in the towns of Concepción, Arauco and Coronel) in the 2010 event (Servicio Sismológico, 2010). Furthermore, emergency warnings and response had been improved since 2010. Warning systems are for the entire Chilean coastline (Bonnefoy & Lyons, 2015), and since 2010, the National Seismic Centre in Chile has been operating constantly, as have many of the regional offices of the government's national emergency bureau (Bonnefoy & Lyons, 2015). Chile has cellular network broadcasting which reaches about 25-40% of people in the evacuation zones, and tsunami warnings were issued 10-12 minutes after the 2015 earthquake. However, most people had already begun to self-evacuate based on the natural cues of earthquake shaking, and mainly used official warnings for confirmation of a tsunami. These better preparations on the part of coastal residents resulted from education programmes, publishing information on evacuation zones, signage of evacuation routes, annual physical drills, and indeed community memory of the 2010 event.

These tsunami events confirm the importance of early evacuation and tsunami awareness, the need to strengthen warning systems, and develop more resilient communities with effective evacuation plans.

1.4.1.2. New Zealand, Christchurch and Sumner

Of the 1,501 tsunami that have been generated around the Pacific Ocean, 5.5% have affected the New Zealand – Tonga region (Bryant, 2014). From 1835-2011, New Zealand has been affected by at least 80 tsunami (Power, 2013), and by about 10 tsunami higher than 4 metres since 1840 (NZEIR, 2015). Of the 80 tsunami that affected New Zealand post-1835, 34% were from distant sources, 15% were from regional sources, 35% were from local sources, and 16% were from unknown sources (Power, 2013). The ring of subduction zones around the Pacific Ocean is responsible for most of the distant source tsunami to affect New Zealand (GNS, n.d.) (Figure 1.4). The six largest historical tsunami in New Zealand were generated by the M_w 8.2 Wairarapa earthquake (1855), M_w Napier Earthquake (February 1931), M_w7.1 earthquake 50 km offshore of Gisborne (March

1947), and distant earthquakes in South America (1868, 1877 and 1960) (Bryant, 2014; Power, 2013). Even though there is only one recorded fatality from a tsunami since European settlement, (McFadgen, 2008) suggests New Zealand experienced repeated large (>10 metres) tsunami that had devastating effects on the indigenous Māori population prior to European contact.

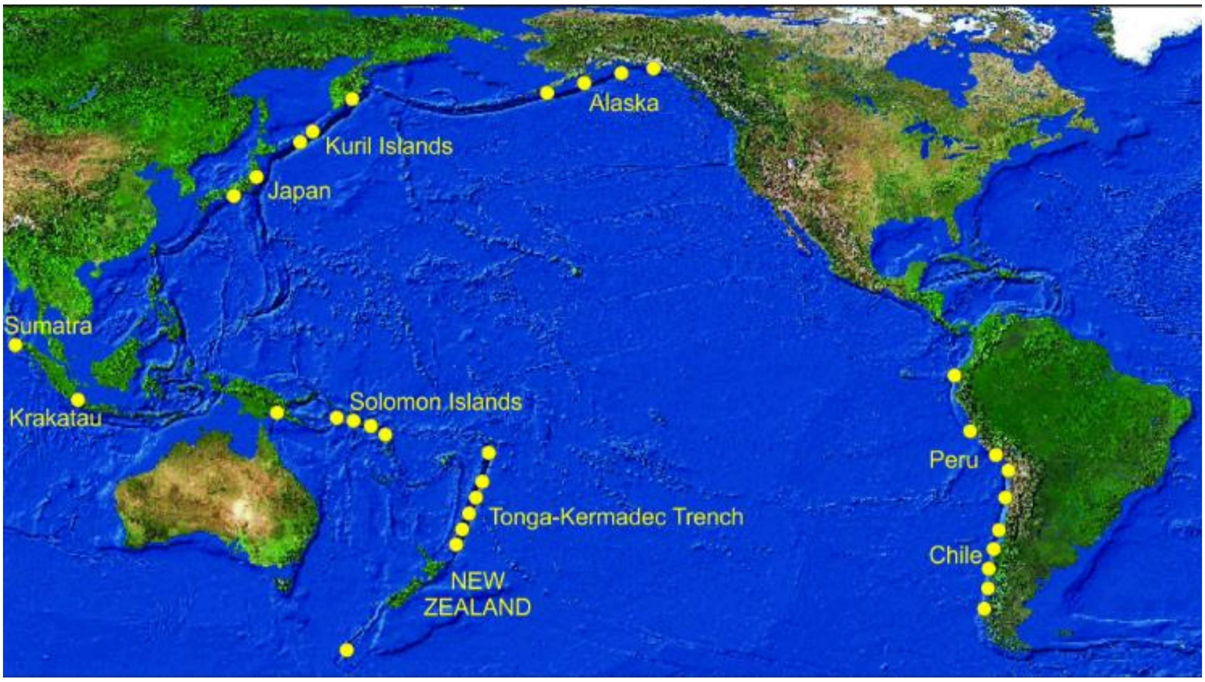

Figure 1.4. Historical and modern records for distant sources tsunami from 1835 to 2011. Yellow dots show sources where tsunami were generated, representing the approximate locations of source events not accurate epicentres. All events were earthquakes, except Krakatau, which was a volcanic eruption (GNS, n.d.).

While there has been relatively little damage and very few recorded casualties in New Zealand due to the Boxing Day tsunami (December 26th, 2004) and Solomon Island tsunami (April 1st, 2007), significant rises in water level have historically been recorded (MCDEM, 2010). The largest wave height recorded in New Zealand from the Boxing Day tsunami was at Timaru where an individual wave reached nearly 1 m (peak to trough) and 1.10 m in Charleston during the Solomon Islands tsunami. New Zealand can expect tsunami with similar, and greater, run-up-heights in the future. Some coasts are more at risk from tsunami than others because of their proximity to local offshore areas of high seismic (earthquake) activity, or may be more exposed to tsunami arriving from distant sources. No part of the New Zealand coast is free from tsunami hazards (MCDEM, 2010).

Several hazard assessments demonstrate the potential high risk of tsunami for coastal communities. A national tsunami hazard review was first conducted by (Berryman, 2005), then by (Power, 2013) and most recently by (Horspool, Cousins, & Power, 2015). Using a probabilistic loss model, (Horspool et al., 2015) assessed the risk of potential fatalities, injuries, property and economic losses from a 1/500 year tsunami event, demonstrating New Zealand’s large exposure to tsunami risk. The estimated fatalities shown in Table 1.2 are assumed to be for ‘worst case’ scenario where there is no evacuation and people remain in their homes.

Table 1.2. The risk from a 1/500 year tsunami event, potential exposure (fatalities, injuries rounded to nearest 000).

Percentile	Fatalities	Injuries	Property loss	Economic loss
84th	33,000	27,000	$45bn	NA
50th	17,000	15,000	$28bn	NA
16th	4,000	4,000	$9bn	NA

Christchurch is subjected to local, regional and distant source tsunami (Lane et al., 2014). Over the past approximate 6,500 years, up to seven paleo-tsuanmi have impacted Christchurch and the most likely sources were South American subduction zone events (Goff, Chagué-Goff, Nichol, Jaffe, & Dominey-Howes, 2012). From 1868 - 2015, there have been five tsunami sourced from South American submarine earthquakes affected Christchurch. Chile was historically the more common tsunami source for this area, although the Peru subduction zone source has been known to cause larger events, with the 1868 Mw=9.1 southern Peru earthquake causing 1-4 m run-up along the South Island of New Zealand (Table 1.3). For a 2,500 year return interval, at the 50th and 84th percentiles, Power, (2013) estimates the tsunami hazard for Christchurch to be >9.5 m and >12.5 m wave heights at the coast, respectively. Power (2013) also indicated that the most likely tsunami source for Christchurch in both a 2,500 and 500 year event, at the 50th percentile, is a Peru subduction zone event. In the event of the Peru subduction zone occurs, Sumner’s geography poses significant constraints for evacuation planning; it is an isolated location with unfavourable exits which are either along the coast, or uphill roads with narrow widths (4-8 m), and located on very steep slopes (Figure 1.5).

Figure 1.5. Topographic map showing Sumner located on the East Coast of Christchurch, New Zealand.

Table 1.3. Historic Christchurch Tsunami, 1868 – 2010 (from Williams, 2016).

Year	Source	Earthquake magnitude	References
1868	Peru	Mw=9.1	((De Lange & Healy, 1986; Goff et al., 2012; Lane et al., 2012)
1877	Chile	Mw=8.7	(De Lange & Healy, 1986)
1960	Chile	Mw=9.5	(Borrero & Goring, 2015; Goff et al., 2012; Lane et al., 2012; Power, 2013)
2010	Chile	Mw=8.8	(Lane et al., 2012)
2015	Chile	Mw=8.3	(National Oceanic and Atmospheric Administration 2015)

Based on a Mw 9.485 earthquake from the Peru subduction zone (2,500 year return period at the 84th percentile confidence interval), the tsunami hazard for Christchurch has been modelled numerically by (Lane et al., 2014) (Figure 1.6). The models, which account for changes in coastal topography following the 2010-2011 Canterbury Earthquake Sequence, represent the highest-resolution tsunami inundation models for

Chrischurch. In the context of this thesis, the (Lane et al., 2014) model will be used as the tsunami hazard scenario. This hazard model indicates Sumner would be one of the six areas along Canterbury coast experiencing the highest levels of inundation (>2.5 metres depth). The specifics of the model are covered in Appendix A1.

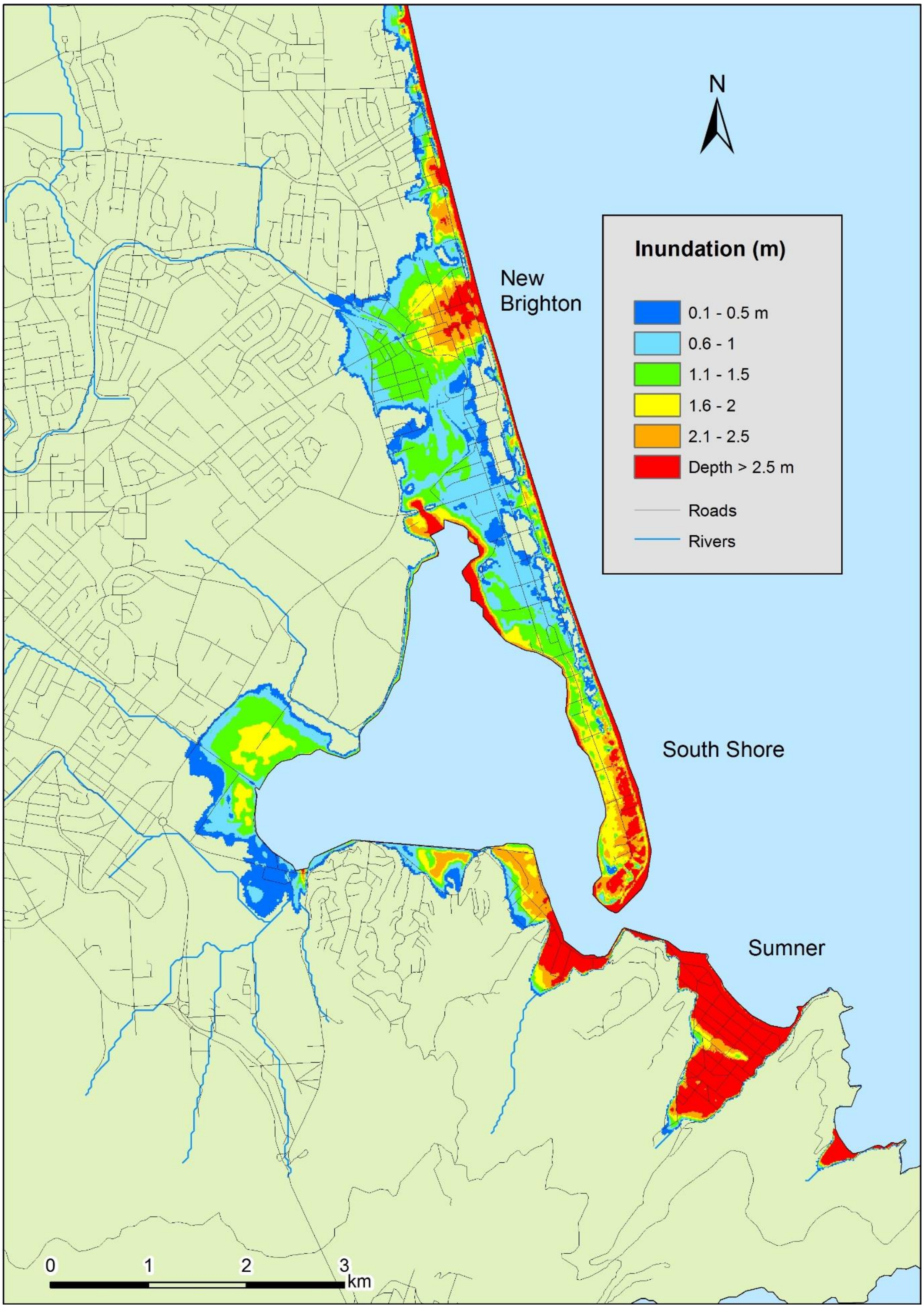

Figure 1.6. Modelled tsunami inundation depths for a 1:2500 year return period Peru subduction zone event in Christchurch (Lane et al., 2014).

The risk of tsunami from the offshore Pacific/Indo-Australian tectonic plate boundary has been apparent to scientists in New Zealand for more than a decade, but political and public traction for mitigation only increased following the Indian Ocean tsunami in 2004 (NZEIR, 2015). Compared to other hazards, tsunami are rare events, but their risk is much greater than other geo-hazards and is more comparable with higher profile commonly recurring risks such as workplace and road accidents (Figure 1.7). However, annual spending on tsunami capability in New Zealand is a tiny fraction of that in comparable risk areas. Spending per unit of tsunami risk is only $0.91, while that of assaults, workplace accidents, vehicles accidents risk is $93.85, $20.73, and $92.83, respectively (NZEIR, 2015)(Table 1.4).

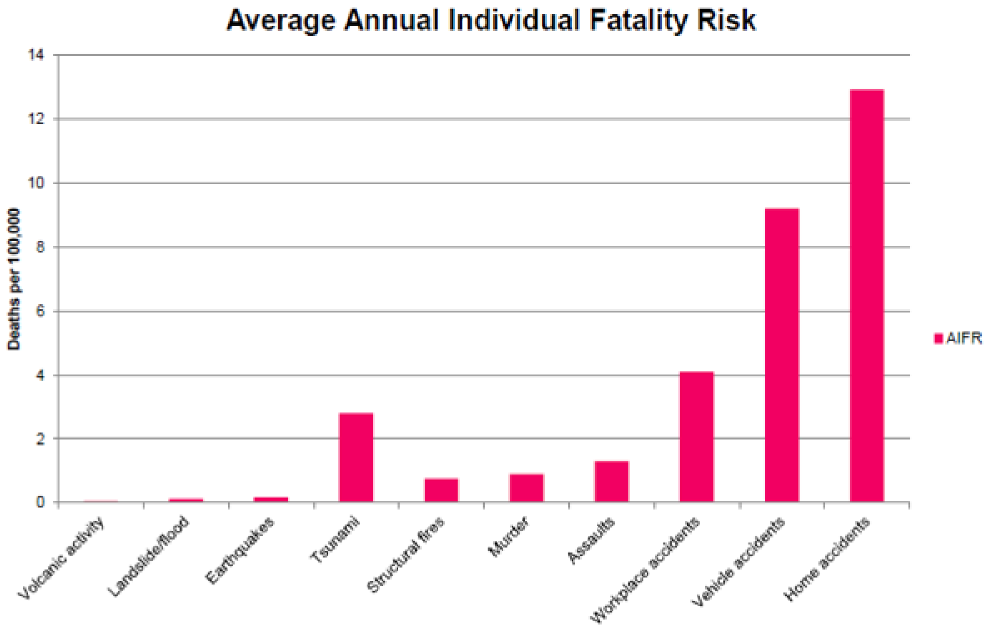

Figure 1.7. Tsunami risk comparison (NZEIR, 2015), after Gisborne District Council, (2013).

Table 1.4. Public spending on tsunami compared with other risks (NZEIR, 2015) after Pedlow et al. (2010); Ministry of Health (2011) (mortality statistics) and NZIER estimates.

Event	Spending by Govt. 2008/9,$m	AIFR/100,000	Spending per unit of risk, $m
Assaults	$122	1.3	$93.85
Workplace accidents	$85	4.1	$20.73
Vehicle accidents	$854	9.2	$92.83
Tsunami	$2.55	2.8	$0.910

The work of NZEIR (2015) demonstrates how effective evacuation in a timely manner can potentially save significant numbers of lives (Table 1.5). Starting with the GNS Science estimates of fatalities based on very limited evacuation, and adjusts this by an estimate of the current evacuation rate that New Zealand would be likely to achieve with current resources and policies. As New Zealand's tsunami preparedness has not been fully tested over the last 50 years, expert judgement was used to develop a plausible target evacuation rate. The results indicate that additional mitigation spending would make it possible to reduce lives lost by around one-third. Improving self-evacuation (for warning times under 1 hour) and developing an official warning capability for regional tsunami (1 – 3 hours lead time) have the most potential. Furthermore, in order to reduce mortality risk alone it could be cost-effective for New Zealand to invest an additional $50 million per annum in tsunami mitigation.

Table 1.5. The opportunity for mitigating national tsunami risks (National Exposure to a composite 1/500 year event (median value) (NZEIR assessment based on workshops with experts).

Tsunami hazard	Warning times below 1 hour	Warning times 1-3 hours	Warning times above 3 hours	Total
*'Worst case' live lost	5,512	3,651	8,108	17,271
Estimated current likely NZ evacuation rate	25%	25%	95%	
Plausible target rate	96%	90%	98%	
Additional lives saved	3,914	2,373	243	6,530
Annual value of lives saved (@$3.88m)	$30m	$18m	$2m	$51m

**'Worst case' scenario where there is no evacuation*

To date, there has been little assessment of potential population exposure to tsunami risk for Christchurch, let alone more specifically for Sumner. Using the methodology used in (Horspool et al., 2015) for the national level, an estimate of potential casualties in Sumner caused by a worst-case far field scenario (Lane et al., 2014) tsunami model for Sumner in worst case scenario is shown in Table 1.6.

Table 1.6. The opportunity for mitigating tsunami risks for Sumner.

Tsunami hazard	Warning times below 1 hour	Warning times 1-3 hours	Warning times above 3 hours
*'Worst case' live lost	Data not available	Data not available	3,305
Estimated current likely NZ evacuation rate	25%	25%	95%
Plausible target rate	96%	90%	98%
Additional lives saved	Data not available	Data not available	96
Annual value of lives saved (@$3.88m)	Data not available	Data not available	$0.79m

**'Worst case' scenario where there is no evacuation*

1.4.2. Tsunami Risk Reduction and Preparedness

Various tsunami risk reduction strategies have been proposed, in which, two examples of holistic risk reduction frameworks are given by (Johnston et al., 2014) and the United States (US) National Tsunami Hazard Mitigation Program (NTHMP) 2001. Risk assessment, land-use planning, appropriate construction, warning, education, and evacuation planning are described as the main components of these frameworks. For more detailed discussion around these risk reduction approaches, refer to (Fraser, 2014; MCDEM, 2008a; NTHMP, 2001)

Among these mitigation options, one of the most effective emergency response strategies during disasters is evacuation, and especially in disasters like tsunami it is considered the main protecting action (Cova, 1999; MCDEM, 2008a; Sorensen & Vogt, 2006). Evacuations are, and most likely will continue to be, the most common and efficient emergency management strategy when a hazardous event threatens and puts at risk the safety of those within the area (Moriarty et al., 2007). However, poorly managed evacuations tend to lead to a strong resentment of government which, in turn, decreases the ability of emergency management organisations to act effectively in the future (MCDEM, 2008a). Therefore, effective evacuation planning is essential, and is the focus of this thesis. This section reviews international literature on evacuation planning options and the current approach of evacuation planning for tsunami risk reduction in New Zealand.

Evacuation planning includes evacuation maps, signs, exercise and vertical evacuation. Each of these items in the paragraphs are discussed below.

Evacuation maps: Maps of evacuation and routes are critical for communicating tsunami risk and emergency response information to the public, and for providing a common platform for integrated evacuation planning (MCDEM, 2008c). For the consistent mapping outputs, guidelines and minimum requirements for evacuation maps are provided in the US (Fraser, 2014) and in New Zealand for local authorities and CDEM groups by the National Tsunami Evacuation Guidelines (MCDEM, 2008c). Examples of tsunami evacuation zones map for Wellington and Tauranga city are presented in Figure 1.8 (left) and Figure 1.9, respectively. Example of the most recent available tsunami evacuation plan for Christchurch is shown in Figure 1.8 (right). The Canterbury CDEM group is currently developing tsunami evacuation maps to be consistent with MCDEM guidelines.

Evacuation signs: To direct the public to safety, signage is an effective tool for identifiable evacuation routes and destinations. A key message that has been applied in all the tsunami sign internationally is a tsunami wave (example of tsunami signs in New Zealand is given in Figure 1.10 (right). New Zealand signage uses blue and white colouring which are consistent with those in the Pacific, however, are different with the designs accepted as an International Standards Office (used by Japan and Caribbean) (Fraser et al., 2012). Meanwhile, Indonesia uses signs with red and blue wave (Fraser et al., 2012). A remarkable project carried out in Wellington, New Zealand is the project with blue line on the streets to mark the inland extend of the 'Yellow zone' (the zone accounts for inundation from the maximum credible local tsunami) has implemented in Wellington, New Zealand (Figure 1.10 (left)).

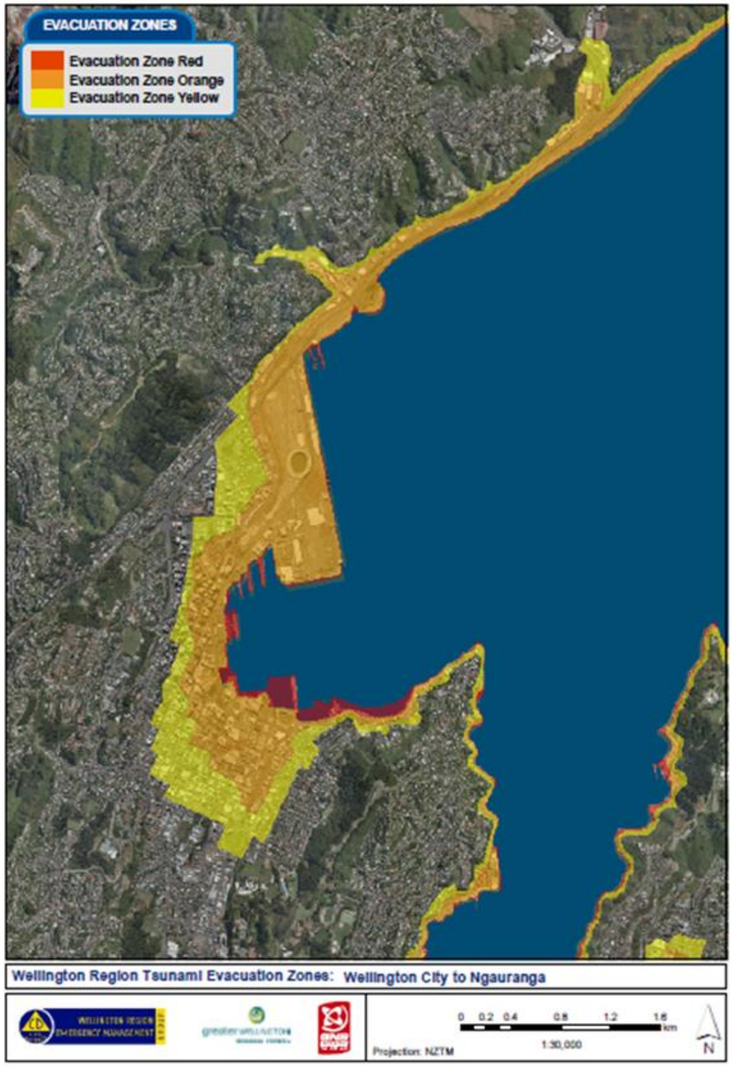

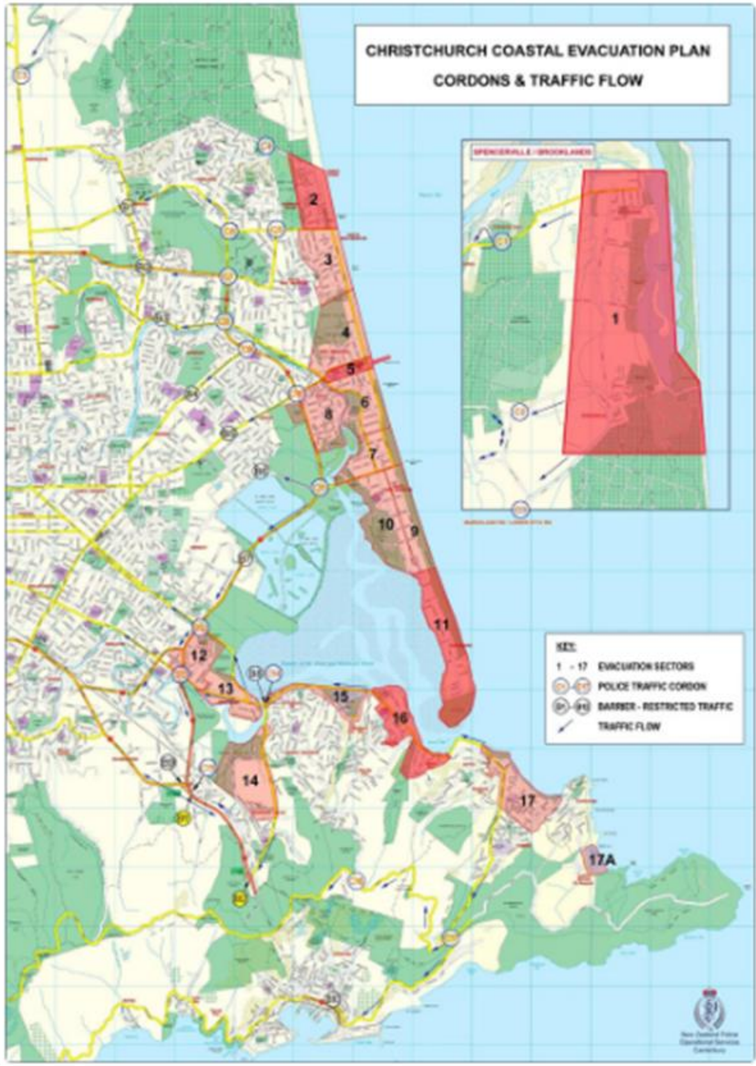

Figure 1.8. Wellington Region Tsunami Evacuation Zones (Wellington City to Ngauranga) (getprepared.org) (left); Christchurch Coastal evacuation plan (right).

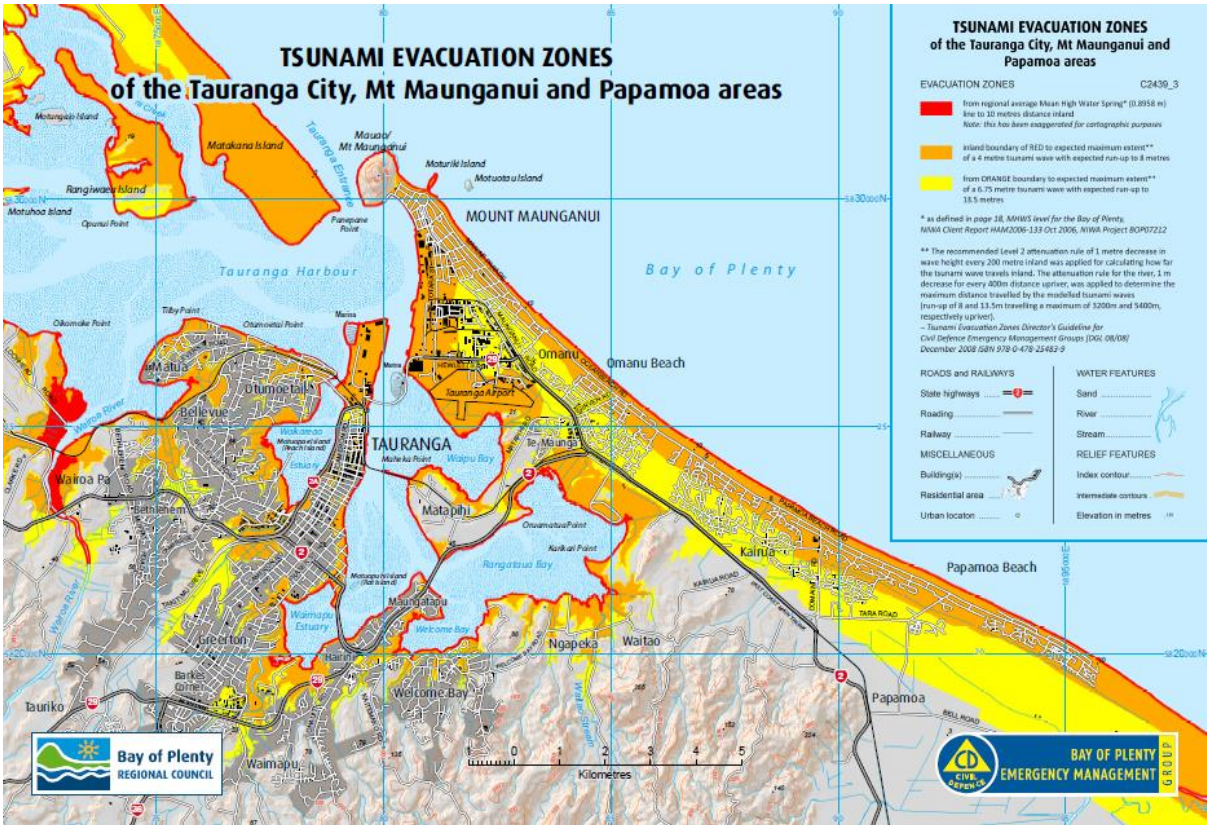

Figure 1.9. Map of the Tauranga coastal area showing Tsunami Evacuation Zones (CDEM Bay of Plenty, 2013).

Figure 1.10. Examples of the blue lines used in Wellington coastal communities (left); and one example of Standard Tsunami signs for New Zealand showing Tsunami evacuation zone (MCDEM, 2008b) (right).

Evacuation exercises: Frequent, well-learned emergency practices are likely to increase the probability that, in a real emergent event, people will respond in an informed manner (Johnston et al., 2011). Although exercises can be unfeasible (costly, time-consuming) (National Research Council, 2011), evacuation exercises provide the valuable opportunities for interactive education, discussion of hazards and appropriate actions, and the assessment and refinement of evacuation plans (Fraser, 2014). Tsunami evacuation exercises are an important component of tsunami preparedness and have been held in many places around the world (Japan, many US States with ShakeOut earthquake drill) (Fraser, 2014). In New Zealand, local CDEM groups (Leonard & Wright, 2011) or individual schools organised tsunami evacuation exercises, however with a very limited involvement (Johnston et al., 2011; McBride et al. 2013).

Vertical Evacuation: Vertical evacuation is to evacuate to elevations above the tsunami flow depth within the hazard zone to tsunami-resistant buildings, towers, or to high areas of natural or artificial high ground (Fraser et al., 2014). Although this approach is often described as a recognised strategy for reducing life risk in hurricanes and flooding (Kolen & Helsloot, 2012; Sorensen, 2000; Wolshon et al., 2005), it also features in tsunami planning guidelines (NTHMP, 2001; Scheer et al., 2012; Scheer et al., 2011). During the 1960 Chilean tsunami, and especially in the 2011 Great East Japan tsunami, a large number of vertical evacuation buildings provided safe refuges in the inundation zone, although some vertical evacuation centres were not high enough to prevent inundation and casualties (Atwater et al., 1999; Fraser et al., 2012). Vertical evacuation structures are used in the US, Japan, and Indonesia (Fraser et al., 2012; Scheer et al., 2012; Velotti et al., 2013), however, in New Zealand, only limited guidelines are available on vertical evacuation. This option is only discussed in the Appendix of MCDEM Guide to the National Plan (MCDEM, 2009). According to (MCDEM, 2008b), vertical evacuation should be considered locally and illustrated on evacuation maps with signage, where this option is applied.

Evacuation plan must be appropriate for the temporal and spatial scales of the hazard. Therefore, this thesis focuses on developing a methodology for better characterising spatio-temporal population exposure, and more realistic evacuation time estimation will help inform emergency management in making evacuation maps, planning evacuation, identify the best locations for evacuation signs and vertical evacuation structures. By doing so, results of this present research also supports the warning and education aspects of tsunami risk reduction.

1.5. Research methodology, and thesis structure

To identify the population exposure, a variable spatial and temporal population distribution model is built. First, the time-profile graphs for different population group are determined based on the 2013 NZ Census data and local knowledge together with expert opinions. Population then will be distributed into buildings according to different time scenarios, seasonal changes (February/June/Oct), between weekday/weekends, and diurnal changes (02:00, 08:00, 12:00, and 17:00). Several rules which take into account the demographics' characteristics (ages, impaired/dependent people, and occupation) were also applied into the model, making the population distribution more realistic.

The structure of this thesis is presented below:

An evacuation model is developed to analyse and evaluate the risk toward humans in a tsunami event. Pedestrian evacuation is determined through applying least cost path distance (LCD) method which takes into account landscape factors (slope degree, up-downhill movements) and demographics' factors (differences in ages' speeds, impaired/unimpaired people, movement/evacuation of group of people). A simplified model for vehicles using different time scenarios is also identified which will quickly help inform the emergency managers of how many vehicles may be used in the event of a tsunami (Chapter 2 and Chapter 3).

A risk treatment is presented as an emergency management tool by using results from the two previous methods. These results are input into the evacuation density map (showing number of people having no or little time to evacuate) and evacuation time curves (presenting number of people corresponding to evacuation time) (Chapter 3). Finally, discussions around limitations and applications research's results, and recommendations for future research are presented (Chapter 4).

Chapter 2 Spatial and temporal distribution models for Sumner

Contents

2.1. Introduction

The purpose of this chapter is to build population, speed and vehicle distribution models for Sumner to inform tsunami evacuation modelling, accounting for spatio-temporal variability. This aims to address the first research objective which is Risk Identification, by assessing the population exposure tsunami hazard in Sumner. This is achieved by (1) presenting an overview of previous research on population distributions for evacuation modelling; and (2) identifying remaining research gaps (Section 2.2). These reviews are used to inform and develop the methodology of characterising spatio-temporal population, speed and vehicle distributions for tsunami evacuation models in Sumner. The results of the population, speed and vehicle distributions inform the different scenarios presented in Section 2.3. The overall chapter structure is depicted in Figure 2.1.

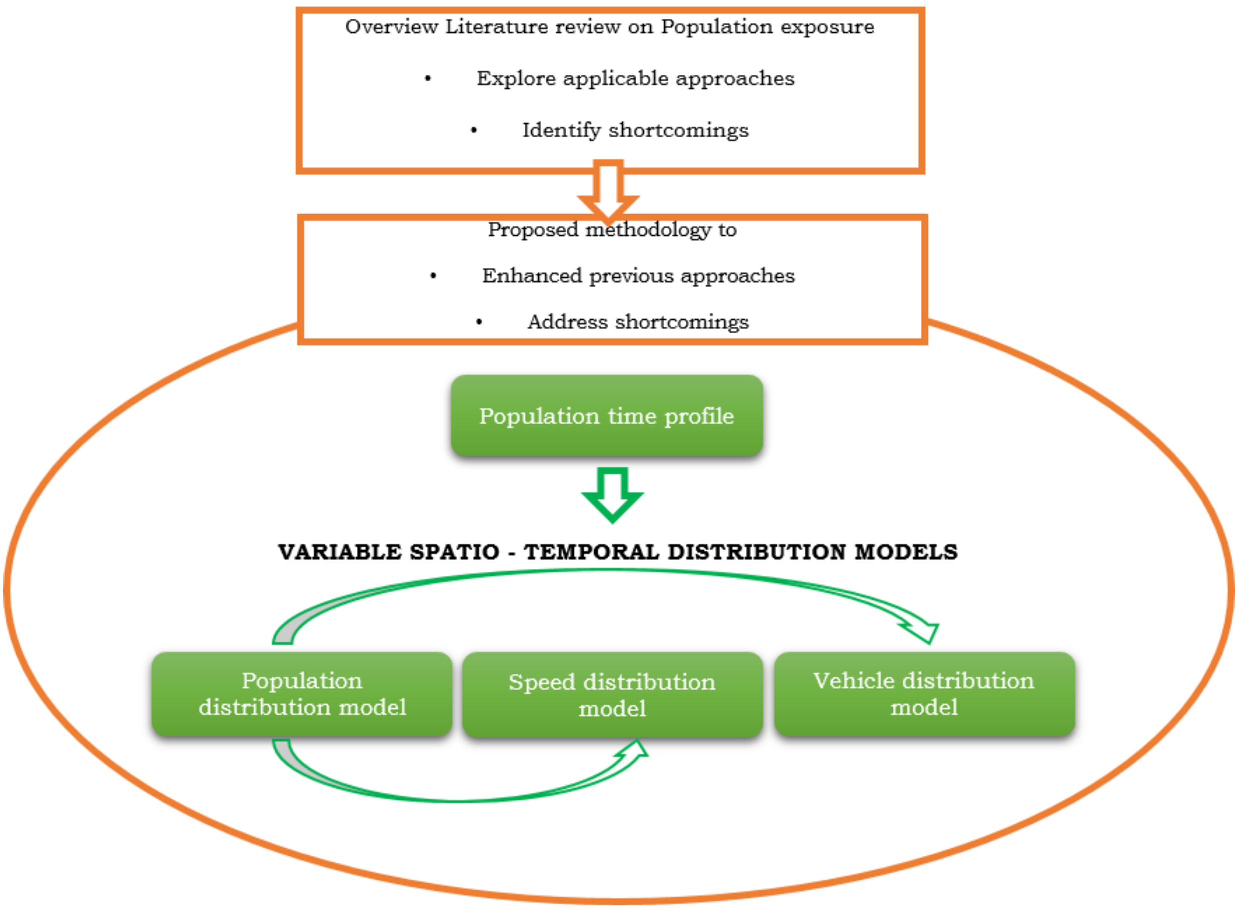

Figure 2.1. Overview of chapter 2 structure.

2.2. Review of population distribution model literature

This section presents an overview of related research by discussing: (1) the importance of determining population distribution for evacuation planning; (2) the importance of high-resolution spatio-temporal data in population distribution models within evacuation models; (3) how previous research addresses these issues; and (4) remaining gaps in the literature. This section helps inform the methodology to develop population, vehicle and speed distributions introduced in Section 2.3.

In the context of hazard and disaster planning and response, determining where people are located at the relevant moment is very important since scientific analyses, operational activities, and policy decisions are significantly influenced by the number of impacted people (Bhaduri et al., 2007; Gatrell et al., 1990; Klepeis et al., 2001; Sutton et al., 2003). By providing spatio-temporal population distributions within the hazard zone (the exposed population), the realistic starting locations of evacuees are determined, and this is a crucial step in preparing an evacuation model (Fraser et al., 2014; Greger, 2014). Despite the importance of proper estimation of the exposed population's size, very little of the existing research is able to thoroughly address two aspects: spatial and temporal changes in population distributions; and consequently gives misleading population exposure models (Glickman, 1986; Greger, 2014; Southworth, 1991).

2.2.1. Temporal distributions

The first shortcoming of much research is the lack of a temporal scale, specifically the daytime population distribution (Cova, 1999; Glickman, 1986; Greger, 2014; Klepeis et al., 2001). Census data are commonly used to present night-time population, and are capable of detecting long-term changes related to life-cycle status (Davies, 1984). However, the large spatial redistribution of population occurring every day, especially in high population density areas, is inadequately demonstrated through census data as the daytime population distribution can be very different from that described by the census (Goodchild et al., 1993; Wu & Kanamori, 2005). Therefore, although the availability of population census data is a positive aspect, it cannot be the only source used to portray the actual population dynamics as functions of space and time (Bhaduri et al., 2007; Wu

& Kanamori, 2005). This downside has already been acknowledged and emphasised by many authors addressing population exposure, where only night-time population was examined (Ahola et al., 2007; Dobson et al. 2000; Schmitt, 1956; Wood et al. 2014).

The lack of modelling daytime shifts in population is understandable as diurnal (day-night) movement is difficult to model due to the complexity of population movements (Cova, 1999; Parrott & Stutz, 1991). This complexity has led to previous research focussing on assumed "worst case" night-time scenarios (Glickman, 1986); however, in the context of emergency planning, accounting for potentially significant diurnal changes needs to be considered for appropriate emergency response. In areas with minor residential use and a greater number of other usages, only considering night-time population, and neglecting daytime population fluctuations, could be problematic and consequently lead to the worst possible decision for emergency management (Glickman, 1986; Greger, 2014). A number of papers have taken into account variations in day-time population; nonetheless, most of the approaches tend to model these temporal fluctuations at highly aggregated levels. For example, some population distribution models account for the temporal scale by either defining it as a two-stage process that contrasts the situations during day and at night (Dewi, 2012), or three scenarios with an additional scenarios for day time and rush hour (Cova & Church, 1997), or daytime residential/workplace population (McPherson & Brown, 2004). From a temporal perspective, (Glickman, 1986; Goodchild et al., 1993; Parrott & Stutz, 1991) mark the first attempts at estimating the variability in the size of exposure population over the course of a day, providing 'any time of day' scenarios rather than specific time scenarios. Similarly, by using available census data and travel surveys or exposure-related human activities surveys, Klepeis et al. (2001) developed a population exposure model accounting for activity for 10 different types of locations, in comparison to the four principal locations used in other research (e.g. Glickman, 1986; Goodchild et al., 1993; Parrott & Stutz, 1991). However, while being detailed in time-of-day human movements and activities, from a temporal aspect the limitations of these studies are a lack of scenarios for days of week (weekday/weekend), seasonal changes, and other 'noise' like special events, or holidays.

2.2.2. Spatial resolution

From a spatial perspective, the aforementioned studies used coarse spatial resolutions, which preclude their applications in the micro-scale context of high-density areas. This is because the commonly used population data source - census data - are limited to census accounting units. For example, in research from the United States the account units are census tracts (aggregated block groups); block groups (aggregated blocks); and census blocks (smallest polygonal unit). Often there is great uncertainty about spatial distribution of residents within these accounting units, as even at the highest resolution (census blocks) the population values are typically an attribute of the block (polygon) centroids (Bhaduri et al., 2007). Therefore, they are normally too generalised in their spatial resolution to be able to adequately represent situations and processes within highly urbanised areas. As natural hazards and vulnerability can vary at smaller geographic scales and even at the household level (Clark et al., 1998), high-resolution population distribution data are critical for successfully addressing important issues, especially from a risk management perspective (Bhaduri et al., 2007). Hence, research needs to address the development of new approaches to estimate population distributions at higher resolutions or at fixed points in time (Cova & Church, 1997; Greger, 2014).

In terms of the spatial scale, Ahola et al., (2007) successfully represented population distribution dynamics by modelling human activities and using census data at the building level. Similarly, Lwin & Murayama, (2009) suggested a variety of calculation methods to estimate populations on a building-level basis, including area-metric and volumetric approaches.

2.2.3. Population groups

Another shortcoming of the above population exposure models are their exclusive focus on residential populations, excluding other population groups (e.g. visitors, people with mobility challenges). As Tobler, (1979) notes, 'the average daily activity space of individuals is dependent upon culture, environment, social, and urban-rural status'. Hence, more detailed information about temporal behaviours in human movements of different population groups, such as visitors (business or leisure reasons), and people with mobility challenges (physically or mentally challenged), could improve the quality of the population exposure model.

Martin (1996) and then Martin et al. (2009) introduced population density estimation models by incorporating available census data, and additional secondary data sets such as prison inmates, hospitalised people and tourists. However, assuming all people of a certain demographic group are engaged in a certain activity at certain corresponding locations, and at a certain time, appears to be too generalised. To overcome this (Greger, 2014) developed an enhanced model, an extension of (Lwin & Murayama, 2009), which utilised multiple usage categories incorporated with temporal variations in human activities that affect building populations. Their underlying assumption was an equal distribution of the population over the available total floor space (per usage category), which allows a more precise estimation of building populations. However, this model was not able to address other temporal scales (over a course of week/season/year and other special events), and lacked other population groups (e.g. visitors, impaired people, young children).

Additionally, the lack of taking maximum required floor per person into consideration in these above research shows a requirement for future research. (Budiarjo, 2006; Dewi, 2012) addressed this problem by developing tsunami evacuation building capacity for a case study in Aceh, Indonesia through setting a capacity score (proportion of available floor area is able to occupied by people) for each building category. This could be a useful approach, however it is only applicable to study areas characterised by high population densities like Indonesia. Despite these limitations, Budiarjo's (2006) and Dewi's (2012) distribution approaches using floor area per different usage of buildings at given times of day, and maximum required floor area per person, serve as the basis for this present research; here, this approach is applied and further developed (further details given in Section 2.3.2).

2.2.4. Spatio-temporal dimensions for population dynamics

Recent progress has been made in modelling population dynamics, by assigning population-time profiles to different types of locations (Cockings et al., 2010) and by using transport data in short time-slices to estimate diurnal changes in population distributions (Kobayashi et al., 2011). However, such time profiles have yet to be applied in tsunami evacuation modelling.

Until now, (Fraser et al., 2014) has been the most comprehensive approach to providing fine-grained spatio-temporal population distribution. This was based on a number of previously published population estimation approaches, which Fraser et al. (2014) developed to be a more realistic representation of human activities in highly urbanised areas. First, Fraser et al., (2014) developed a method called variable time profile graphs which showed the proportion of each population group for three different location groups (home, work, and unspecified locations) according to the time of day (described in Section 2.3.1). In addition, other time scenarios were considered for weekday/weekend, season (peak – medium- low tourist season). It is worth noting that in Fraser et al., (2014)'s model people are distributed into buildings, and also "unspecified locations" (roads, beaches, and recreational areas) to account for those who are doing outdoor activities or are in transit. Unlike (Greger, 2014), instead of assigning population into all types of buildings through a floor area ratio, (Fraser et al., 2014) only applied this approach for the work location category (which are commercial and community use buildings). With the home category (residential buildings) people are assigned at random; however, the total number of people from different age groups were still constrained by the number of people in each age group in each census meshblock. This is a better approach as in reality a bigger house does not necessarily contain more people.

Compared to previous research, Fraser et al. (2014) present a better approach by addressing the fluctuations of population distribution both spatially and temporally; however, there are some limitations to this approach. First, by randomly distributing the number of people at home into residential buildings, the research did not take into consideration those who are able to be home alone and those who are not. For example, it would be unrealistic for a child under 5 years of age or an impaired person to stay home alone. A more realistic assumption would be that at least one adult is at home with the dependent person. Second, the research only focuses on pedestrian evacuation and does not incorporate other transportation types such as personal vehicles or public transportation, which in reality are likely to be used in the event of far field tsunami scenario where people have more time to evacuate. Therefore, in this present research, several rules will be applied to address these limitations to enhance the spatial-temporal population estimation method. Hence, this research provides a more realistic model of the underlying real-world processes that are the result of human actions, especially in urban areas.

2.3. Population, speed and vehicle distribution: methodology and results

This section introduces the methodology used in this research to develop population, travel speed and vehicle distribution models. This is based on the benefits and shortcomings of previous methods (Section 2.2). Data preparation for population (Section 2.3.1.1), locations (Section 2.3.1.2), and time scenarios (Section 2.3.1.3) are presented below. Methodologies and results for all population groups, travel speed and vehicle distribution models are given in Section 2.3.2.

2.3.1. Data preparation

2.3.1.1. Population

The Sumner population is divided into six different groups; *children under five*, *children from five to 14*, *working age adults* (people in the ages of 15 to 64), *elderly independent* (>= 65 years old), *impaired groups* (people with physical mobility challenges), and *visitors.* These population groups are defined based on: (1) the predominant diurnal activity and age; (2) available data on population, and research related to mobility in different groups; and (3) social and demographic factors influencing evacuation as defined in Section 2.2. Data on the first four groups is taken from Census 2013, employment data, local education rolls, and local care facility capacities. Data for visitors is obtained indirectly from census data for Christchurch: monthly numbers of tourists from January 2000 to March 2015. The six different demographic groups are used in the model to assign exposure locations, travel speed distributions (different demographic groups travelling at different speeds, especially on foot), and vehicle distributions.

In this study, total night-time population is obtained from 2013 Census Population by Age at meshblock resolution. A meshblock is a New Zealand cadastral entity, generally covering less than 4km^2 in Sumner (Figure 2.3.1). Diurnal movement patterns of all population groups are defined by *Population time profiles* (Section 2.3.2.1) which show the proportions of each group at different types of location according to a given time scenario.

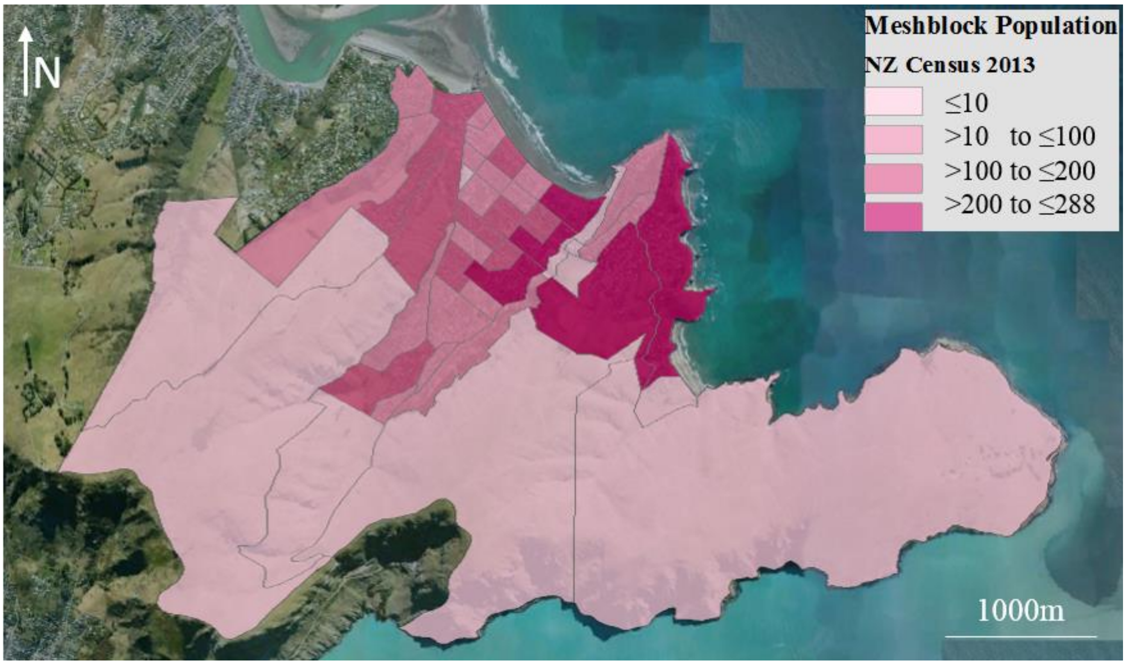

Figure 2.2. Meshblock boundaries and the 2013 estimate of total population (all age groups) for each meshblock in Sumner.

2.3.1.2. Population Locations

There are three types of population locations defined in this research: *Home* (residential buildings), *Work* (business buildings, motel/bed and breakfast accommodation, community, schools and rest homes), and *Unspecified locations* to represent people in transit or outdoors. Building locations, floor area and usage categories are obtained from building data within the loss estimation software RiskScape (https://riskscape.niwa.co.nz/) and the Christchurch Building Footprint shapefile from the data portal Koordinates (https://koordinates.com/layer/6676-christchurch-city-building-footprints/) (Table 2.1). Data for Residential Red Zone areas (those areas impacted by the 2010-2011 Canterbury Earthquake Sequence), updated in 2014, were obtained from CERA and used to assess the current building stock. There are 513 buildings missing from the RiskScape building dataset, therefore those buildings' information was obtained from the Koordinates Building Footprint data, assuming that those buildings have one storey only. A total of 2545 buildings were examined within the study area, with the numbers of residential buildings, workplaces, and combined schools and rest homes being 2476, 50 and 18, respectively. Populations for each of these three location types were determined from the results of generated population time profiles (Section 2.3.2.2).

Table 2.1. Summary of building data

Data sources	**Number of buildings**	**Year**	**Shapefile types**	**Attributes**			
				Location	**Usage category**	**Floor area**	**Storeys**
RiskScape	2034	2013	Point	✓	✓	Floor area	✓
Koordinates	2958	2013	Polygon	✓	N/A	Footprints	N/A

2.3.1.3. Time scenarios

Nine time scenarios are examined (presented in 24-hour format, New Zealand Standard Time): 02:00 weekday; 08:00 weekday; 17:00 weekday; 12:00 weekday and weekend in February. 02:00 weekday and 12:00 weekend are repeated for February, June and October to represent peak, mid- and low-tourist season, respectively, and also to compare night versus peak commuting times (Table 2.2). The differences between population exposures in the three examined months reflect fluctuations in the visitor numbers between the months; other population groups are uniform throughout the year. The range of scenarios allows for a more realistic time-variable exposure model, better identifying evacuation demand.

Table 2.2. Time scenarios analysed in this research

Months	Weekday				Weekend
	02:00	08:00	12:00	17:00	12:00
February	✓	✓	✓	✓	✓
June	✓	N/A	N/A	N/A	✓
October	✓	N/A	N/A	N/A	✓

2.3.2. Methodologies and results

2.3.2.1. Population time profile

This section explains the methods used for developing each time profile for the individual population groups. These time profiles are used as the foundation for the next steps; building the population distribution model and then the respective models for speed and vehicle distributions.

2.3.2.1.a. Children under five

A total of 207 children under 5 is used, with 50 children going to pre-school accounting for 25% of the total children under 5 in Sumner. The number of children staying at home is assumed to be 157 (75%). This type of data is not available and is likely to be an over estimation as some children will attend pre-school outside of Sumner. Pre-school hours for these children is between 08:00 – 17:00 (taken from Pebbles School, Table 2.3). Commuting hours are at 07:00 and 18:00, before and after school starts and finishes, respectively. Figure 2.3, and Figure 2.4 show the flow chart for children under 5 time profile graph, and weekday time profile graph for this group, respectively.

Table 2.3. Pebbles School's population and school hours.

School	***School rolls***	***Staff***	***Staff/students ratio***	***School's pop***	***School hours***
Pebbles school	*50*	*11*	*0.22*	*61*	*08:00 -17:00*

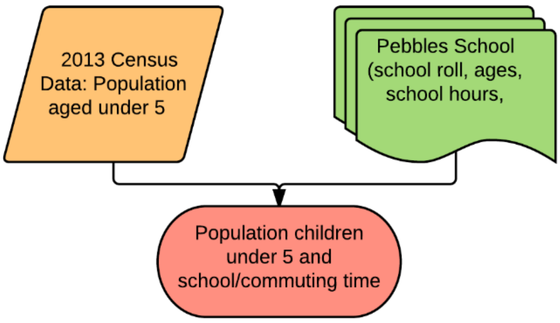

Figure 2.3. Flow chart for children under 5 groups' time.

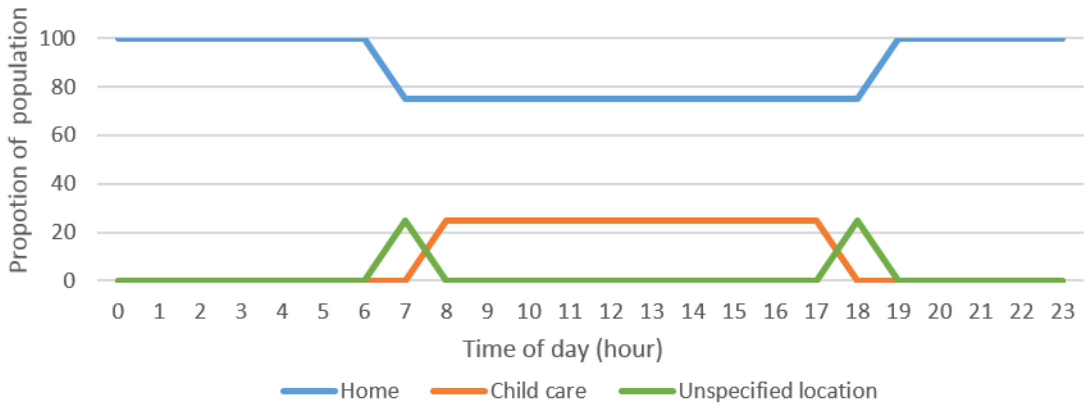

Figure 2.4. Weekday time profile for children under 5.

2.3.2.1.b. Children from five to fourteen

The number of children from 5 to 14 in Sumner is 600; the number of children from 10 to 14 is 270. The age of 14 is used as the upper limit because the pedestrian seed literature uses this an upper bound for this age group (Knoblauch, Pietrucha, & Nitzburg, 1996; Park, van de Lindt, Gupta, & Cox, 2012; Post et al., 2009). As there is no exact number for the population of 13 and 14 year-olds available, the population of this group was calculated as 2/5 of the total 270 (total of 108), assuming the number of children aged 13 and 14 is equal. Therefore, the number of children under 13 going to the three schools in Sumner is estimated to be 492 (600-108).

However, school rolls for the three schools is 736 students (in 2015) which is 244 higher than the number of children under 13 living in Sumner (Table 2.4). Although subsequent to the 2013 Census the population of under 13 year-olds might have increased, to ensure consistent data throughout the research these 244 students were assumed to be living outside Sumner. The total population for children between 5 to 14 is taken as the total number living inside and outside Sumner, which is 844 (600 + 244) (Table 2.5).

School starts at 09:00 and finishes at 15:00, therefore children under 13 (accounting for 87% of total children from five to fourteen year old) are assumed to leave home or travel to Sumner (for children living outside Sumner) at 08:00 and leave school at 16:00. Meanwhile, 13% of this population group, which are students over 12 studying outside of Sumner, need to leave home at 07:00 and will come back to Sumner at 17:00.

From 18:00 to 6:00, all children from 5 to 14 living in Sumner are staying at home which accounts for 71% of the total 844 children in this group. At 7:00 children living in Sumner, at the ages of 13 and 14 years old, leave Sumner and travel to town (13%), while children under 13 are still at home (53%). At 8:00, children under 13 (both living inside and outside Sumner) go to schools in Sumner, accounting for 87% of total children from 5 to 14. Figure 2.5 and Figure 2.6 show a flow chart to develop the time profile graph for this group, and weekday time profiles, respectively. The total proportion of children aged five to 14 does not always equal 100% because some attend school in Sumner but live elsewhere, and others who live in Sumner but attend school elsewhere.

Table 2.4. Primary schools population and school hours in Sumner.

School	School rolls	Staff	Staff/students ratio	School's pop	School hours
Sumner	459	41	0.09	500	09:00- 15:00
Our Lady Star of the Sea	69	8	0.12	77	
Redcliffs	208	30	0.14	238	
Total students 5-12	**736**				

Table 2.5. Population ages 5 to 14.

Ages	**Living**	**Number**
5 to 12	In Sumner	492
	Outside Sumner	244
13 to 14	In Sumner	108
	Population of 5 to 14	**844**

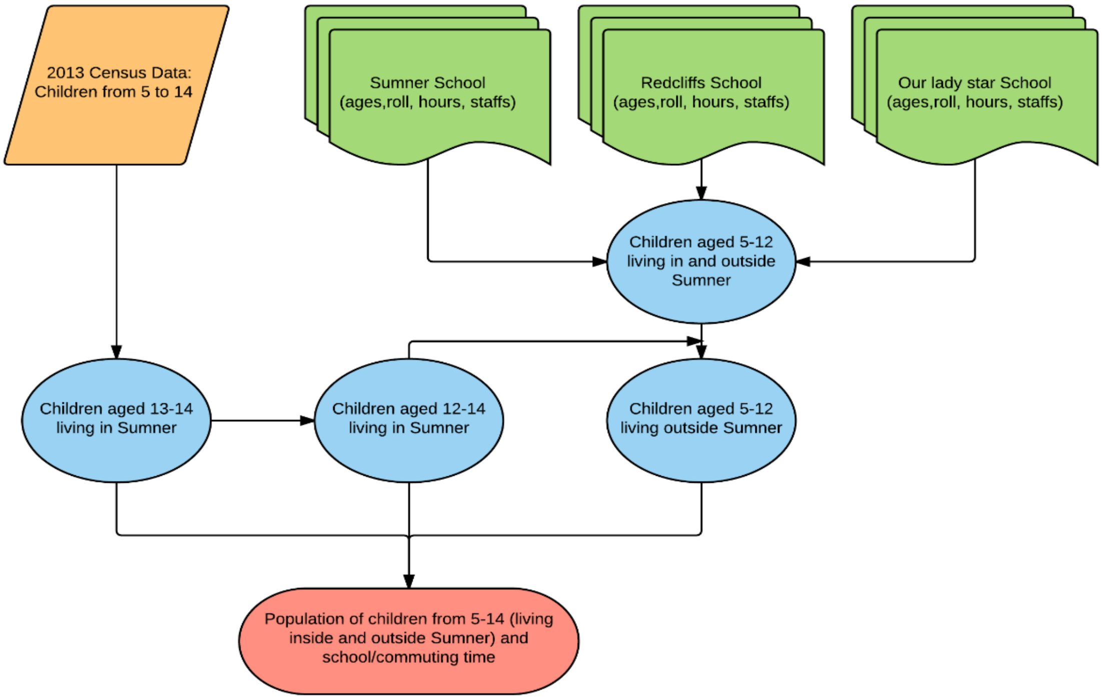

Figure 2.5. Flow chart for developing children under 15 group's time profile.

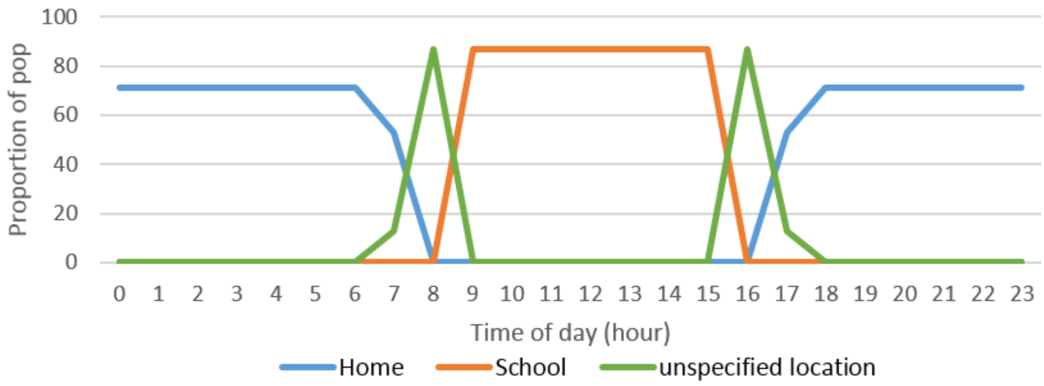

Figure 2.6. Weekday time profile for children from 5 to 14.

Weekend time profile for children under 15 (under five and from five to 15)

Children under 15 (both children under 5 and from 5 to 15) do not go to school on the weekend, and therefore, the time profile of these two groups is assumed to be the same in the weekend. This model assumes all children remain in Sumner in the weekend. Note that the number of children from 5 to 14 counted here excludes the number of children under 13 living outside Sumner. Results are shown in Figure 2.7.

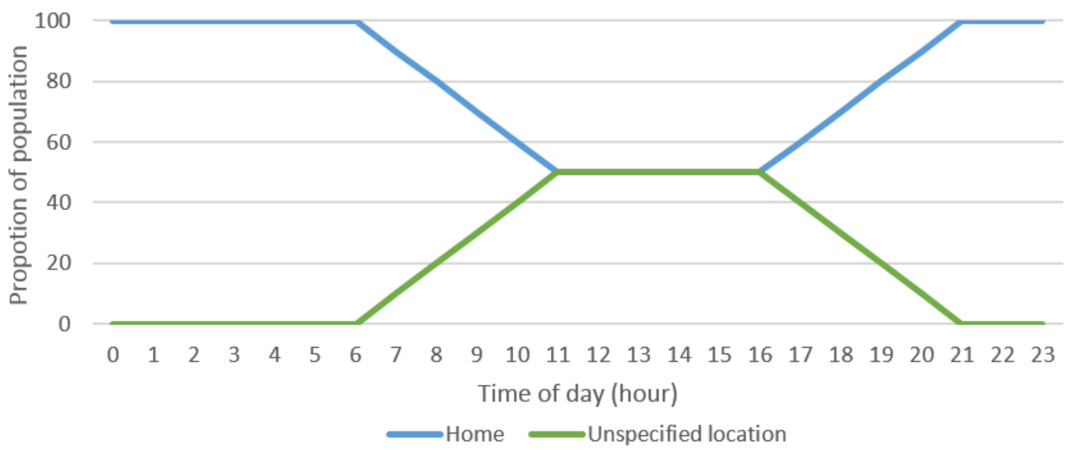

Figure 2.7. Weekend graph time profile for children under 15.

2.3.2.1.c. Working age adults

Employment and commuting patterns have been characterised using occupation for the employed resident population and for work places (aged 15 and over) (Statistics New Zealand, 2013), and local knowledge of commuting times. Other previous work on a similar topics (e.g. (Glickman, 1986; Goodchild et al., 1993; Klepeis et al., 2001; Parrott & Stutz, 1991) and especially (Fraser et al., 2014) (as this study is also conducted in New Zealand (Napier, North Island)), are helpful references for establishing time profiles. Due to their detailed and informative descriptions, (Glickman, 1986) and (Southworth, 1991) provide a clear method to determine the time profile for working adults. Equation (2.1) presents an improvement over Glickman's (1986) and Southworth's (1991) method for modelling the spatio-temporal distribution of working adults:

$$W_{At}=R_{st}-R_{ot}+NR_{it} \tag{2.1}$$

where, W_{At} is the number of working adults at time t; R_{st} is the number of working adults who are residents and stay in Sumner at time t; R_{ot} is the number of working adults who are residents, leaving from Sumner at time t; and NR_{it} is the number of working adults who are non-residents of Sumner, coming in to Sumner at time t.

Based on employment shift data (Statistics New Zealand, 2013), the ratios of residents who work in Sumner, residents who work outside Sumner and non-residents who work in Sumner over usual residential employees are 55:45:11 for weekdays, and 20:10:5 in the weekend. Therefore, the total proportion of working-age group in the graph time profile does not always equal 100% due to the absence of the number of residents working outside Sumner. The model also takes into consideration full- and part-time jobs, with the ratio of the two job types being 70:30, respectively (Statistics New Zealand, 2013) . With full-time workers, there are two main shifts; day and night (ratio of 98:2). For part-time workers, the ratio is 8:92.

The process for estimating the working age adult population and distribution is shown in flow chart Figure 2.8, and Appendices 2 and 3. Results of time profile graphs for this group are shown in Figure 2.9.

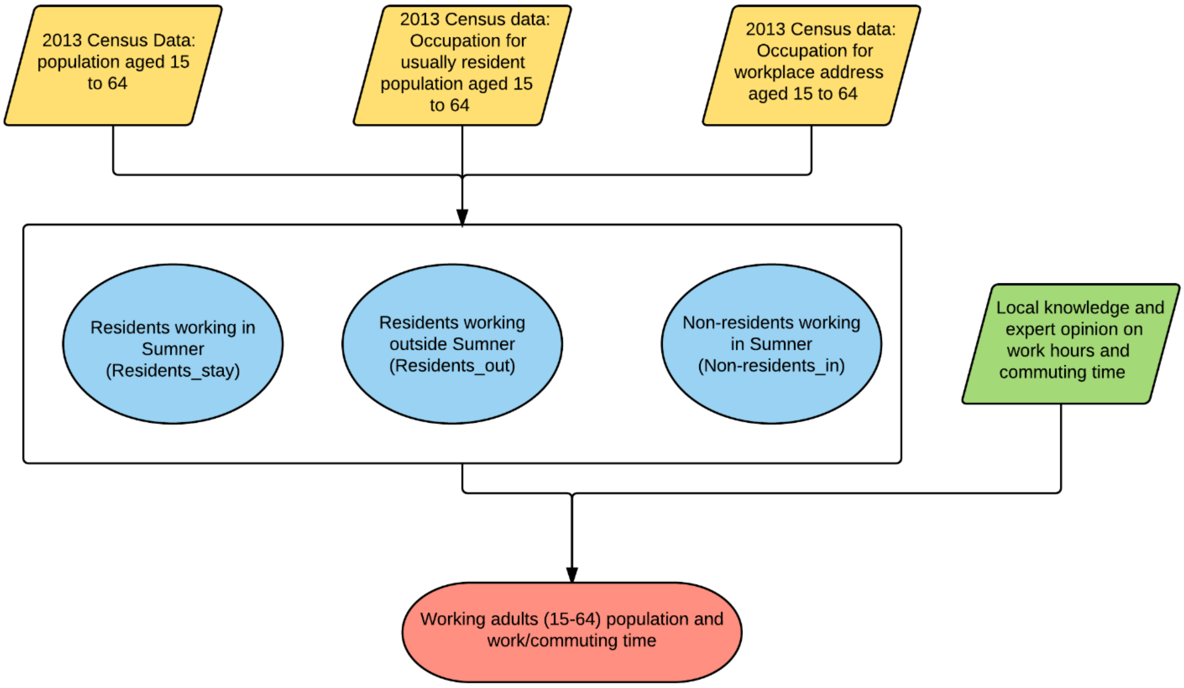

Figure 2.8. Flow chart for developing working adult group time profile.

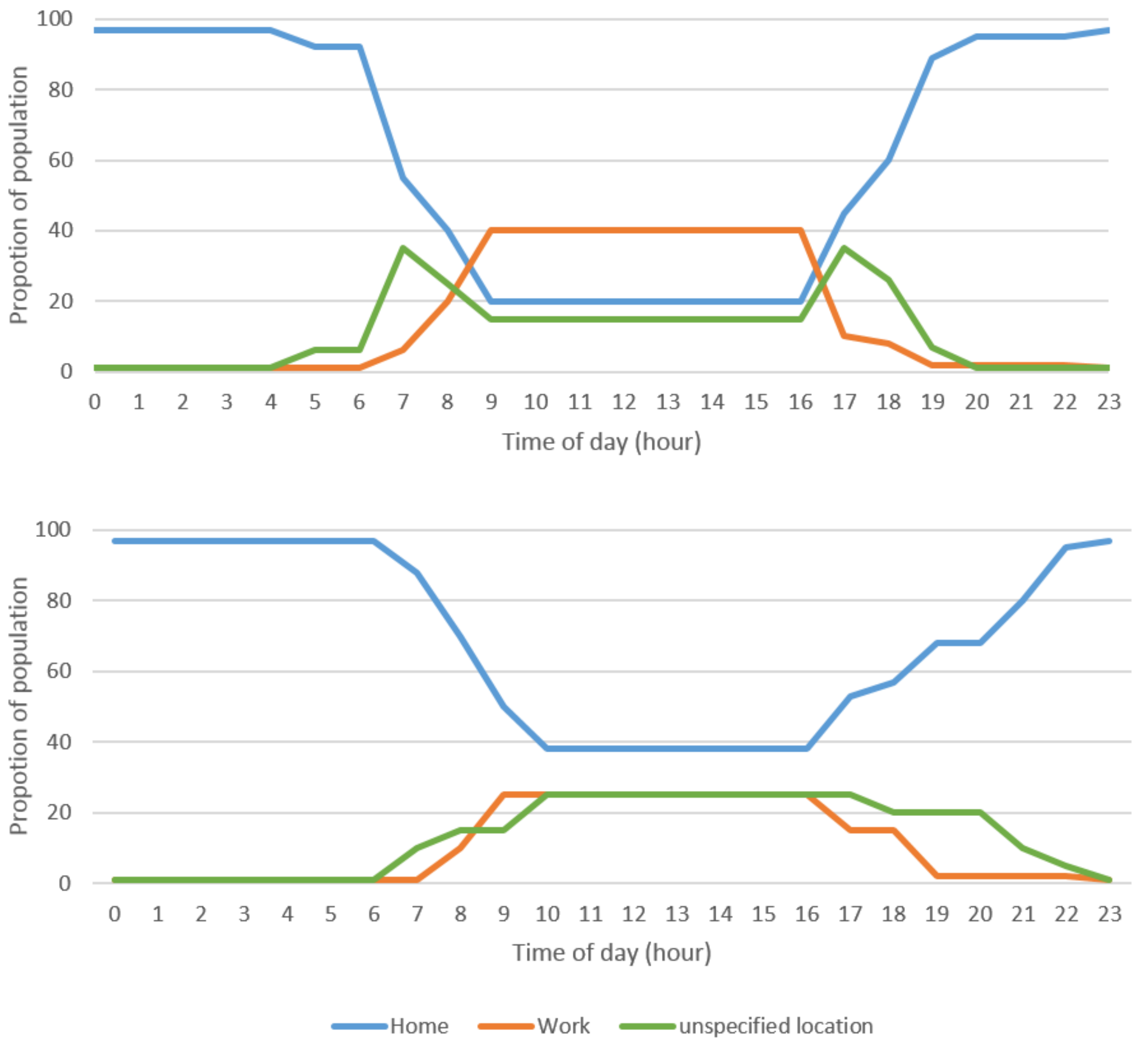

Figure 2.9. Time profiles for working adults; top – weekday; bottom – weekend.

2.3.2.1.d. Impaired people

Impaired people are assumed to be those people living in the Edith Cavell care facility and those that are Home-based (60 elderly people living at home, and in need of assistance), and 11 students in Van Ash Deaf School (under 13 years old). The Home-based group is assumed to be elderly (over 65 years old) and impaired adults (from 15 to 64 years old) (73 people). This number is estimated through unpaid work from household data (Statistics New Zealand, 2013), where 10% of people staying at home are looking after someone who is an ill/disabled. The number of the unpaid workers in households group is assumed to be in the unemployed group, and not in working group that accounts for 30% of the population from 15 to 54 years old.

The staff at Edith Cavell (60) and Van Ash Deaf School (50 on weekdays and 13 on weekends) are also considered to belong to the impaired people group as they are expected to assist these dependent people, and are assumed to have the same speed while evacuating. Of this group, 20% are assumed to commute into Sumner between 10:00 to 16:00, and 10% are assumed to be at unspecified locations at 09:00 and 17:00. The population of Van Ash Deaf School and Edith Cavell rest home are shown in Table 2.6. The resulting time profile graph for this group, and a flow chart for building the time profile are given in Figure 2.10 and Figure 2.11, respectively. Note that the time profile for this group for weekdays and weekends are the same.

Table 2.6. Population in Van Ash Deaf School and Edith Cavell rest home.

Name		Rolls/Residents	Time of day	Staff
Van Ash	Weekdays	11	02:00	13/3
			08:00	50
			12:00	50
			17:00	50
	Weekend	11	12:00	13/3
Edith Cavell	Weekdays	63	02:00	3
			08:00	13
			12:00	18
			17:00	12
	Weekend	63	12:00	14

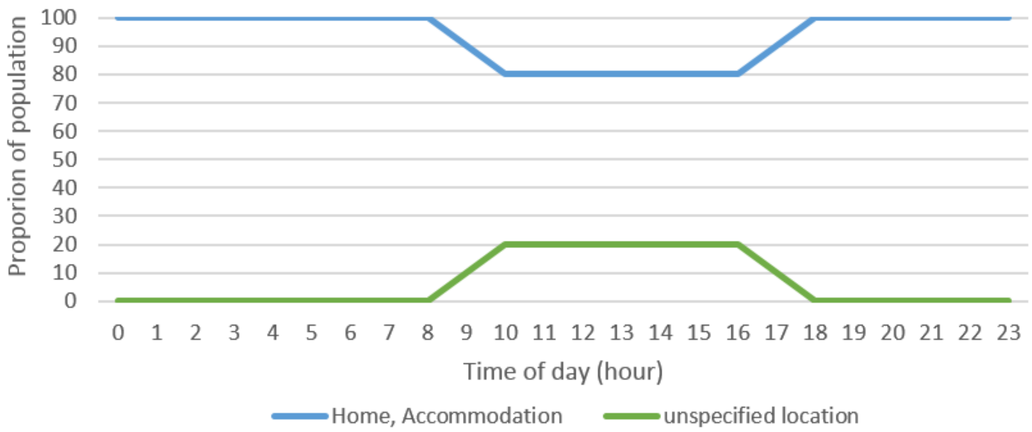

Figure 2.10. Time profile for the impaired people group.

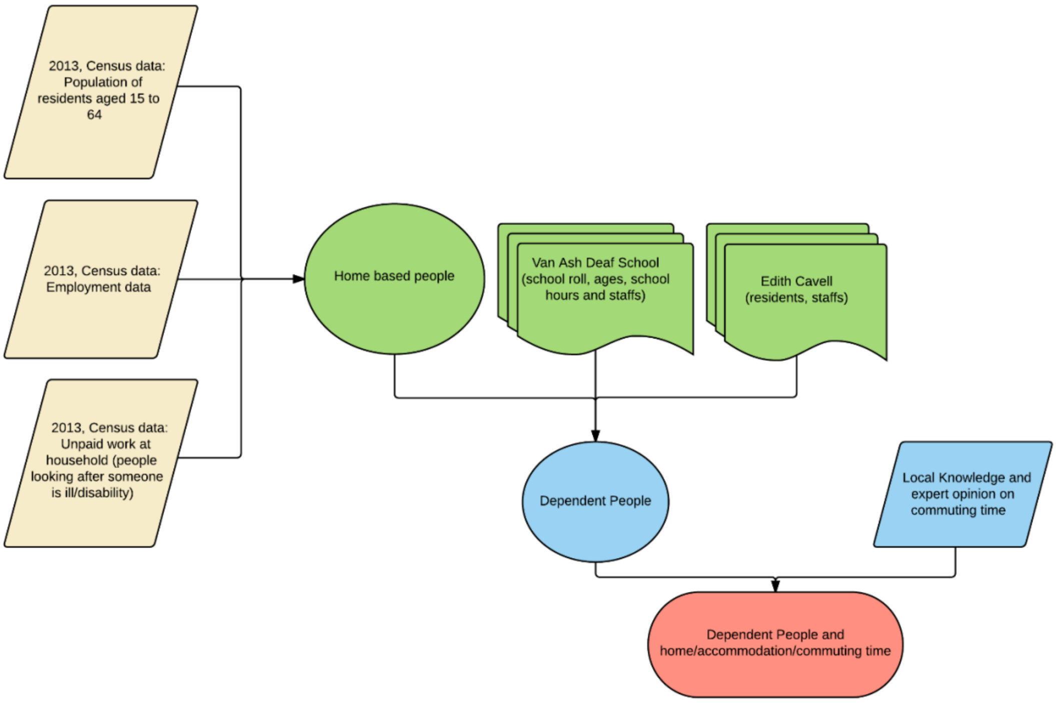

Figure 2.11. Flow chart for impaired people group's time profile graph.

2.3.2.1.e. Elderly Independent

The number of elderly independent people is calculated based on the number of people over 65 years old (Statistics New Zealand, 2013) subtracting the number of dependent living in Edith Cavell and Home based (Table 2.7).

Table 2.7: Population of impaired and elderly group.

Impaired	Edith Cavell	60
	Home based	68
Elderly over 65 (NZ Census, 2013)		528
Total Independent		400
Ratio Independent/Elderly over 65		0.76

The time profile for this group is shown in Figure 2.12 where the busiest commuting times are from 09:00 to 15:00 with 60% are at home and 40% are in unspecified locations. A flow chart explaining the process to develop time profile is shown in Figure 2.13.

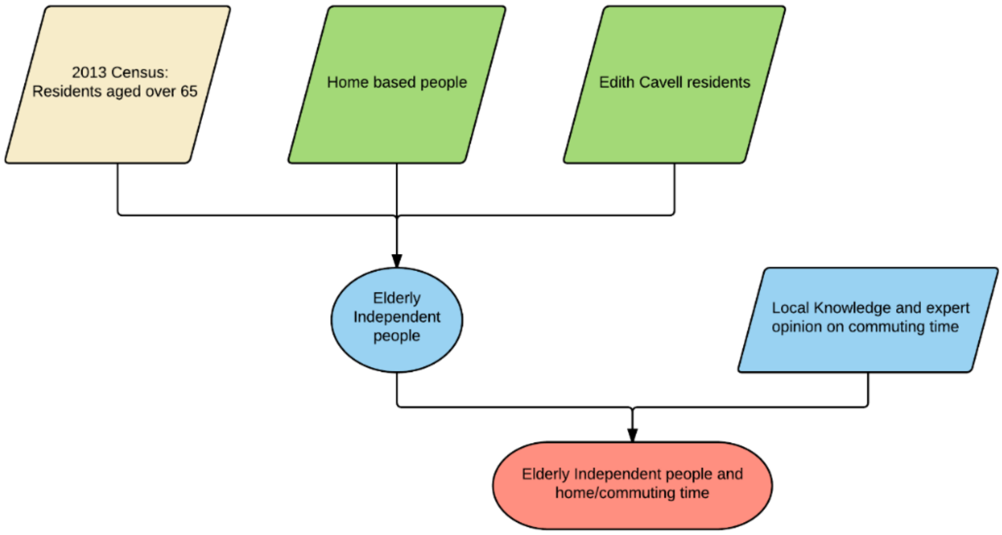

Figure 2.12. Flow chart for developing independent elderly group's time profile.

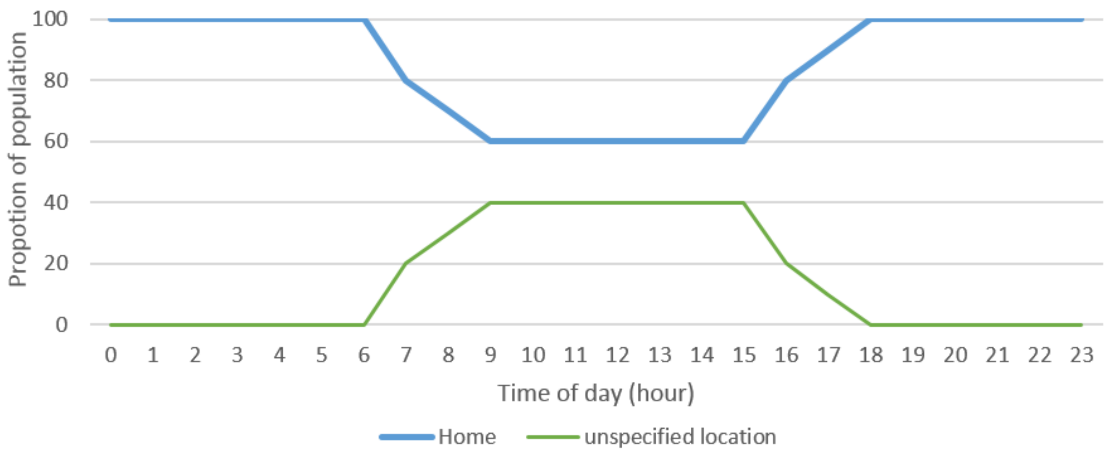

Figure 2.13. Time profile for independent elderly group.

2.3.2.1.f. Visitors

Based on the Census 2013 data for visitors to Christchurch, peak visitor season is in January and February (summer), lowest in June (winter) and mid-season is in October (spring). January is summer holidays for students, therefore they might travel with family away from Sumner. To estimate the highest population of both residents in Sumner and visitors, February is chosen as the peak season instead of January. Together with expert judgement and local knowledge, the number of visitors at the peak time (12:00) on a weekend in February is estimated to be approximately 10,000. The percentage of visitors arriving in Christchurch in June and October compared to February are 50% and 80%, respectively (Census data for visitors to Christchurch). Therefore, the number of visitors to Sumner in June and October are 5000, and 8000, respectively. In the absence of reliable information, it is assumed here that the number of visitors on weekdays is 2/3 of those in the weekend.

According to regional and Christchurch tourist data, 35% of visitors stay overnight and 11% of visitors stay in commercial accommodation (the other 24% of visitors are day visitors). There are two types of accommodation considered in this study; commercial and private accommodation. The former is commercial accommodation in Sumner (eight establishments), and the latter for this study are randomly selected residential buildings. Thus, at 02:00 11% of visitors are distributed to commercial accommodation, 23% of those are in private accommodation, and 1% are distributed to unspecified locations. Similarly, with other scenarios, the ratio between visitors in commercial and private accommodation is 1:2. Peak commuting time for this group is from 12:00 to 14:00, and they are located mainly near Sumner beach and business areas. Results for visitor numbers at different time scenarios are given in Table 2.8, and visitor distributions among different locations at nine time scenarios are given in Table 2.9. A flow chart and time profile for this group are given in Figure 2.15 and Figure 2.14, respectively.

Table 2.8. Population for visitors at different time scenarios

Season	**Month**	**Weekend**		**Weekday**	
		Over night	Peak time	Over night	Peak time
Peak	Feb	3500	10000	2333	6667
Low	Jun	1750	5000	1167	3333
Mid	Oct	2800	8000	1867	5333

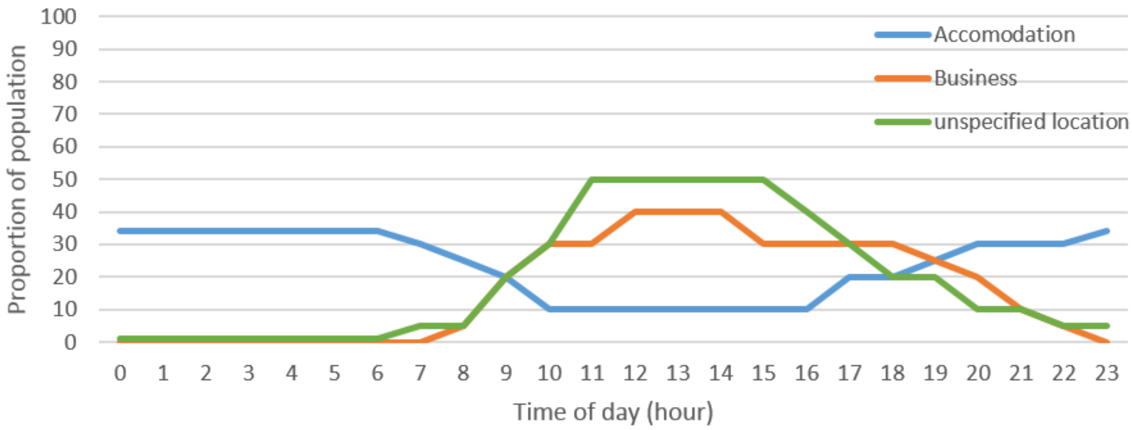

Figure 2.14. Time profile for the visitors group.

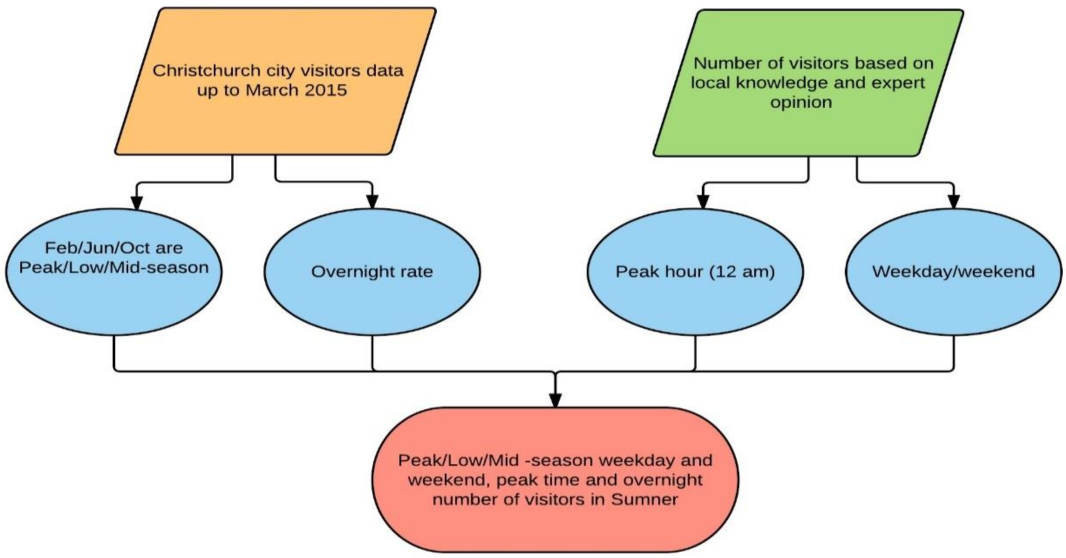

Figure 2.15. Flow chart for developing the visitors group's time profiles.

Table 2.9. Results of visitors' population at nine times scenarios (weekday 2:00, and weekend 12:00 for February, June, October).

Time scenarios	**Months (tourist seasons)**	**Accommodation**		**Business**	**Unspecified locations**
		Commercial	**Private**		
Weekday 02:00	Feb	257	537	0	23
	June	128	268	0	12
	Oct	205	429	0	19
Weekend 12:00	Feb	175	175	4000	5000
	June	88	88	2000	2500
	Oct	140	140	3200	4000
Weekday 08:00	Feb	556	1111	333	333
Weekday 12:00	Feb	222	445	2667	3334
Weekday 17:00	Feb	445	889	2000	2000

2.3.2.2. Population distribution model

In this section more details are presented on the method used to distribute the population groups into three location types: *home*, *work*, and *unspecified locations*. The first step for the population distribution model is to calculate the total number of people from different population groups in each meshblock for the nine time scenarios, at three location categories. This is achieved by using the proportion of each population group in each scenario from the previous Section 2.3.2.1 and presented in Appendix 3.

2.3.2.2.a. Home location distribution

The derived population of each meshblock from the step mentioned above is distributed to randomly selected residential buildings in that meshblock. This method for randomly distributing people in residential buildings has been used by (Fraser et al., 2014). However, to improve the accuracy of the model, two rules are applied as below:

- There are no more than five people at home;
- Dependent people (children under 5 and impaired people) need to be home with at least one working age adult.

These two assumptions are based on (1) real population census data where the proportion of household having six people is minor (1%), and (2) from expert opinion together with local knowledge, as in reality it would be unrealistic for children under five and impaired people to stay home alone without caregivers. These factors have not been taken into consideration in previous studies, and therefore makes this model better reflect a real life situation. While it is recognised that children around the ages of six to ten are also not likely to be home alone, it is not possible to determine the exact number of children at these ages staying home as Census 2013 does not specify this group's population. Home distributions for all of the age groups in February at 12:00 on a weekend day is shown in Figure 2.16. Results for all time scenarios are given in

Table 2.10.

Table 2.10. Home population distribution results for five residential groups throughout different time scenarios.

Time scenario	Under 5	From 5 to 14	From 15 to 64	Independent Elderly	Impaired people	Total population
Weekday 2:00	219	599	2322	550	74	3764
Weekday 8:00	164	0	958	385	74	1581
Weekday 12:00	164	0	479	330	59.2	1032
Weekday 17:00	164	447	1077	495	66.6	2250
Weekend 12:00	109	422	909	330	59.2	1830

Figure 2.16: Home population results for all residential groups in Sumner, February Weekday 12:00.

2.3.2.2.b. Work location distribution

Schools and rest home buildings

Populations assigned to schools and rest homes are based on the school rolls, residents, and staff according to the population time profiles developed above. Results are shown in Table 2.11, and an example of a map showing results of the scenario at 12:00 on a weekday is shown in Figure 2.17.

Table 2.11. Population in schools and rest home (staff are also counted).

Schools and Rest Home	Weekday 2:00	Weekday 8:00	Weekday 12:00	Weekday 17:00	Weekend 12:00
Sumner School	0	0	500	0	0
Our Lady Star of the Sea School	0	0	77	0	0
Pebbles School	0	61	61	61	0
Van Ash Deaf School	15	61	61	60	13
Red-cliffs school	0	0.0	238	0	0
Edith Cavell Rest home	66	76	68	69	64

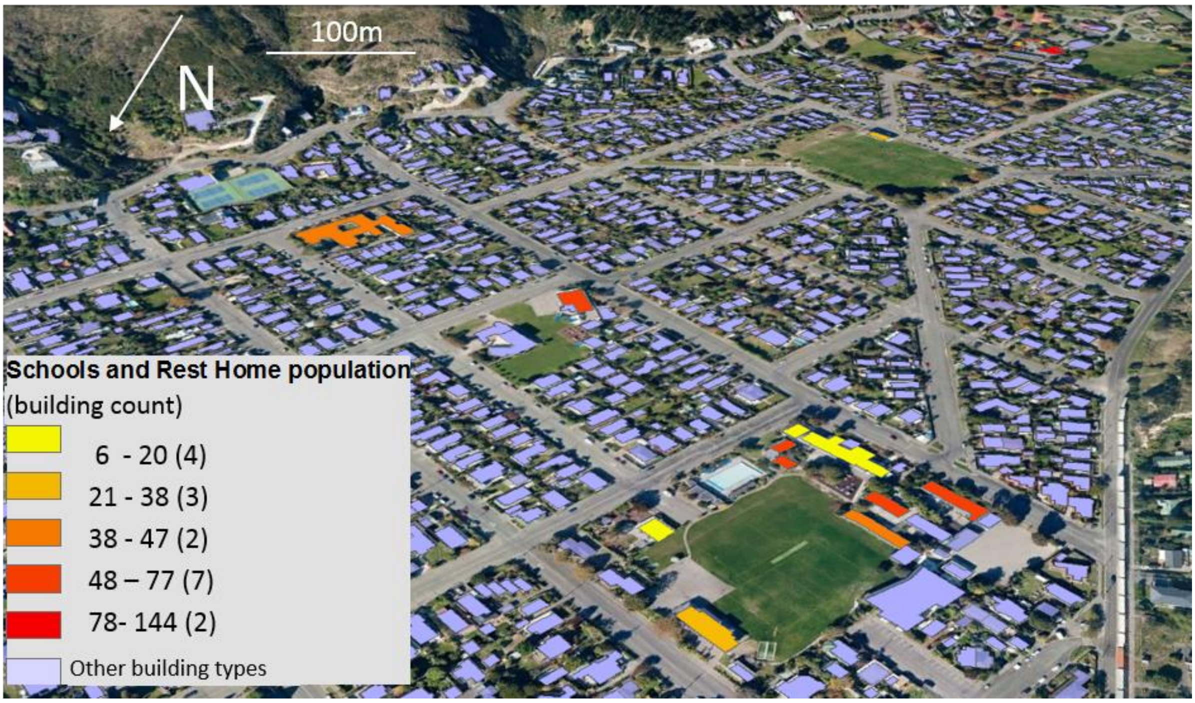

Figure 2.17: Schools and Rest Home population (staff included) in Sumner, February Weekday 12:00.

Remaining work buildings (commercial and community use buildings)

As it is not possible to determine the ages of the visitor group, these people are assumed to be in the same range of ages as the working age group, and therefore both groups will be distributed into the remaining work buildings, and later assigned *unimpaired adult* travel speed (more details in Section 2.3.2.3).

The total number of working age people (excluding number of staff in schools and rest home at the same time), and visitor groups in each meshblock at a given time scenario, are calculated based on results from the time profiles and then distributed to workplaces. This is achieved by assigning the population to commercial or community-use buildings according to their ratio of floor space in the cumulative floor space of all buildings. The maximum occupancy of the building is determined by using the building floor area (m^2) and required floor area per person. If the number of assigned people in the building is higher than its population capacity, those 'overflow' people will then be distributed in to unspecified locations (Section 2.3.2.2.c). The process to develop this approach is discussed below.

(Cousins, 2009), and (Fraser et al., 2014) defined different categories of use for buildings and their occupancy rates. People were distributed into those buildings in proportion to the available floor area based on these occupancy rates. These case studies (e.g. Cousins, 2009; Fraser et al., 2014) are from New Zealand (Hawkes Bay, and Napier), however when applying their method to Sumner, it gives unrealistic results. For example, the commercial category (e.g. shop, office, clinic – according to Cousins, (2009)) has occupancy rates of $60m^2$ per person during the daytime and $400m^2$ per person at night time. These two numbers are relatively high, and therefore out of total $22,707m^2$ floor area for all business buildings in Sumner, only 378 people (with the $60m^2$ per person case) are able to occupy these buildings. Therefore, from the perspective of this current study, a different and more realistic approach needs to be developed.

The International Building Code (IBC, 2006) provides the minimum required floor area per person for different occupancy types. (CBRE, 2012) also reported that the US's workspace ratios are similar to those in New Zealand (at around $15\text{-}16m^2$ per worker). (CBRE, 2012; IBC, 2006) and Christchurch Council standard requirements for restaurants/cafés (Christchurch City Council, 2016b), together with local knowledge, are used in this research to assess the assumptions regarding the number of occupants for different types of space. The occupancy load for different occupancy types used in this research are defined in Figure 2.18.

Table 2.12. Examples of results for work location distribution for working adults and visitors at 12:00 weekday in February are given in Figure 2.18.

Table 2.12. Occupancy type and load in IBC, 2006 and used this research.

Occupancy type (IBC, 2006)		**Occupancy load (m^2) (IBC, 2006)**	**Occupancy type in this research**	**Occupancy load estimated in this research (m^2)**
Business		9.29	Office	15
Dormitories		4.65	Accommodation	7.5
Exercise room		4.65	Community use -REC	7.5
Assembly without fixed seats*	Table and chai	1.39	Restaurant, shops	3
	Chair only (not fixed)	0.64	Community Centre, Church	1.4

Note that Sumner's cinema can seat 337 patrons in total (Hollywood 3, 2015), therefore its maximum capacity is simply assumed to be this number.

People at workplaces in the working age group are assigned into this location category first, then those in the visitor group are allocated to accommodation/business buildings until the maximum occupancy of the buildings is satisfied. The remaining visitors in workplaces are distributed in the next type of location – *unspecified locations* (Section 2.3.2.2.c).

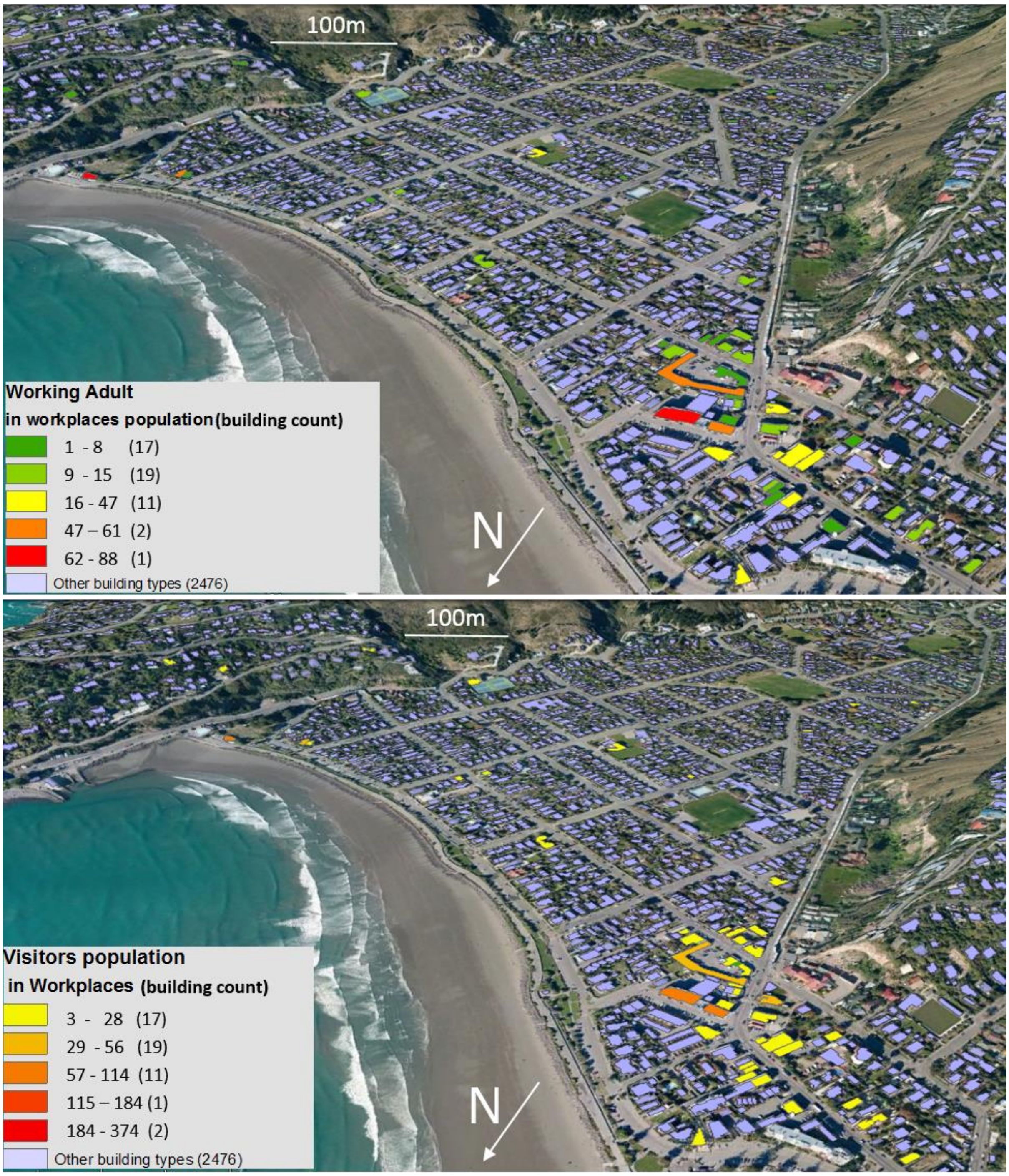

Figure 2.18: Workplaces population in Sumner, February Weekday 12:00; top – working adult population; below – visitors population.

2.3.2.2.c. Unspecified locations

Unspecified locations are defined as roads and open spaces including Sumner Beach, the Esplanade Beach, Taylor's Mistake Beach, and St. Leonard Park. Before assigning the population into *unspecified location*, the number of 'overflow' working age adults and visitor groups, described in the in the previous section (Section 2.3.2.2.b), was subtracted from the total number of those two population groups at a given time. Results of the subtraction are then allocated into the unspecified location category.

For assigning populations to unspecified locations, the number of assigned people in each category are weighted based on these following criteria:

- Popular/Busy levels, with proportions of roads and open spaces shown in Table 2.13.
- Area: All other roads are then weighted based on area - larger areas are weighted more heavily for assigned numbers.

Table 2.13. Unspecified locations types and their weighted ratio.

Types		**Weighted based on activity level (%)**
Open spaces	Sumner Beach	35
	Esplanade Beach	45
	Taylor Mistake Beach	15
	Leonard Park	5
Roads	The Esplanade	15
	Wiggins St	10
	Nayland St	10
	Head St	6.5
	Menzies St	6.5
	Hardwicke St	6.5
	Stoke St	6.5
	Wakefield Ave	6.5
	Marriner St	6.5
	All other roads	26

An example of results for distributing population to *unspecified locations* for the visitor group, for a February weekend at 12:00 time scenario, is shown in Figure 2.19. For details on road locations see Appendix C1.

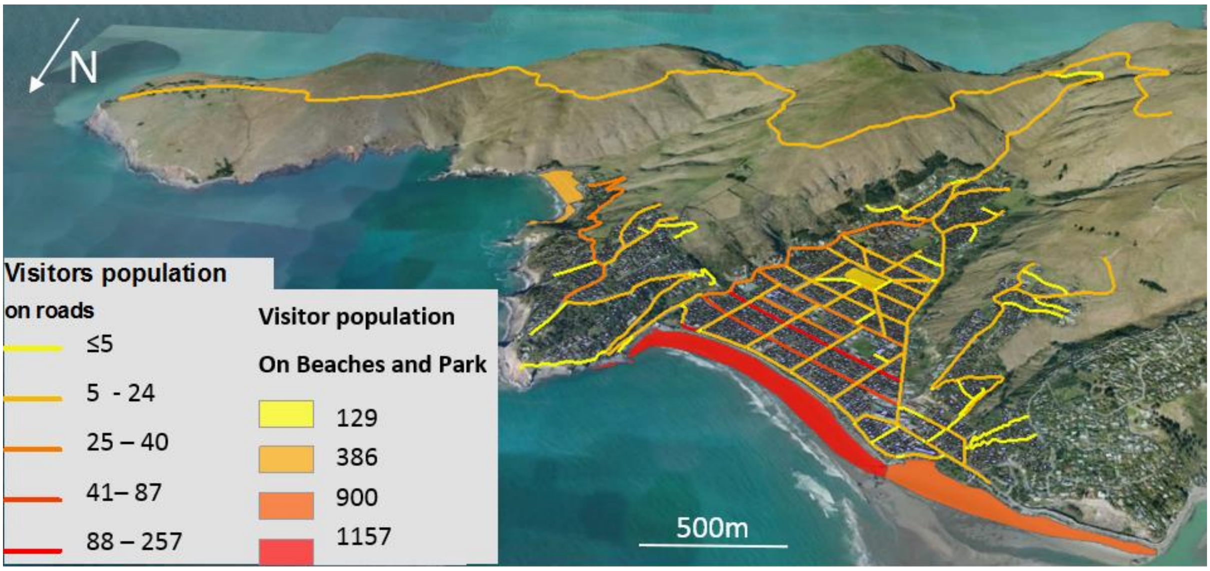

Figure 2.19. Visitor's population allocated into unspecified locations, February Weekday 12:00.

2.3.2.3. Speed distribution model

Speed considered in this study includes two types: walking speeds for pedestrians and vehicle speeds. Vehicle speeds are assumed to be the common limited speed in Sumner which is 50 km/hr. Walking speeds distributed amongst the population modelled above are defined as five travel speed groups: *Elderly, Child, Adult Impaired, Adult unimpaired,* and *Running* (Table 2.14). These speed groups are based on (Fraser et al., 2014) who developed these walking speed groups from other literature (e.g. Chooramun et al., 2012; Knoblauch et al., 1996; Liu et al. 2006; Liu et al., 2009; Mas et al., 2012; Park et al., 2012; Post et al., 2009; Revi & Singh, 2007; Sugimoto et al. 2003; Wood & Schmidtlein, 2012). Most published studies have only applied a fixed speed for their evacuation models, while the approach (Fraser et al., 2014) proposed enables the model to capture the variability in walking speeds. The motivation for the detailed population distributions (Section 2.3.2.2) is to identify how many people need to evacuate, and to determine how long that person takes to evacuate, which depends significantly on the person's travel speed. Therefore, by assigning different travel speeds to each population group, the mobility of the population is effectively characterised.

When assigning speeds to population groups, one important factor that is taken into account in this study is group evacuation. A large body of research over the past decade, which mainly focus on casualty research and models, has addressed this topic, with a focus on difficulties experienced during evacuation for people with small children and group evacuation of families or schools (Charnkol & Tanaboriboon, 2006b; Koshimura et al., 2006; MacDonald, 2005; Phillips & Morrow, 2007; Rees et al., 2005; Wilmot & Mei, 2004; Yeh, 2010). However, work is required to translate the empirical information contained in the literature into useful and practical measures of evacuation in different scenarios. (Fraser et al., 2014) classified all people distributed in schools with *child* travel speeds, with the expectation of school class groups evacuating together in the event of a tsunami. In this study, the approach is extended to address both education locations and other location types. The rules applied in the speed distribution model are:

- For a building with only one person, the assigned speed is the speed of the population group that the person belongs to;

- For a building with two or more people, the speed assigned is that of the slowest population group that an individual belongs to.

Note that these rules are only applied for building type locations. For unspecified locations people are assumed to evacuate separately regardless of whether those people are with or without company. Results of the speed distributions for home locations for February weekdays at 12:00 are presented in Figure 2.20.

Table 2.14. Speed distribution (m/s) for different population groups compiled from (from Fraser et al., 2014).

Level	Elderly	Child	Adult Impaired	Adult unimpaired	Running
Min	0.21	0.56	0.58	0.88	1.79
Max	1.3	2.1	1.07	2.8	3.83
Average	0.9	1.29	0.87	1.43	2.77

Figure 2.20: Average speed distribution at residential locations for all population groups, February weekday 12:00.

2.3.2.4. Vehicle distribution model

In this study, vehicle distributions are developed based on the population model (Section 2.3.2.2) together with census data regarding the number of vehicles per household (Statistics New Zealand, 2013), and several assumptions outlined below.

For consistency and to ensure the high spatio-temporal resolution of the model, vehicles are also assigned into three type of locations: *home, work* and *unspecified locations.* Definitions for each location are kept the same – which means each location represents where the 'object' is located corresponding to their activities. However, the vehicle location descriptions are adjusted to make them more appropriate for assigning to vehicles (Table 2.15).

In this study, each car parking space is defined as 2 x 5 metres; the average size of parking spaces in car parks. However, this may be an over simplification as there are differences in sizes of parking spaces, especially parallel parks on the streets. Furthermore, it is also very difficult to account for areas where cars are not allowed to park in the model (e.g. in front of driveways). Available car park capacity in Sumner is given in Table 2.16.

Table 2.15. Location's types, descriptions, and example snapshots for vehicle distribution.

Location types	**Locations descriptions**	**Example snapshots (taken from Google Earth, 2016)**
Home	In driveways around residential buildings	
Work	Car parks surrounding commercial buildings	
Unspecified location	• Car parks on Esplanade road • Car parks for Sumner and Taylors Mistake beaches • Car parks on roads	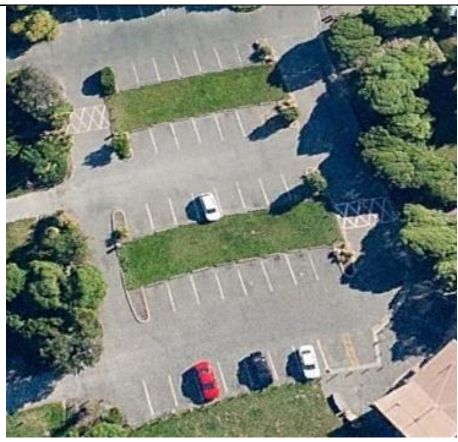

While distributing cars on roads, roads less than 8 metres wide will only have parking on one side whereas roads greater than 8 metres will have parking on both sides. Furthermore, some parts of roads with steep slopes and hairpin turns do not allow cars to be parked. Based on the car parking space, width requirements and the no car parking rule, car-capacity is calculated for each road, and total car capacity on roads in the study area is estimated as 9757 cars.

Table 2.16. Available car park capacity in Sumner.

Car park locations	Capacity (number of cars)
Esplanade	431
Sumner beach	56
Taylor Mistake beach	49
Sumner Shopping mall	42
On Nayland St	16
Sumner Coffee Culture	19
Tart Cafes and Deli	26
DotCom Café	11
Cave rock	23
Sumner Bay	15
Joe Garage	20
Sumner Primary school	23
Van Ash School	20
Accommodation	6
Total	**747**

In addition to car capacity requirements, when distributing vehicles into each location category, several rules are applied as follows:

Home

With the *Home* category, a vehicle is only assigned to houses with at least one working age adult or (unimpaired) elderly person. Given that no more than five people have been distributed to each house (Section 2.3.2.2.a), it is assumed here that one car per household will suffice for evacuation; this will inform the vehicle evacuation model (Section 3.3.4).

Work and Unspecified locations

People over 15 years old located in *work* and *unspecified locations* are assigned with one vehicle per person, while the visitor group are assigned with the ratio of five people per vehicle, assuming people travel to Sumner mostly with friends or family. This is subjectively assigned based on local knowledge and experiences. It is acknowledged that many visitors might travel alone or as a couple (the number of people ranges from 1 to 4 per car), meaning the actual number of visitors' vehicles might be higher. However, as non-residents working in Sumner and visitors might travel to Sumner by other means (e.g. bus, or bike), the assumptions for number of assigned private vehicles in this study are therefore reasonable.

Cars for these groups are allocated into available car parks first, the remaining cars are then distributed onto roads following the abovementioned rules for pedestrians. Results for vehicle distribution with different locations on a February weekday at 17:00 is given in Figure 2.21.

Several network analysis studies have addressed vehicle distributions, although at highly aggregated spatio-temporal resolutions (Cova & Church, 1997; Dewi, 2012; Franzese & Liu, 2008; Lindell & Prater, 2007; Southworth, 1991; Tomsen et al., 2014; Urbanik, 1979). Thus, this current study marks the first attempt at vehicle distribution with a higher spatial-temporal resolution, and more importantly incorporates vehicle distribution into the population distribution model, to help future work produce a more realistic mixed vehicle model.

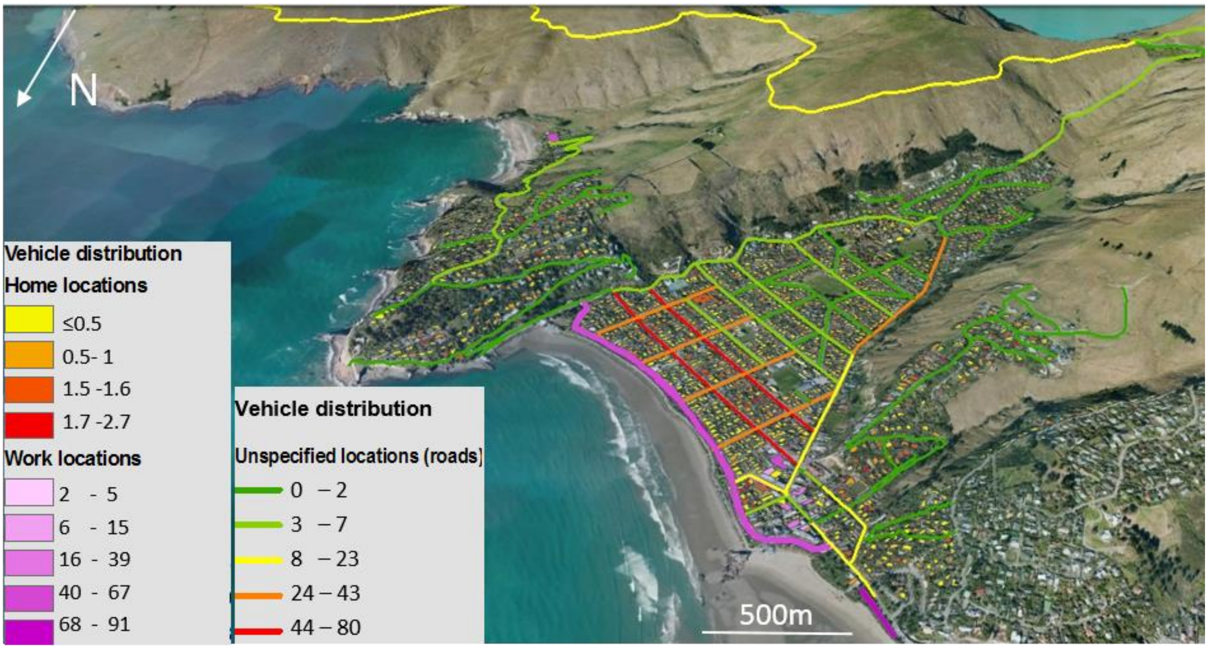

Figure 2.21. Vehicle distribution at car parks, roads and at home, February weekday 17:00 scenario (scale of 1:10000).

2.4. Summary and link to the next chapter

This chapter presented methods modelling spatio-temporal distributions of different population groups, their relevant speeds, and private vehicles in Sumner. The methods address the spatio-temporal variation based on the dynamics of daily human activity. The results of the distribution models are the inputs for evacuation models employed in Chapter 3.

Chapter 3

Evacuation models for Sumner

Contents

3.1. Introduction

This chapter presents a tsunami evacuation model for Sumner, Christchurch. This model is intended to contribute toward tsunami risk assessment and evacuation planning for Sumner, as outlined in the thesis objectives (see Section 1.2). The chapter firstly presents an overview of relevant tsunami evacuation model literature (Section 3.2) to identify evacuation modelling approaches to be applied to Sumner. Secondly, the chapter presents how 'Least Cost Path Distance' analysis is applied for tsunami evacuation models in Sumner for both pedestrians and vehicles, and presents visualisations of evacuations times. Also presented here is a preliminary test of the pedestrian model using a real-life subject (Section 3.3). Finally, Section 3.4 summarises this chapter and links to the next.

3.2. Review of tsunami evacuation model literature

Although tsunami evacuation drills are important for at risk communities to be prepared for such disasters, they are very difficult to carry out (Anh et al., 2012). Thus, evacuation modelling is carried out to identify optimal evacuation routes and the time needed for the at risk population to evacuate so as to minimize the number of casualties (González Riancho et al., 2013).

A brief overview of tsunami evacuation models is covered in this Section, with an emphasis on the two most common approaches; agent-based models and the Least Cost Path Distance model (Section 3.2.1). The Least Cost Path Distance analysis method is identified as most appropriate for this study and its application to Sumner is described here. Section 3.2.2 compares Least Cost Distance isotropic and anisotropic approaches, and presents the rationale for applying the latter in this research.

3.2.1. Tsunami evacuation modelling literature

Since 1970, studies of evacuation modelling from around the world have flourished in various disciplines, starting with works focused on hurricane evacuation (Tomsen, 2010). In comparison to other types of hazards such as floods, hurricanes, nuclear disasters and structure fires, relatively little attention has been given to tsunami evacuation until 2004 (Tomsen, 2010). However, since the 2004 Indian Ocean tsunami and the associated massive loss of life and property damage, tsunami evacuation research has substantially improved to support tsunami preparedness and education efforts (Wood & Schmidtlein, 2012). There have been several approaches applied to tsunami evacuation models, mainly the following: genetic algorithms (GAs) (Park et al., 2012); distinct or discrete element methods (DEMs) (Abustan, 2013); system dynamic approaches (Kietpawan, 2008; Simonovic & Ahmad, 2005); agent based models (ABM); and Geography Information System (GIS) analyses, in particular the Least Cost Distance (LCD). The advantages and disadvantages of GAs, DEMs, and system dynamic approaches are discussed extensively in (Mas et al., 2015). Here, the two most common approaches in tsunami evacuation modelling, ABMs and LCD, are reviewed. This Section does not provide an extensive review of all models available, as it is beyond the scope of the study; the rationale for focusing on the LCD approach is described below.

The use of both ABM (Affan et al., 2012; Anh et al., 2012; Charnkol & Tanaboriboon, 2006a; Imamura et al., 2012; Johnston, 2013; Mas et al., 2012; Yeh, 2014) and LCD (Fraser et al., 2014; Riancho et al., 2013; Graehl & Dengler, 2008; Laghi et al. 2006; Post et al., 2009; Scheer et al., 2012; Wood & Schmidtlein, 2012, 2013) approaches has been increasing in tsunami evacuation studies. In the context of tsunami evacuation, modellers use ABM to simulate the action and interaction of autonomous agents (both individuals and organisations/groups) within a system. Agents with sets of characteristics (determined physically or experimentally) follow particular rules according to their roles within the system to determine evacuation actions (and efficiency of the actions) they will likely take in the event of tsunami (Anh et al., 2012; Mas et al., 2015). Least Cost Distance analysis, a GIS-based method, focuses on characteristics of the evacuation landscape, such as slope and land cover, to calculate the most efficient path or minimum cost of travel (expended energy or time) to safety from every location in a hazard zone. The cost surface, which represents the difficulty of travelling through each location, is defined based on static landscape characteristics (e.g. slope and land cover) (Wood & Schmidtlein, 2012).

ABMs potentially provide great flexibility in that they can be used with both theoretical and empirical data, and is aim to simulate disaster emergency evacuations (Manson et al., 2012; Mas et al., 2012; Munadi et al., 2012). However, this method is computationally expensive and the time taken for each simulation is a major disadvantage (Anh et al., 2012; Wood & Schmidtlein, 2012; O'Sullivan, 2012). Furthermore, to inform assumptions within the ABMs, prior knowledge about the influence of personal characteristics and experience on likely behaviours is essential. This is a level of data that, to date, is still difficult to constrain for tsunami evacuation studies, especially for New Zealand (Fraser et al., 2014) because although there is a significant tsunami risk there is limited first-hand experience (NZEIR, 2015). In addition, most of the ABMs only account for evacuating on roads, which in reality is not always the case, especially for pedestrians who might choose different routes to evacuate rather than roads, or their starting locations are not on the roads (beaches, open parks/other recreation areas).

Therefore, in this research, LCD model is chosen to generate an aggregate view of evacuation, focusing on understanding the spatial distribution of evacuation times. However, it is recognised that the micro-scale phenomena captured by ABMs (Johnston, 2013) could be incorporated within future LCD models, which will be well suited to tracking the complexity and diversity of behaviours that underpin dynamic changes (Mas et al., 2015). Hence, applying a mixed-methods approach could be ideal in future for modelling the complexity of emergent phenomena through agent interactions over space and time (Wood & Schmidtlein, 2012). In future studies ABMs could be applied to investigate the influence of evacuation behaviour on aggregate evacuation outcomes.

3.2.2. Least Cost Distance model literature

There are various ways to develop LCD models to examine evacuations, from simple models based solely on horizontal distances between hazard and safety zones, to more complex models that incorporate variable effects of land cover and terrain. The two most common LCD approaches are: (1) an isotropic approach that incorporates land-cover conditions and vertical slope characteristics (slope angle) to accommodate travel outside of the road network; and (2) an anisotropic approach that incorporates land-cover condition and slope, but additionally takes into account slope directionality (e.g. uphill and downhill movements). Within the ArcGIS platform, the former approach uses the Cost Distance tool (ArcGIS, 2009b) while the latter uses the Path Distance tool (ArcGIS, 2009a). An overview of these two approaches will be given in this Section, providing the rationale for applying the anisotropic in preference to the isotropic approach used in this present research.

Both of these approaches are based on the development of a spatial matrix of cells where each cell contains a value representing the difficulty, or cost, of movement across a landscape. Differences in land cover (e.g. roads, light/heavy shrub-land, sand, open water) and slope characteristics (e.g. slope angle) are taken into account in these two approaches, when examining the cost distance surface, and in the end suggest a *least cost path*, i.e. the most efficient path. In addition, to determine whether individuals could evacuate from an area before tsunami waves arrive, travel speed values can be applied to the cost distance surface to generate a time surface which represents the time to travel from source to destination. Even though these two approaches both determine the minimum accumulative travel cost from a source to each cell location on a raster, an *anisotropic approach* accounts for the impact of slope directionality (uphill versus downhill) on travel costs while the *isotropic approach* does not. This means that the anisotropic approach is a better measure of actual distance that must be travelled.

Isotropic approaches have been applied in previous tsunami studies (Riancho et al., 2013; Graehl & Dengler, 2008; Laghi et al., 2006; Post et al., 2009; S. J. Scheer et al., 2012) and flooding (Freire et al., 2012) evacuation models. (Post et al., 2009) increased complexity of LCD analysis by including critical facilities and evacuee density as modifiers of travel cost. Extending Post et al.'s (2009) methodology, Freire et al. (2012) developed isotropic methods for flood evacuation modelling based on a LCD approach, but also included an assumption that it would take one minute to climb or descend each storey while during vertical evacuation in higher buildings. Although improvements to isotropic approaches have been proposed, this approach is still inferior to anisotropic approaches (Wood & Schmidtlein, 2012). After determining the influences of different LCD models on tsunami evacuation potential and testing their sensitivities to elevation and land cover data, (Wood & Schmidtlein, 2012) concluded that an anisotropic approach provides the most realistic representation of an actual pedestrian evacuation.

Following Wood & Schmidtlein (2012), Schmidtlein & Wood (2015), Wood & Schmidtlein (2013) and Fraser et al. (2014) also applied anisotropic path distance approaches to their tsunami evacuation models for pedestrians. Fraser et al. (2014) introduced the most comprehensive method by using variable spatio-temporal population distributions of different population groups to determine dynamic travel speeds. This approach better reflects evacuee behaviour in a real evacuation event, and thus is applied to the pedestrian evacuation model in this present research (Section 3.3.2). From now on, anisotropic approach is referred as LCD in this research. Furthermore, as discussed in Chapter 2, for a far field tsunami scenario that allows longer time to prepare and evacuate, vehicles are most likely used for evacuation. Therefore, a new method has also been developed to model vehicle evacuation (Section 3.3.3).

3.3. Method and results of evacuation models

In this section, the steps implemented in the LCD method and results of the Sumner tsunami evacuation models are described. First, an overview of LCD analysis is introduced with basic concepts of accumulative grid cell calculation, the path distance formula and its required parameters/inputs (Section 3.3.1). Second, details of the method applied in Sumner and results for each model are given (Sections 3.3.2 and 3.3.3).

The LCD method is applied here for three Sumner evacuation scenarios:

1. Pedestrian evacuation (people evacuating on foot) (Section 3.3.2)
    a. all people evacuate to higher elevation ground;
    b. all people evacuate to a bus stop.
2. Vehicle evacuation where all people use private vehicles to evacuate out of the inundation area (Section 3.3.3).

By using these three scenarios, this study covers all possible end-member options for people evacuating out of the hazard zone, accounting for people evacuate by foot, by using public transportation, and by using private vehicle. It is acknowledged that the assumption of 100% compliance rate, and 100% of people choosing one particular means to evacuate in each scenario, might not be realistic as people's real-world decisions will differ. Nevertheless, results from these models are still useful for decision makers in evacuation planning, and establish a key foundation to enable future research in this field.

3.3.1. Overview of the Least Cost Path Distance Method

This section explains the basis of the path distance tool, including how travel cost is accumulated between cells, the mathematics of how path distance is calculated, the determination of input parameters, and how these act as inputs for the LCD models.

3.3.1.1. Understanding how the path distance tool works

3.3.1.1.a. Node Travel Cost

The path distance tools create a total accumulative cost distance raster, in which each cell is assigned the minimum accumulative cost distance between a specified source and destination cell. Nodes and links represent each cell and the connections from it to neighbouring nodes respectively. Spatial orientation of the nodes, and how the cells are connected, determine the cost to travel from one node to the next. Different types of node travel costs and how they calculated are presented in Figure 1.1Figure 3.1.

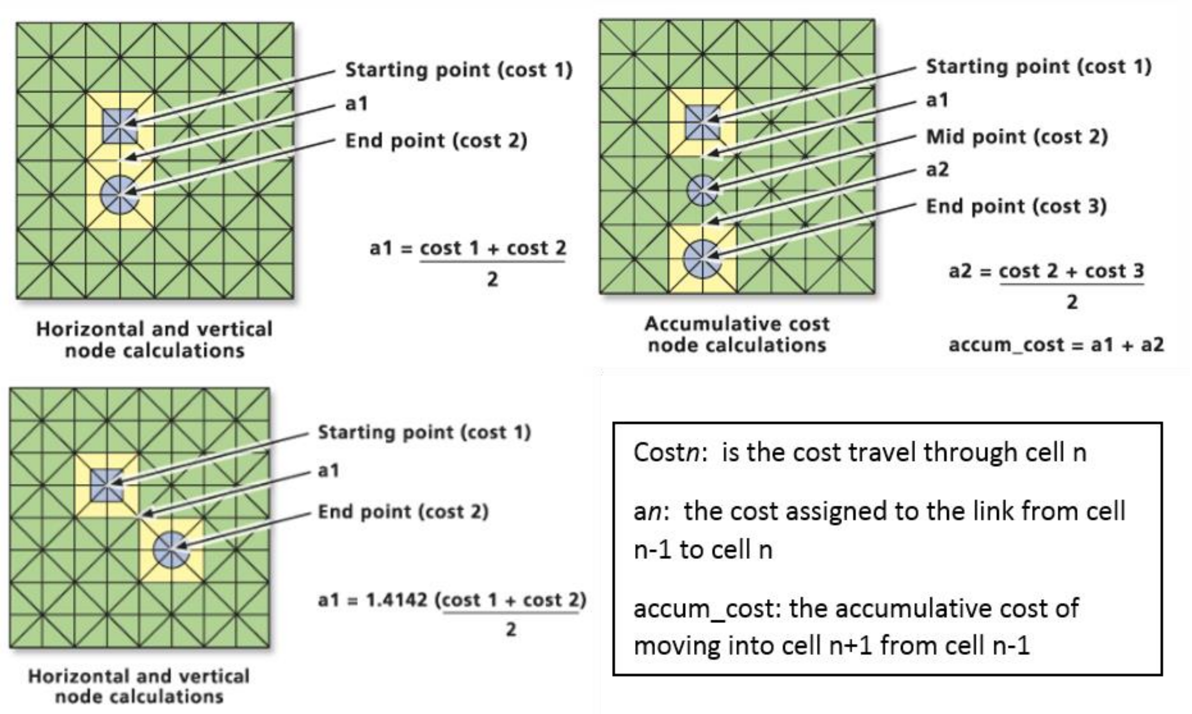

Figure 3.1. Travel node cost for three different cases. Top-left - adjacent node cost when moving from one cell to one of its four directly connected neighbours; top-right – accumulative perpendicular cost when moving from one cell, passing through other cells before arriving in the end cell; bottom-left – diagonal node cost when the movement is diagonal (1.4142 is approximately the square root of 2) (ArcGIS, 2009a).

3.3.1.1.b. Accumulative Cost distance raster

An accumulative cost-distance raster is created by identifying the source cell and then the cost to travel to each neighbour cell. Those neighbour cells are listed from least to most costly, and the least accumulative cost to each of the neighbours is identified. This process is repeated until all cells on the raster have been assigned an accumulative cost (Figure 3.2).

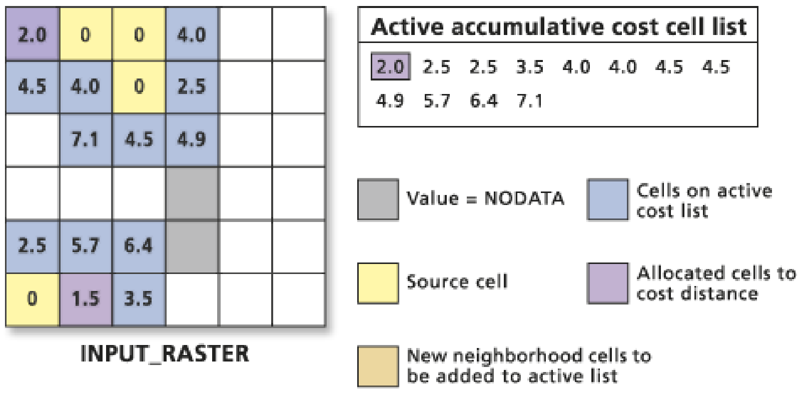

Figure 3.2. Accumulative cost cell list (ArcGIS, 2009a).

3.3.1.2. Inputs for Path Distance tools

3.3.1.2.a. Path distance formula

The cost distance in LCD involves multiplying the cost surface, surface distance, horizontal and vertical factors. All of these components account for factors that influence the total cost or difficulty of moving from one cell to another. In this study, the effect of the horizontal factor (e.g. wind speed) is ignored as it beyond the scope of this research. Figure 3.3 shows the model structure of the LCD approach applied in this study, and the inputs for each parameter in the path distance formula.

The two main outputs in the LCD model are the Least Cost Path and the Least Evacuation Time surfaces. A Least Cost Path Surface is the set of cells containing 'cost value', and those cells connect together to make a 'path'. This is the path which connects between the Origin points within the hazard zone to its 'preferred' Destination points within the safe zones. The main inputs to produce the raster layer Least Cost Path include: Land cover layer, 5 metre Digital Elevation Model (DEM) (Canterbury Geotechnical Database, 2015), Origin and Destination points. Each least cost path raster was converted to polyline to calculate the length of the path. The result of the Speed Conservation Value (SCV) for slope and land are the average values of all the SCVs collected (using the ArcMap Sample tool) from all the cells that the path runs through. These two average SCVs surfaces are multiplied together to get the mean SCV of the path – or the Travel base rate. This travel base rate is multiplied with the walking speeds determined by demographics and physical ability (assigned to each of the Origin points, generated from the Speed distribution models in Section 2.3.2.3), to obtain the travel speed. Finally, the inverse travel speed is multiplied with the path length to obtain the Least Evacuation Time. Details of each parameter are discussed in turn below.

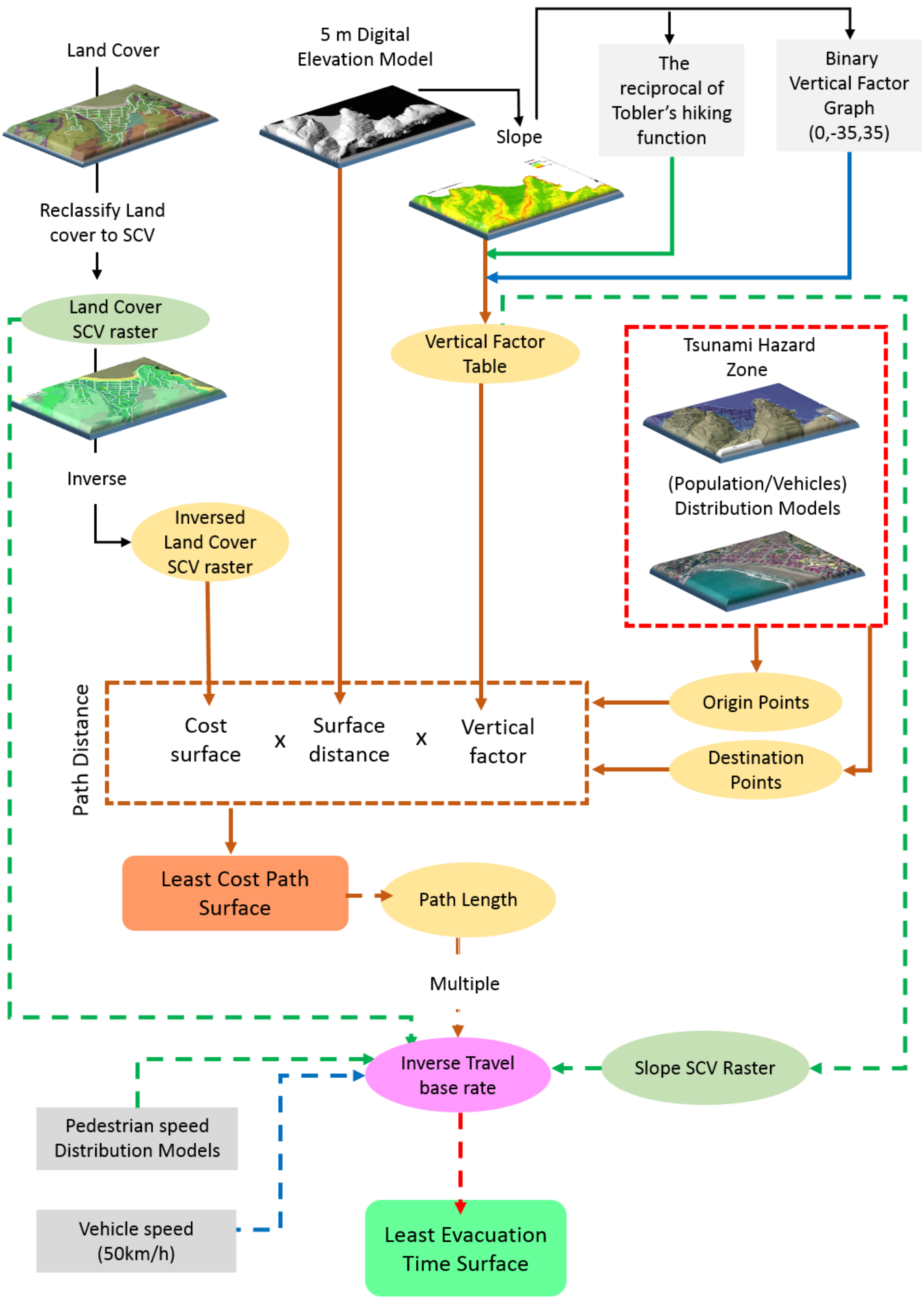

Figure 3.3. Diagram of the Least Cost Path Distance approach applied in this study. Dashed arrows represents processes implemented after calculating Least Cost Path Surface. Green and blue dashed arrows represent processes in pedestrian and vehicle models, respectively. The process from the red dashed box to the brown dashed box is presented in more detail in Figure 3.7. SCV stands for Slope Conservation Value.

3.3.1.2.b. Cost Surface and Speed Conservation value

In this study, the cost surface consists of a regular two-dimensional grid where each cell value represents the cost to travel through it depending on costs introduced by land cover and slope. In terms of tsunami evacuation, the cost surface is effectively a measure of travel time (evacuation time) needed to travel to a safe area.

The cost surface is an inverse speed raster determining the time needed for travelling through a particular path, and depends on the raster spatial resolution, distance and land cover. For example, it is more costly to travel through heavy bush rather than along concrete roads, and thus heavy bush will be assigned a higher cost when reclassifying the dataset. Therefore, each land cover's cost must be quantified such that it can be used to calculate speed and travel time for each path generated from the LCD model.

The relationship between slope and speed also needs to be considered. However, the raw numerical value of the slope cannot be equated with the cost of overcoming that slope. For example, it may seem reasonable that the cost of overcoming a zero degree slope is zero, but it is not necessarily reasonable to say that overcoming a two degree slope is twice as difficult as overcoming a one degree slope. Therefore, the numerical value of slope (dh/dx or degrees) must be transformed to a cost (Pingel, 2010).

Speed conservation values (SCV) have been utilsed to represent the percentage of maximum travel speeds that would occur on a given land cover or slope. For example, if the maximum speed for pedestrians/vehicles is assumed to be on roads, the SCV will be 1 (100% of the maximum speed) and any other types of land cover surface would be some lower number. This approach was first introduced by (Wood & Schmidtlein, 2012) and has been applied in other studies (Fraser et al., 2014; Wood et al., 2014; Wood, Schmidtlein, & Peters, 2014). Land cover and the slope SCV raster surfaces are discussed in Section 3.3.2 for the pedestrian model, and Section 3.3.3 for the vehicle model.

3.3.1.2.c. Vertical factor

Vertical factors (VFs) determine the difficulty overcoming the negative (downhill) or positive (uphill) slopes associated with changes in the slope angle from one cell to another. The higher the VFs the higher the cost or more difficult the movement. A VF of 1 does not affect the cost to move between cells. However, a VF less than 1 decreases the cost while factor greater than 1 increases the cost.

The cost for these movements is calculated from the Vertical Relative Moving Angle (VRMA – the slope angle between two cell centres) and accompanying VFs. The raster used to determine VRMA in this study is a 5m DEM which is also used for the input surface raster. This VRMA is calculated using trigonometry (Figure 3.4), and compensates for both positive (uphill) and negative (downhill) slopes between 90 and -90 degrees. By plotting VRMA values on the specified VF graph, the VFs are obtained and used in the calculations to determine the cost to travel to the destination cell. There are several types of VF graph which could be used; those provided with the ArcGIS software or a custom graph with an ASCII file. In this study, different VF graphs were used for the pedestrian and vehicle evacuation models because these agents overcome uphill and downhill slopes differently. These graphs are discussed in Sections 3.3.2.1 and 3.3.4.2

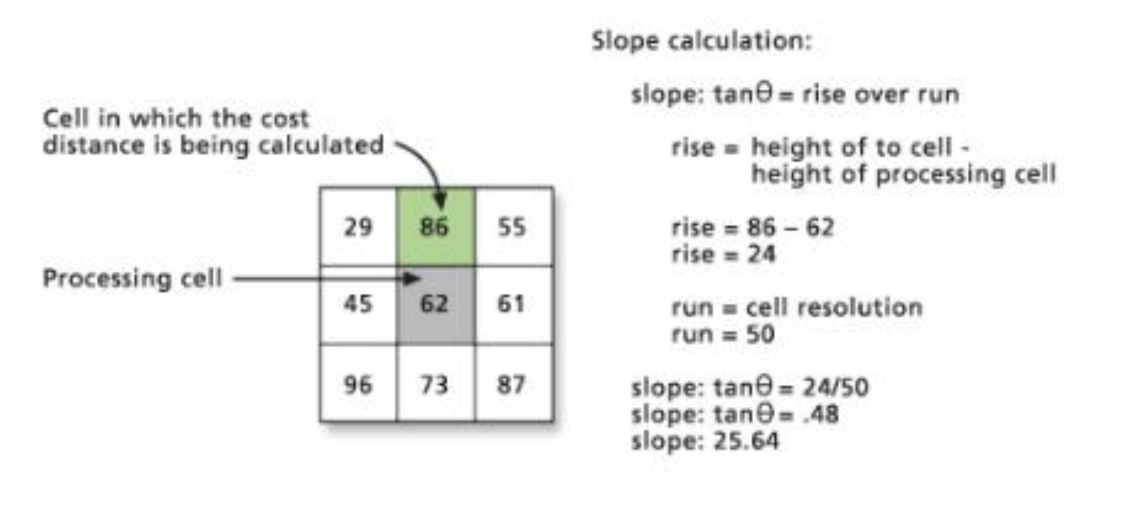

Figure 3.4. Slope calculation between two cells (ArcGIS, 2009a).

3.3.1.2.d. Surface distance (or true surface distance)

For the purpose of evacuation, the actual/true distance (including distance travelled up or downhill) needs to be calculated rather than just the straight line distance between two cells. The actual/true surface distance is calculated based on the Pythagorean theorem (Figure 3.5).

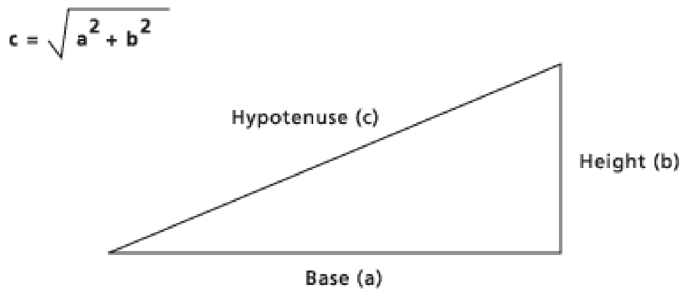

Figure 3.5. True surface distance calculation based on Pythagorean theorem (ArcGIS).

In this study, the input raster for this component is the aforementioned 5 m DEM raster. The length of base (a) is based on the node travel cost, while the height (b) is determined by the difference in the height of the destination cell and source cell. True surface distance shows that if the surface is not flat, the travel distance is longer and hence the cost (travel time) is greater.

3.3.1.2.e. Origin and Destination Points

The origin points (or Origins) are all points located in the tsunami inundation zone and used as source points for LCD models. In the pedestrian evacuation model these points represent population exposed to tsunami, while in the vehicle evacuation model they represent vehicles distributed in the inundation area. Destination points (or Destinations) are all points located in the safe zone and used as locations that evacuees/vehicles are expected to travel to. Criteria for Origins and Destinations selections are different for each model and are discussed in Section 3.3.2. The tsunami inundation model of Lane et al. (2014) (Figure 3.6) and population/vehicle distribution models are used to define the origin and destination points as inputs for LCD analysis for the pedestrian/vehicle evacuation models.

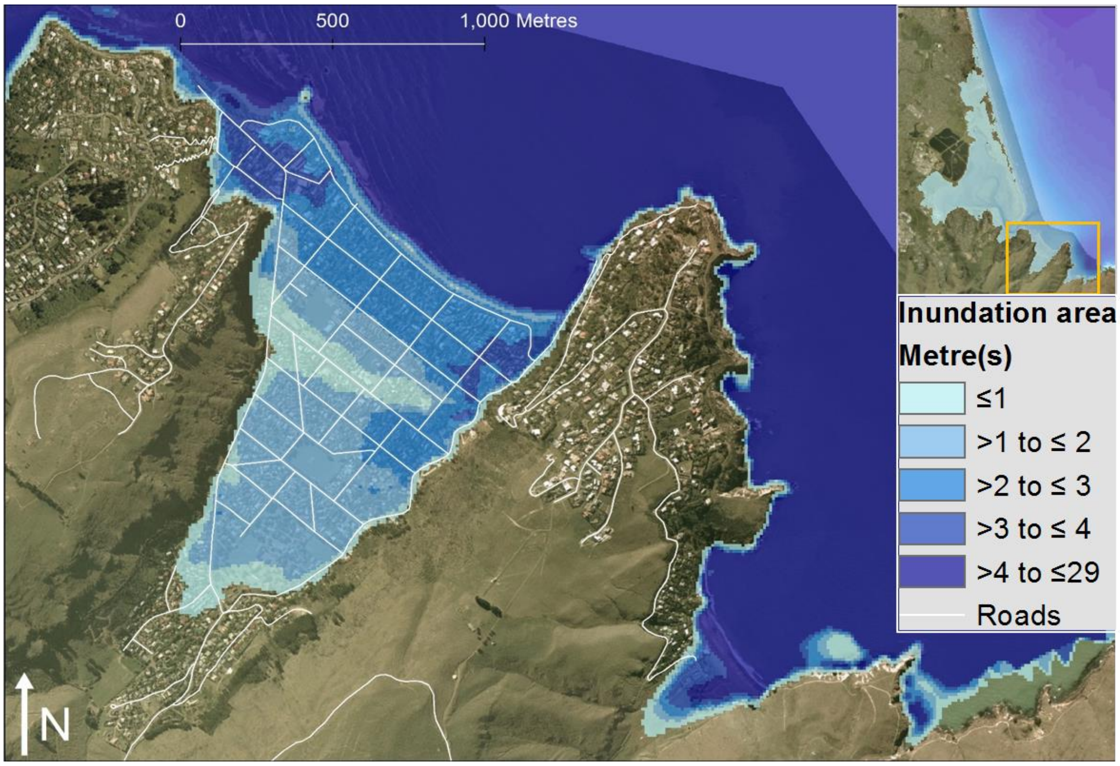

Figure 3.6: Tsunami inundation model (repoduced from Lane, et al, 2014).

Essentially, the LCD model will find the optimum path from each Origins to each Destinations. All paths are then compared to choose the best Destination (with the least costly path). The process keeps going until all Origins pair with their best 'preferred' Destinations. See Figure 3.7 for the process of LCD model, and Appendix C1 for an example of six representative Origins and their best paired Destinations).

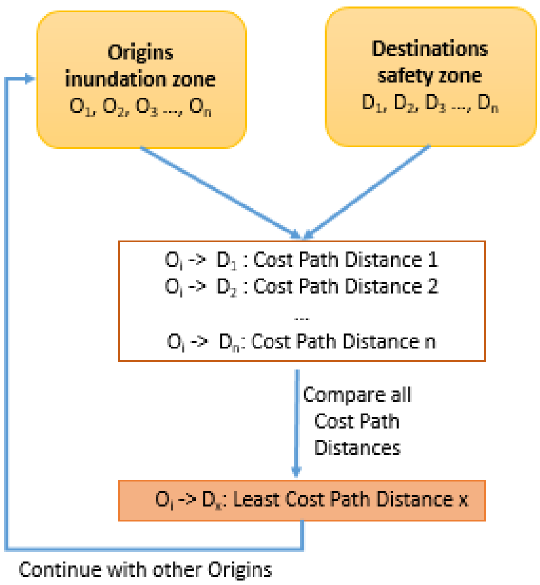

Figure 3.7. LCD models processing the least cost path distance. The process shown here represents the process from red dashed box to the brown dashed box in Figure 3.3.

3.3.2. Pedestrian evacuation model

This section first discusses the inputs used in the two pedestrian evacuation models (Section 3.3.2.1). As mentioned above, the two pedestrian evacuation models are pedestrians evacuating to higher ground and to bus stops. Therefore, the Destination inputs differ between the two models. Details specific to each model are given in Section 3.3.2.2 (evacuation to higher ground) and Section 3.3.2.3 (evacuation to bus stops).

Note that although the speeds used to estimate evacuation times presented here account for the demographic composition and physical ability of the at-risk population, it is only one realisation of the speed distributions model developed in Section 2.3.2.3. Future research should calculate average speeds resulted from multiple simulations of speed distributions to estimate more reliable average evacuation times.

3.3.2.1. Inputs for pedestrian evacuation models

3.3.2.1.a. Cost Surface – Effects of Land Cover

In this study, land cover data are compiled from aggregated polygon data (Land Resources Information Systems, 2014) representing ground surface cover divided into 11 classes. Additional polygon shapefiles representing roads, buildings and beaches (described in Section 2.3.1) are combined into a single comprehensive land cover layer. Fences were not considered in this analysis due to the limitations of the imagery and elevation data. Therefore, fences, if present, were assumed to be on individual properties and not continuous obstacles for significant distances.

To assign walking speeds to land cover type, land cover is represented in the LCD analysis by using the SCVs (Section 3.3.1.2). For this study, the SCVs are the inverse of energy cost terrain coefficients for certain land-cover types (Soule & Goldman, 1972). This was first developed and applied in LCD analysis by Wood & Schmidtlein (2012). This approach assumes walking speeds will decrease in proportion to the changes in energy required to move across different land-cover types. Compared to several previous studies (Anguelova et al., 2010; Jobe & White, 2009; Laghi et al., 2006; Post et al., 2009) which have reclassified land cover layers into SCV surfaces, the approach proposed by Wood &

Schmidtlein (2012) and later applied by Fraser et al. (2014) seemed most appropriate until field-derived relationships can be developed.

Table 3.1 matches the 2012 land cover classified in New Zealand (Land Resources Information Systems, 2014) with that in Soule & Goldman (1972), and the corresponding SCVs. Cells classified as buildings and water are considered impassable (hence SCV = 0) while cells representing roads are assigned SCV=1.0 (no hindrance to movement).

Table 3.1. Land- cover classes with corresponding SCVs

Land Cover classes (Land Resources Information Systems, 2014)	**Soule and Goldman categories (1972)**	**SCV**
Broadleaved Indigenous Hardwoods	Light Brush	0.8333
Built up Area (Settlement)*	Dirt Road	0.9091
Deciduous hardwoods	Light Brush	0.8333
Estuarine Open Water	Open water	0
Exotic Forest	Light Brush	0.8333
Gorse and/or Broom	Heavy Brush	0.6667
High Producing Exotic Grassland	Light Brush	0.8333
Low Producing Grassland	Light Brush	0.8333
Mixed Exotic Shrub-land	Heavy brush	0.6667
Sand or Gravel	Hard Sand	0.5556
Urban Parkland/Open Space	Dirt Road	0.9091
Additional land cover layers	**Soule and Goldman categories (1972)**	**SCV**
Beaches	Hard Sand	0.5556
Buildings	None	0
Roads	Blacktop	1

**Excludes buildings*

3.3.2.1.b. Vertical factor

In this study the transformation from slope to cost is via the hiking function described by Tobler (1993), which was developed from empirical data collected by Imhoff (1950, in Pingel, 2010) (Figure 3.8 and Equation 3.1). The equation Tobler (1993) derived determines the hiking speed based on an exponential function that takes into account the slope of the surface the hiker is passing over, and has the form:

$$V = 6.e^{-3.5.\left|\frac{dh}{dx}+0.05\right|} \tag{3.1}$$

where V is walking velocity (km/h), *dh* is slope high and *dx* is slope base. The equation takes into account the fact that travel in the downhill direction is beneficial, and uphill travel has an additional travel cost. Although it is acknowledged that moving downhill on steep slopes is potentially more dangerous than uphill travel (Pingel, 2010), this issue is not addressed here. A maximum walking speed of 6 km/h occurs at approximately 3 degrees of downward slope while on level ground walking speed is approximately 5 km/h (Figure 3.8).

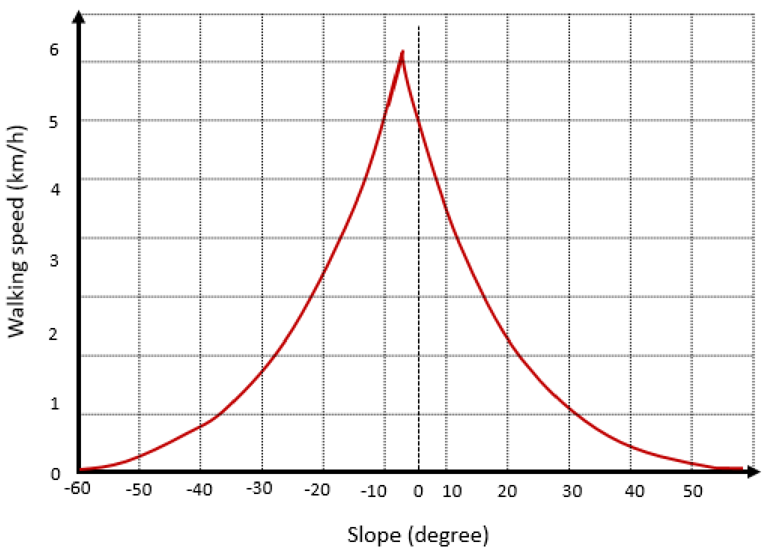

Figure 3.8. Tobler's hiking function and its derivative cost functions. Negative and positive slope degrees mean downhill and uphill movements, respectively (compiled from Tobler, 1993).

Other studies (Wood et al., 2014; Wood & Schmidtlein, 2013; Wood et al., 2014), and most recently Fraser et al. (2014), also utilised Tobler's hiking function to convert directional slope into a travel speed cost.

Typically, the cost functions derived from speed data are represented as the inverse of the slope/speed relationship. As Pingel (2010) discussed, this approach is correct when solving for time, and models utilising such a cost function will produce least-time routes. Whitley & Hicks, (2003) used this approach when estimating likely routes of Indigenous North Americans through hilly terrain in North Georgia, U.S.A. This approach was also applied by Tripcevich (2007) to identify probable routes of pre-Hispanic llama caravans in the Andes of South America. In this present study, the reciprocal of Tobler's hiking function proposed by (Tripcevich, 2008) is applied to estimate the cost, in this case time (hours), to travel one metre of the calculated path:

$$\text{Time (hours) to cross 1 metre} = 0.000166666\, e^{\left(3.5.\left(\left(\left|tan\left(RADIANS(slope\ in\ degrees)\right)+0.05\right|\right)\right)\right)} \quad (3.2)$$

where the *slope in degrees* includes all values between -90 and 90 degrees.

The Path Distance tool in ArcGIS creates a custom VF graph with a customised VF Table, containing slope in degrees and the appropriate VF (Table 3.2).

Table 3.2. Abbreviated version of slope and corresponding cost (time/hours) to travel one metre. Vertical Factor equal to -1 means people cannot traverse slopes of that angle (Tripcevich, 2008).

Slope (degree)	Vertical Factor
-90	-1
-80	-1
-70	2.099409721
-50	0.009064613
-30	0.001055449
-10	0.00025934
-5	0.000190035
-4	0.000178706
-3	0.000168077
-2	0.000175699
-1	0.000186775
0	0.000198541
5	0.000269672
10	0.000368021
30	0.001497754
50	0.012863298
70	2.979204206
80	-1
90	-1

Slope SCVs were developed by dividing the speeds calculated from the inverse of Equation (3.1) above by the maximum potential walking speed. The Slope SCV was then multiple with the Land Cover SCV collected along the path generated from LCD model (using *Sample* tool in ArcGIS) to produce a travel base rate layer (refer to LCD model's flow chart, Figure 3.3).

The search direction of the LCD model is very important as it decides the direction of slope – which is downhill from one direction but is uphill in another case. In this study, the direction is defined from Origins to Destinations, which means from hazard zone to safe zones - direction of evacuation. Equation (3.2) is specifically applied for this case of direction.

3.3.2.1.c. Origin points for pedestrian evacuation

The origin points in all evacuation models are the pedestrian and private vehicle distribution points that intersect the tsunami inundation hazard layer. These origin points represent population exposure to the modelled tsunami hazard. In this study, people who are in zones outside of the modelled tsunami hazard are not considered in the evacuation model. As discussed in Chapter 2, the spatio-temporal population exposure is distributed among home, work and unspecified location categories, hence origin points are also distributed accordingly. The method for assigning origin points for each of these categories is described below:

- *Home and work locations*: the origin point is the centroid of the polygon representing each home and work building. Each point holds a corresponding population value for the building it represents at a given time.
- *Unspecified locations* (includes open spaces and road locations):
    - *Open spaces (park and beaches):* the origin points are distributed randomly inside the open space area category. Each open space holds the number of points according to its ratio discussed in Section 2.3.2.2.c (Table 2.13), therefore, the total number of origin points is 100. The population is then divided equally among the origins points based on the population located in open spaces at given time.
    - *Roads:* the origin points are distributed randomly on all of the roads within the study area, with intervals of approximately 120 m. These points are then manually adjusted such that there are no points on road intersections. This helps eliminate the possibility that one point represents two roads and omits population data of one of those two roads.

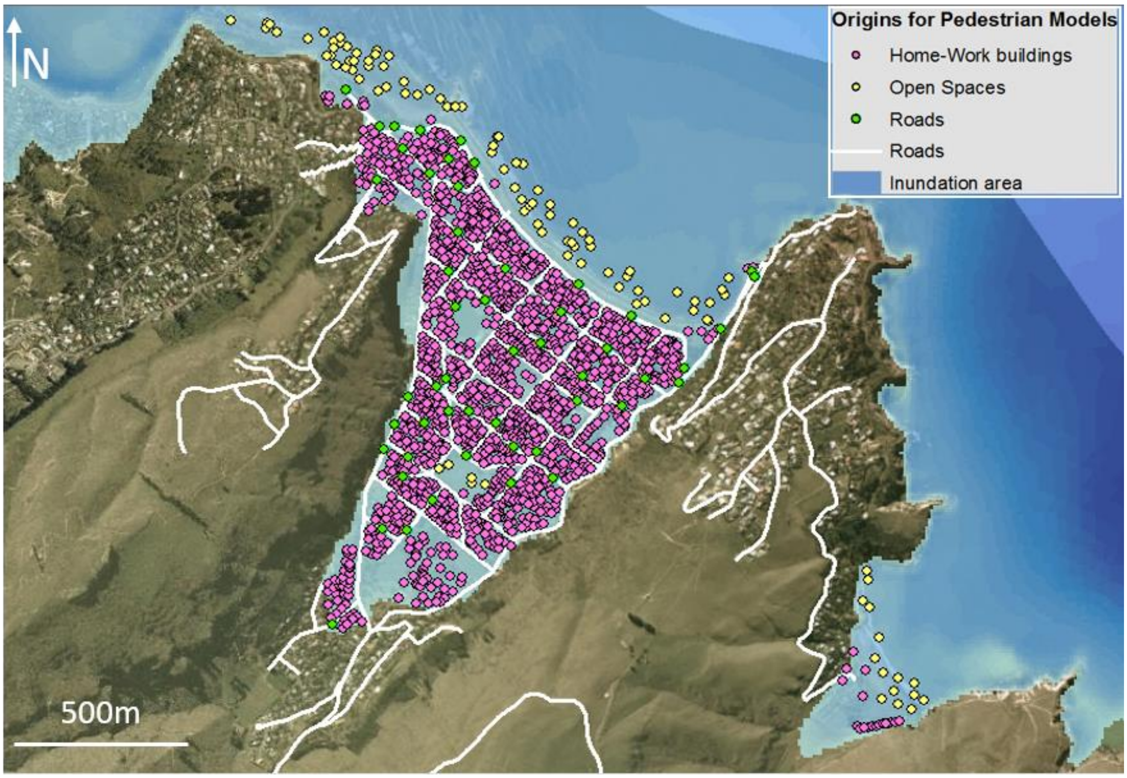

Figure 3.9. Origin points for the pedestrian evacuation model.

3.3.2.1.d. Destination points for pedestrian evacuation models

There are various ways to select destination points for evacuation, including the boundary of the hazard zone (Wood & Peters, 2015) or vertical evacuation to high buildings/refuges in the case where high ground is unreachable (Wood et al., 2014). High buildings/refuges can be effective risk-reduction options; during the 2011 Tohoku M_w 9.0 earthquake and tsunami, many high buildings provided safe vertical evacuation refuges for thousands of people in several Japanese coastal communities (Fraser et al., 2012; G. Leonard et al., 2011). Therefore, the potential of vertical evacuation refuges is being planned in the United States (Doughton, 2013) and Sumatra (Geohaz, 2008). However, in Sumner there is no existing plan for refuges, and the most recent evacuation plan also does not mention any refuges close to the study area (Christchurch City Council, n.d). The decision to construct or designate buildings as refuges is a difficult policy matter, and should be addressed in future. In other research (Wood & Schmidtlein, 2013), destinations are simply referred to as 'safe areas' or 'areas outside of the hazard zone' without specifically introducing the criteria for these areas and how they are defined.

Hence, deciding upon destinations depends on expert judgements. The only criterion that is true in all cases is that the destinations are typically outside of the hazard zones.

In this study, the destination points for pedestrian evacuation models are based on (1) pedestrian evacuating to higher elevations and (2) pedestrians evacuating to bus stops for subsequent transport out of the hazard zone. More details for defining destination points of each model are given in Sections 3.3.2.2 and 3.3.2.3.

3.3.2.2. Evacuating to higher elevations

3.3.2.2.a. Destination points for pedestrian evacuation to higher elevation

In this study, the boundary between safe zones and evacuation zones is the20 m height contour line (taken from the 5m DEM) as this is the contour closest to the inundation area. Destination points are created along this line at 50 m intervals (Figure 3.10). Points were removed manually from areas impossible to access due to their steep and dangerous nature. Currently, most of these areas are protected from rock fall by shipping containers, emplaced after the 22 February 2011 Christchurch Earthquake. These containers are now being removed as geotechnical remediation works are completed; however, these areas will remain inaccessible for pedestrian tsunami evacuation (Figure 3.10 numbered (1) and (2) show the removed points).

Figure 3.10. (Top-left) Destinations for pedestrian evacuation to higher ground. The total number of Destinations is 105 points; (Top-right) Photo shows steep slopes on Wakefield Road, numbered 1 in the destinations map (May, 2015); (Bottom-left) Photo shows rock fall protection containers on Wakefield Avenue, numbered 2 in the destinations map (May, 2015); (Bottom-right) Photo shows steep slopes on the other side of the valley, chosen to be destinations in model – these points were kept as destinations within the model to test whether or not the model would evacuate people to these unrealistic locations, numbered 3 in the destination maps (May, 2016).

3.3.2.2.b. Results of pedestrian evacuation to higher elevation

The purpose of the LCD model is to determine the recommended directions to evacuate from the tsunami hazard zone for different locations in the inundation area. Figure 3.11 shows six zones in the study area with their optimal (shortest time) evacuation direction. Zone boundaries were manually delineated along areas separating domination evacuation directions. This product enables emergency managers to evaluate evacuation routing options.

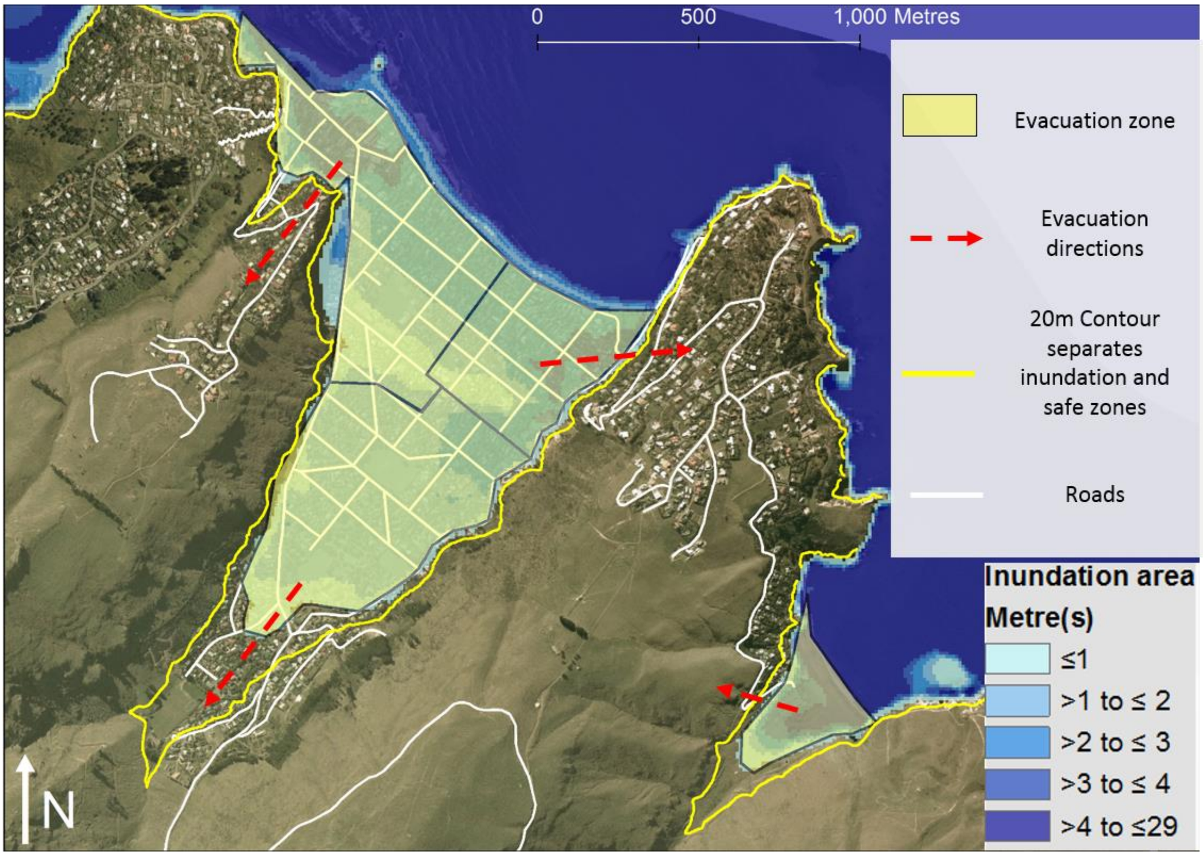

Figure 3.11. Tsunami evacuation zones suggested by the pedestrian evacuating to higher ground model.

Figure 3.12 shows evacuation times for the population evacuating to higher ground in Sumner. Each point on this map represents an individual or group of individuals. This evacuation time surface is overlaid with tsunami inundation depth values. Emergency managers can use these results to prioritise the evacuation of different locations by combining information of evacuation times and inundation depths. Figure 3.12 shows areas with the longest evacuation times are in the vicinity of Wakefield Avenue and from the vicinity of Campbell Street towards the coast.

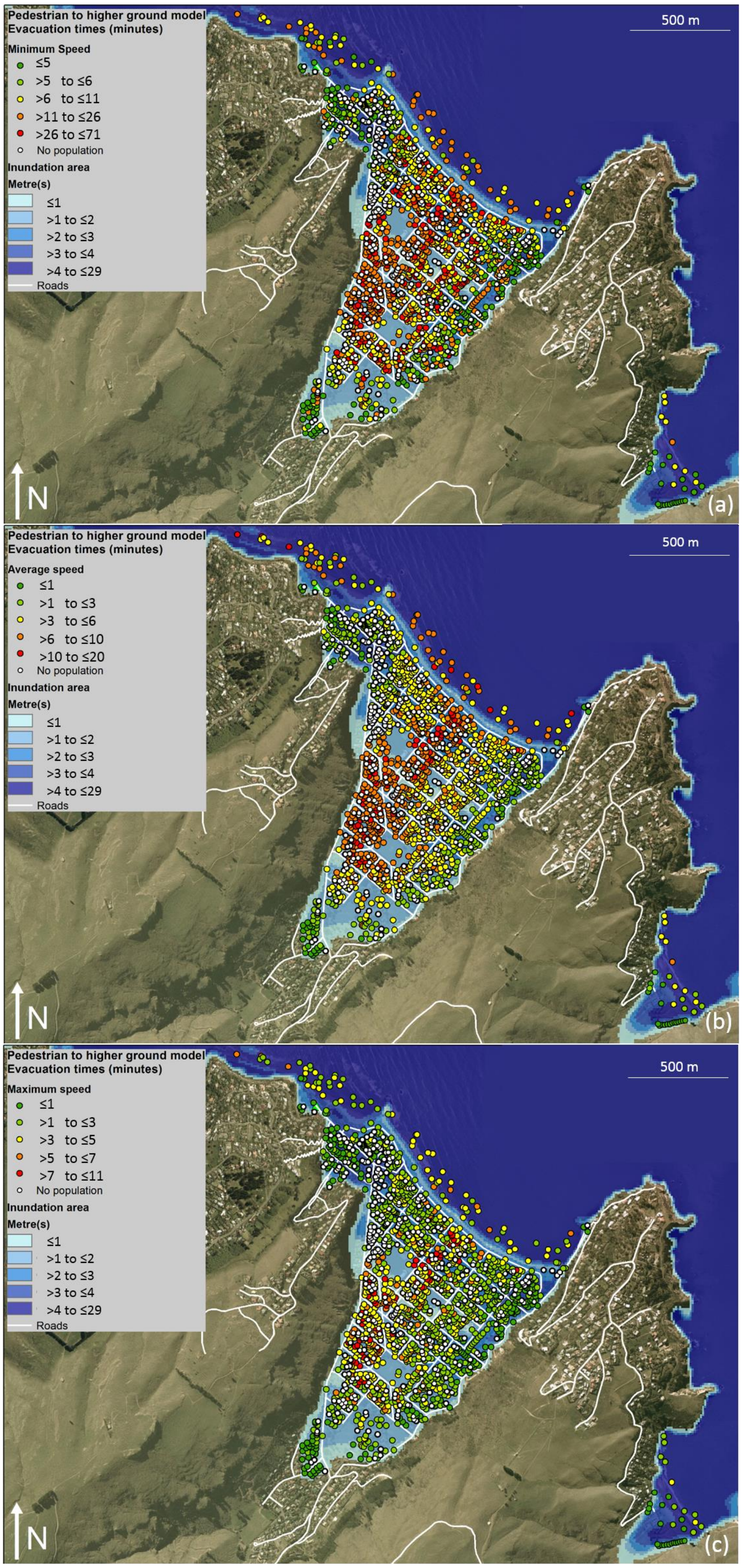

Figure 3.12. Evacuation times for the population in Sumner in a February weekend 12:00 scenario with (a) minimum speed; (b) average speed; and (c) maximum speed. Time data are overlaid on inundation depth values.

The LCD model also produces travel time and the corresponding number of evacuees. Travel time is obtained by calculating the length of each recommended path, and by determining the travel base rate. The travel base rate resulted from multiplying mean values of land and slope SCV for all cells the paths cross. Variable spatio-temporal population and speed distributions are used with results of path length and SCV to produce evacuation time curves, showing the population corresponding to evacuation time in each scenario (Figure 3.13). This set of evacuation time curves enables emergency managers to make a quick assessment of the total population and their evacuation time in different scenarios.

Evacuation time curves for all models in this study are presented in the same format: a graph starting with three weekend time scenarios of at 12:00 for each of February, June and October, to examine the impacts of seasonal changes on exposure distribution, and evacuation time; a graph for three time scenarios, weekday at 02:00 for the February, June, and October, to show the changes in exposure distribution at night; and a graph comparing five time scenarios (02:00, 08:00, 17:00, and 12:00 weekday and weekend) to understand the impact of diurnal, and seasonal variation on evacuation time and exposure distribution. Abbreviations for different time scenarios in the graphs are: weekday at 02:00 (wd2); weekday at 08:00 (wd8); weekday at 12:00; weekend at 12:00 (wk12); weekday at 17:00 (wd17); F, J and O stand for February, January and October, respectively.

At 02:00 the most common time to evacuate from the hazard zone was five minutes (Figure 3.13b; 10% of the number of evacuees), and with the rest of time scenarios was six minutes (Figure 3.13a,c; 13% of the number of evacuees). The second most common evacuation time was seven to eight minutes at 02:00, and nine to ten minutes with the rest of time scenarios, accounting for 14% and 11% of the number of evacuees, respectively. A small number of people (around 2% of the at risk population) take longer than 12 minutes to evacuate. Fewer people at 02:00 compared to 17:00 scenario characterise the commuting patterns in Sumner. At 17:00, residents coming back to Sumner from work, and daily visitors who only leave Sumner at night-time, make the number of evacuee higher than at 02:00. Refer to Appendix 3.1 for absolute numbers of evacuees and corresponding evacuation times for each scenario.

Across all time scenarios, the pedestrian evacuation times to higher elevations beyond the inundation zone range from 0.5 to 20.5 minutes (Figure 3.13. Evacuation time curves for pedestrian evacuate to higher ground comparing between different time scenarios; (a) February weekend 12:00 (Fwk12), June weekend 12:00 (Jwk12); October weekend 12:00 (Owk12); (b) February weekend 02:00 (Fwk2), June weekend 02:00 (Jwk2), October weekend 02:00 (Owk2); (c) Weekday 02:00 (Wd2), Weekday 08:00 (Wd8), Weekday 12:00 (Wd12), Weekend 12:00 (Wk12), Weekday 17:00 (Wd17). Time scale presented as 30 seconds interval.). This means that for regional and distal tsunami sources, where the arrival times are estimated to be <3 hours and >3 hours (Section 1.4.1) respectively, people will have sufficient time to evacuate. However, several relevant factors are not taken into account here such as departure delay time, people's behaviour during evacuation, congestion and potential disruptions to evacuation routes, which might lead to longer total evacuation times (discussed further in Chapter 4). For local-source scenarios (i.e. < 1 hour until the tsunami arrives), the modelled evacuation times plus these delaying factors may prove problematic.

Note that in this research, the speed applied for all scenarios is average walking speeds. Examples of evacuation maps and evacuation time curves resulted from utilising minimum, average and maximum speeds into the model specifically for February weekend 12:00 shown in Figure 3.12 and Figure 3.14 (refer to Table 2.14) for details of different minimum, average, and maximum speeds of each population group). The most common required evacuation time are ten, six, and three minutes with minimum, average, and maximum speeds, respectively, for more than 60% of the evacuees. More details on these results are discussed in Section 3.3.3

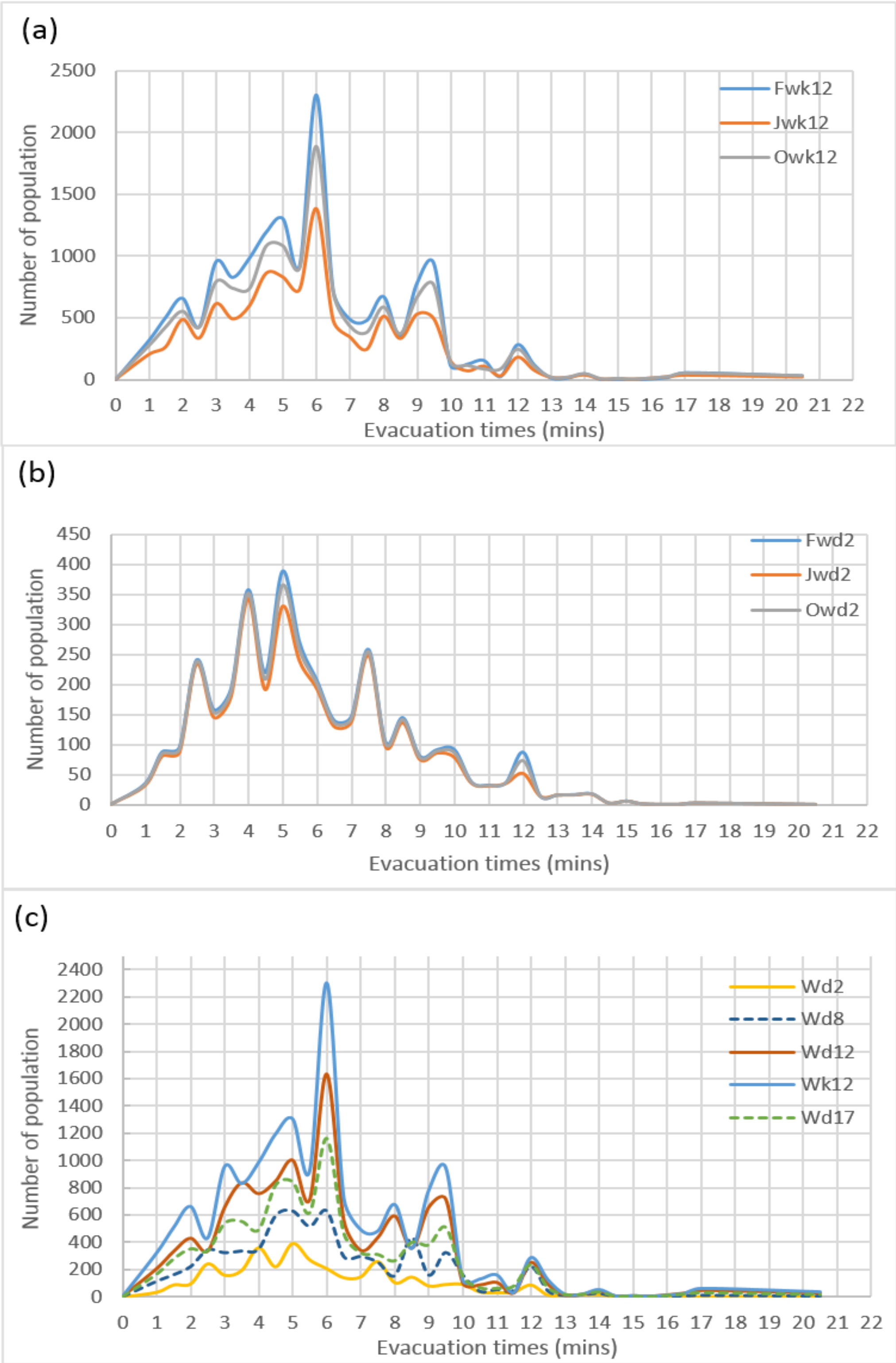

Figure 3.13. Evacuation time curves for pedestrian evacuate to higher ground comparing between different time scenarios; (a) February weekend 12:00 (Fwk12), June weekend 12:00 (Jwk12); October weekend 12:00 (Owk12); (b) February weekend 02:00 (Fwk2), June weekend 02:00 (Jwk2), October weekend 02:00 (Owk2); (c) Weekday 02:00 (Wd2), Weekday 08:00 (Wd8), Weekday 12:00 (Wd12), Weekend 12:00 (Wk12), Weekday 17:00 (Wd17). Time scale presented as 30 seconds interval.

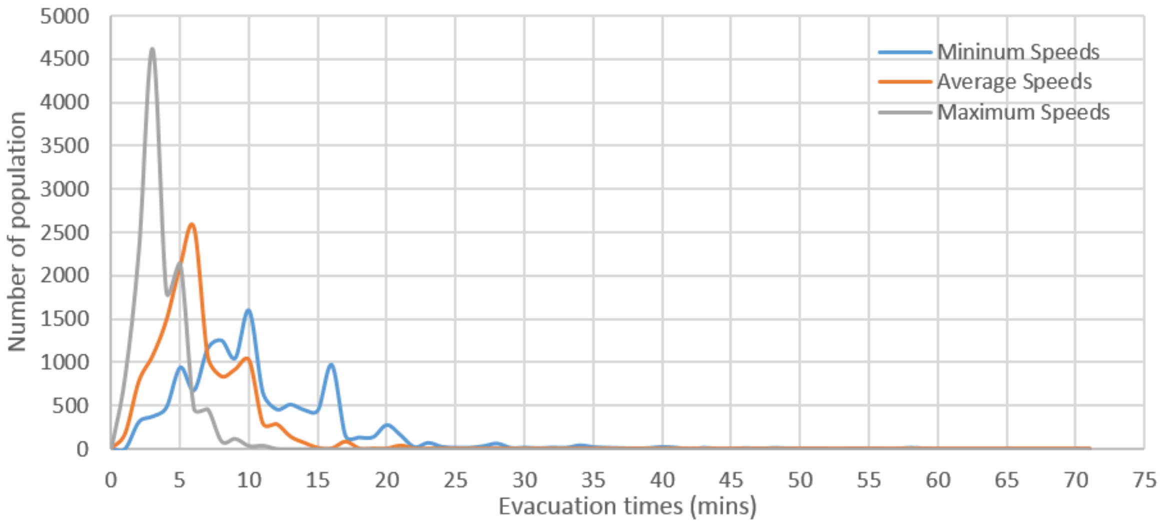

Figure 3.14. Evacuations time curves for pedestrian evacuate to higher ground February weekend 12:00, with three different speeds (minimum, average, and maximum speeds). Time scale presented as a minutes interval.

3.3.2.3. Evacuation to bus stops

Alternative forms of transportation, in addition to private vehicles, are assessed in this study. Public transportation can reduce traffic congestion, which is likely to be present in a tsunami event, and is especially important for low-mobility populations who normally depend on public transportation (Tomsen, 2010). One of the most common forms of public transportation in most urban areas is buses, and this is also true for Sumner. Therefore, in this study, the number of pedestrians and their travel times to different bus stop locations for different time scenarios are estimated. Input parameters are the same as for the previous pedestrian model, and only the destinations are different. Note that it is unnecessary to include people from Taylors Mistake (Figure 1.10) in this model, because before reaching the bus stop they already reach higher ground and are in a safe zone. The method for selecting destinations and results for pedestrian evacuation to bus stops are presented below.

3.3.2.3.a. Destination points for pedestrian evacuation to bus stops

Three bus stop scenarios are presented here (Figure 3.15): (1) A single designated bus stop on Marriner Street, on the main route exiting Sumner; (2) a second additional bus stop on Nayland Street near Sumner School; and (3) a third additional bus stop on Duncan Street near St Leonard Square. The Marriner Street stop was selected because it is a logical muster point at the exit route from Sumner, and the other two stops were selected to explore pedestrian travel times to locations well-known to the community. Choosing three different scenarios gives local and emergency manager information which they can use to decide which scenarios would be the best, depending on their priority between numbers of evacuees, evacuation time, and human resources.

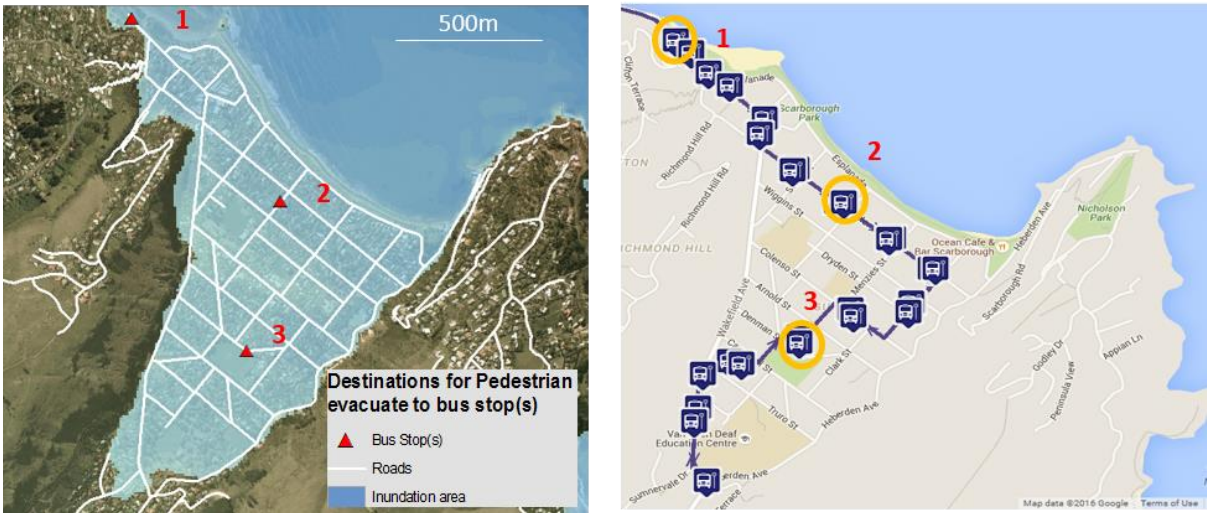

Figure 3.15. The three bus stop destinations analysed here;(left) Locations of the three bus stops used in the model; (right) locations of bus stop(s) taken from Metroinfo page (Metroinfo, n.d.).

3.3.2.3.b. Results of pedestrian evacuation to bus stops

Similar to the model of pedestrian evacuation to higher ground, optimal paths to the destinations from all origins have been determined for Sumner (i.e. the recommended evacuation paths to bus stops). To make the maps (Figures 3.16) easier to interpret, all origins are grouped into different colour zones with their recommended evacuation directions for two and three bus stops scenarios. Zone boundaries were manually delineated along areas separating domination evacuation directions. The one bus stop scenario is excluded from this grouping process as there is only one destination choice.

The recommended usage of bus stops for different evacuation zones is based on the least cost (shortest time) paths generated by the LCD for vehicle model (Section 3.3.3). One factor not considered here is the maximum holding capacity of evacuees at each bus stop. For example, in the case of the two bus stops scenario (1 and 2), nearly 80% of the population at risk is recommended to evacuate to bus stop 2 due to its easy accessibility. This may lead to overcrowding issues at bus stop 2, and this potential problem should be addressed in future research. Expanding zone 1 and reducing zone 2, the dashed line area in Figure 3.16, could solve the issues of overcrowding at bus stop 2.

The recommended usage of bus stops for different evacuation zones is based on the least cost (shortest time) paths generated by the LCD for vehicle model (section 3.3.3). One factor not considered here is the maximum holding capacity of evacuees at each bus stop. For example, in the case of the two bus stops scenario (1 and 2), nearly 80% of the population at risk is recommended to evacuate to bus stop 2 due to its easy accessibility. This may lead to overcrowding issues at bus stop 2, and this potential problem should be addressed in future research. Expanding zone 1 and reducing zone 2, the dashed line area in Figure 3.16, could solve the issues of overcrowding at bus stop 2.

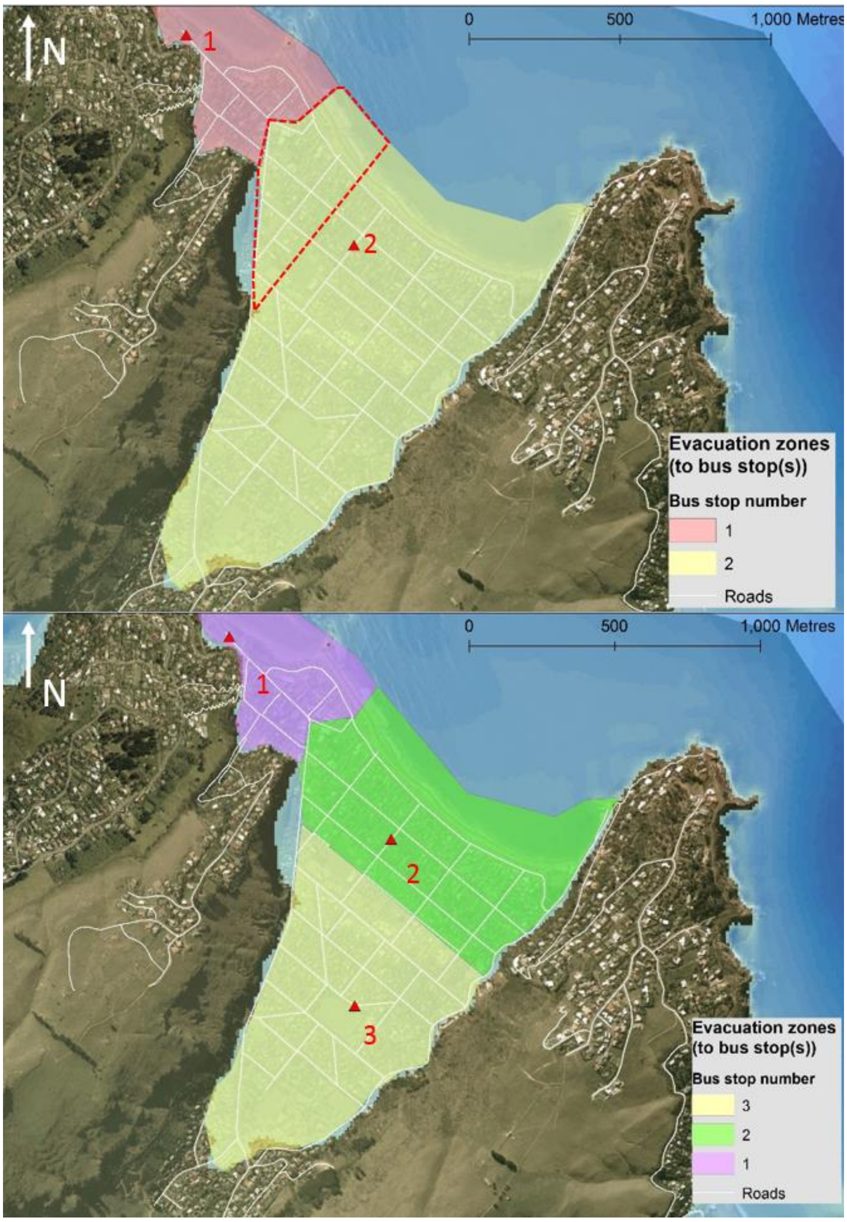

Figure 3.16. Evacuation zones recommended for the two (top) and three (bottom) bus stop scenarios. Dashed line shows the recommended extended evacuation zone 1.

Evacuation time maps for the population to evacuate to one, two and three bus stops for a February 1200 weekend scenario are shown in Figure 3.17. Warm colours indicate longer time to travel to the bus stops. In all three cases, areas in the vicinity of Wakefield Avenue, Heberdeen Avenue and the corner of Heberdeen Avenue/Esplanade Road have the longest times.

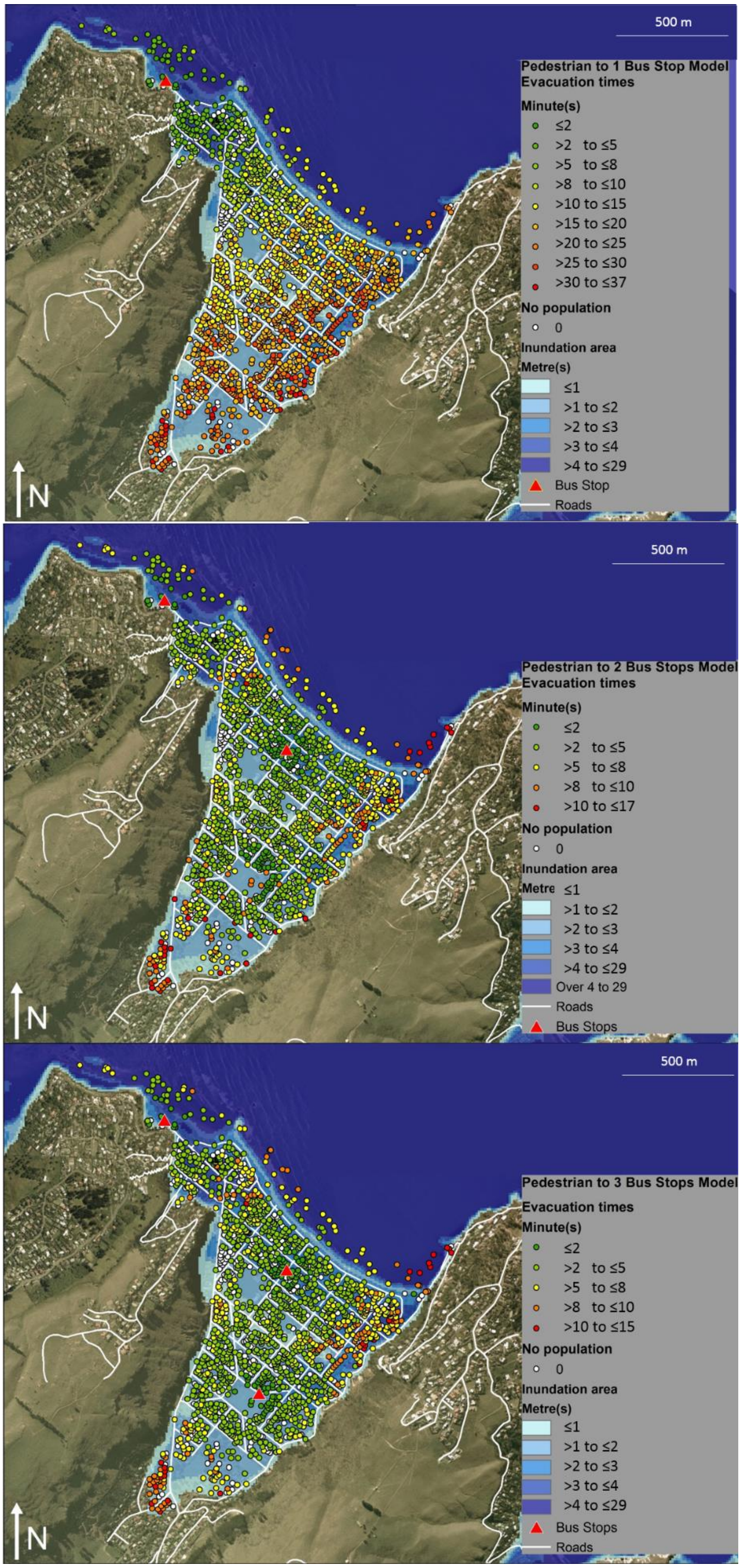

Figure 3.17. Evacuation times for the Sumner population to evacuate to one, two, and three bus stop(s) (top to bottom), for a February 12:00 weekend scenario. Time data are overlaid on the tsunami inundation model indicating depth values.

Evacuation time curves are also presented (Figure 3.18, 3.19 and 3.20).If all evacuees start departing at the same time, it is estimated that 28%, 73%, and 80% of exposure people are able to reach bus stop(s) after six mins in cases of one, two and three bus stops sceanrios, respectively. These numbers increase to 41%, 97%, and 98% of the total population at risk after 10 mins of evacuation time (refer to Appendices 3.2, 3.3, and 3.4 for absolute number of evacuee and corresponding evacuation times at given time scenario).

It is clear that the three bus stops scenario gives the shortest required evacuation time for the greater number of successful evacuees, but compared to two bus stop scenarios the differences are insignificant. For example, if all people departed at the same time, within 14.5 minutes 100% will have arrived at the three bus stops; 99% will have arrived at the two bus stops; and 59% will have arrived at the one bus stop. However, it also means within within 14.5 minutes there would be ~3000 to >12,000 people arriving at bus stops, which will require 90 to 360 buses (with 33 seated passenger per bus) (NZTA, 2014). This might create severe traffic congestion. Another factor should be considered when choosing the appropriate bus stop scenario is that the functionality of the public transport sector which is highly dependent on employee reliability. Tomsen (2010) cited a similar concern when giving an example that if bus drivers or train conductors choose to evacuate with their families then they will not be available for public service. Therefore, it is very important to have prior arrangements with public bus companies, in addition to other organisations possessing necessary evacuation resources before the disaster. Furthermore, the compliance rate in this study is assumed to be 100% in all scenarios, in reality it is highly unlikely that all people choose public transportation as their only mode of evacuation. Thus, evacuation demand for this transportation mode will be smaller, and as a consequence, bus capacity required is also reduced. More discussion in terms of utilising public transport (in this case is buses) in evacuation will be given in Chapter 4.

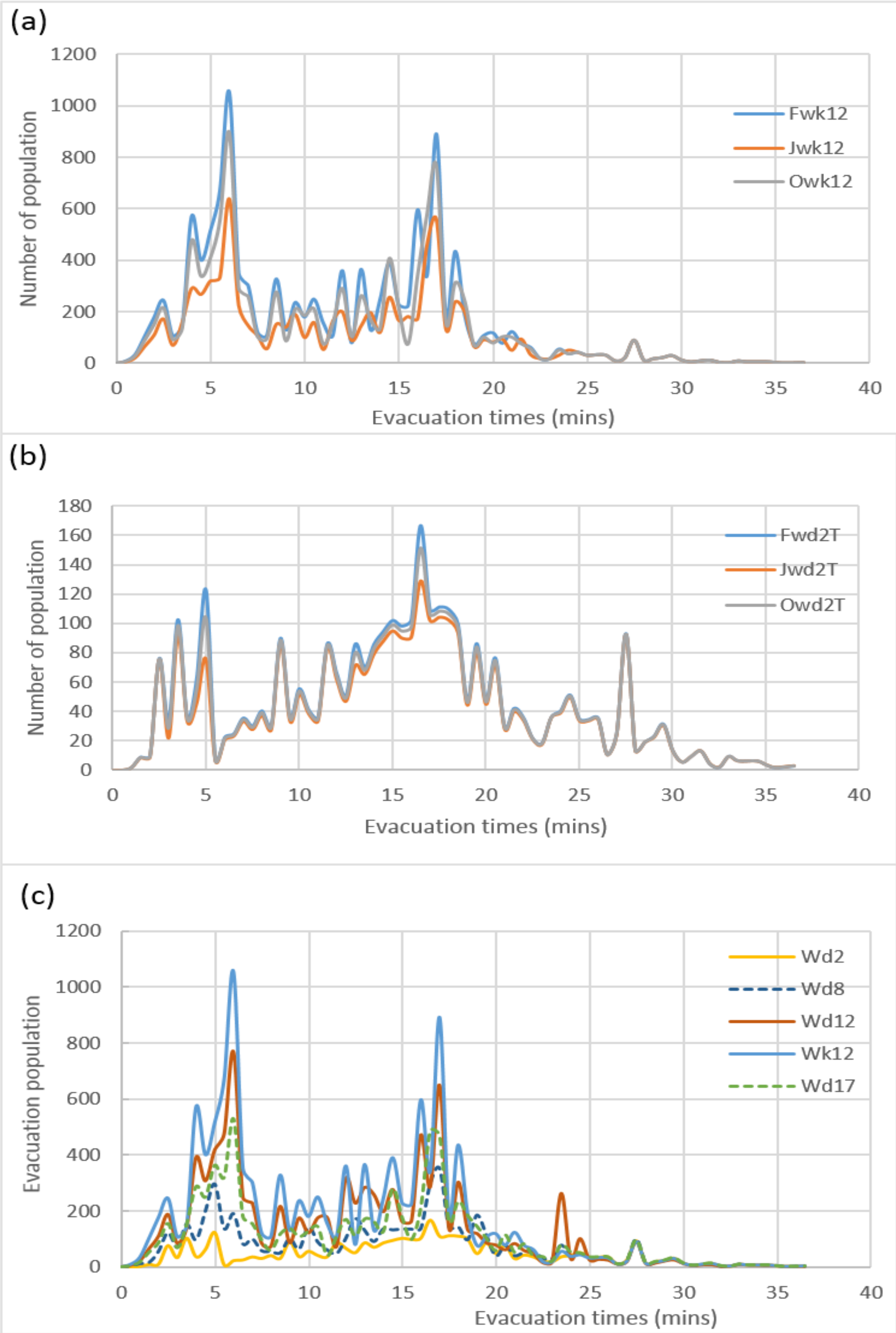

Figure 3.18. Evacuation time curves for bus stop 1 scenario comparing between different time scenarios; (a) February weekend 12:00 (Fwk12), June weekend 12:00 (Jwk12); October weekend 12:00 (Owk12); (b) February weekend 02:00 (Fwk2), June weekend 02:00 (Jwk2), October weekend 02:00 (Owk2); (c) Weekday 02:00 (Wd2), Weekday 08:00 (Wd8), Weekday 12:00 (Wd12), Weekend 12:00 (Wk12), Weekday 17:00 (Wd17).

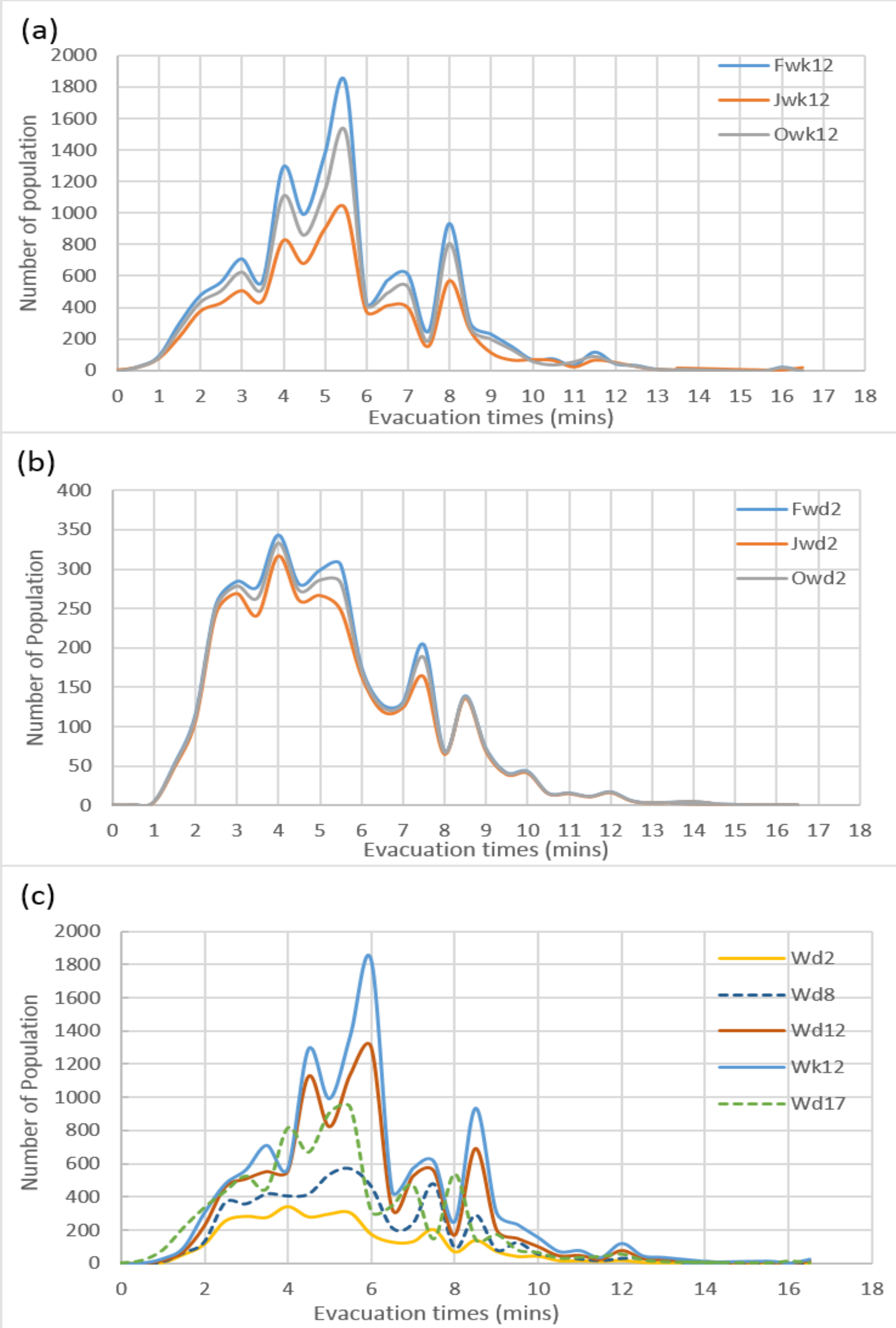

Figure 3.19. Evacuation time curves for 2 bus stops scenario comparing between different time scenarios; (a) February weekend 12:00 (Fwk12), June weekend 12:00 (Jwk12); October weekend 12:00 (Owk12); (b) February weekend 02:00 (Fwk2), June weekend 02:00 (Jwk2), October weekend 02:00 (Owk2); (c) Weekday 02:00 (Wd2), Weekday 08:00 (Wd8), Weekday 12:00 (Wd12), Weekend 12:00 (Wk12), Weekday 17:00 (Wd17).

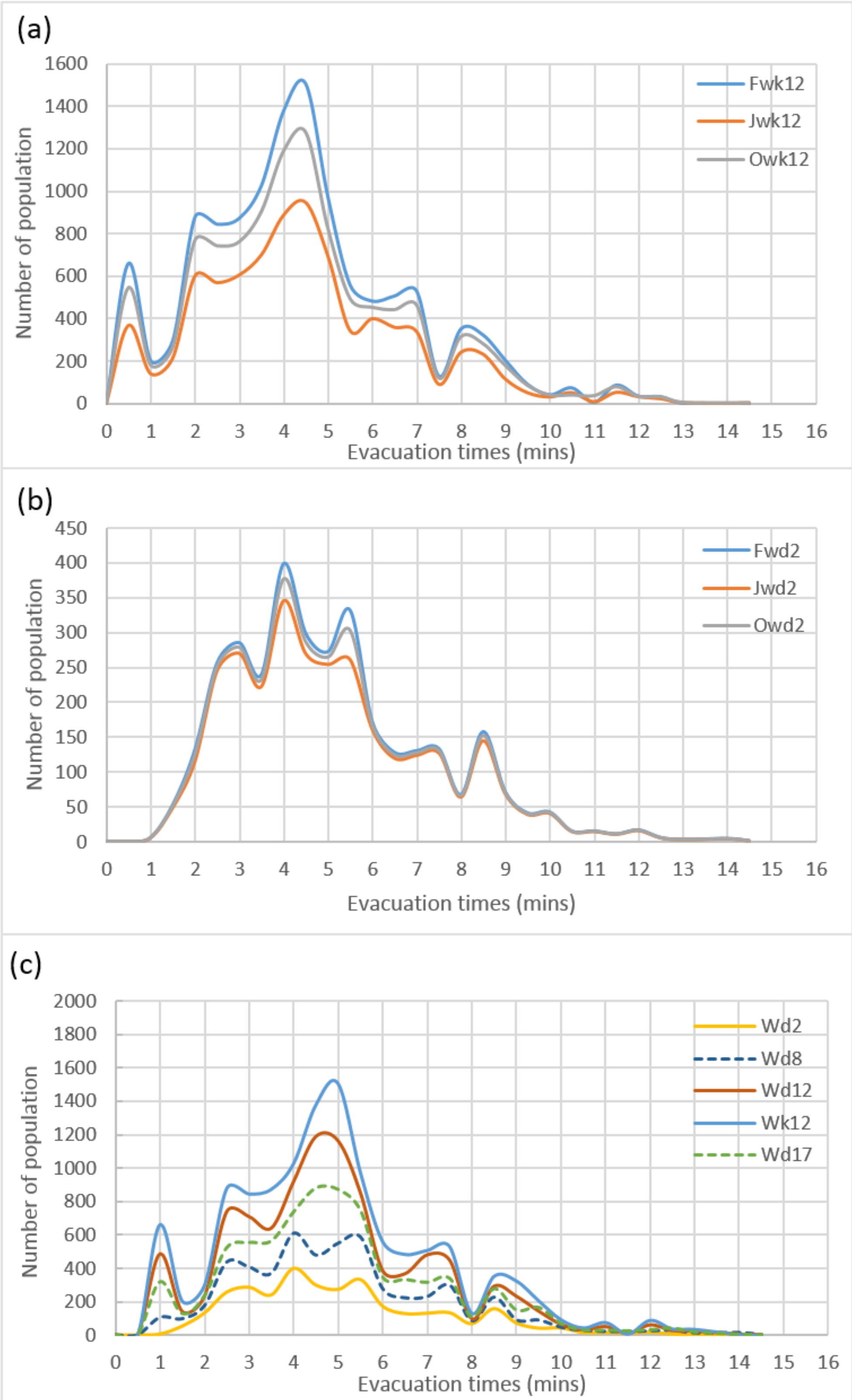

Figure 3.20. Evacuation time curves for 3 bus stops scenario comparing between different time scenarios; ; (a) February weekend 12:00 (Fwk12), June weekend 12:00 (Jwk12); October weekend 12:00 (Owk12); (b) February weekend 02:00 (Fwk2), June weekend 02:00 (Jwk2), October weekend 02:00 (Owk2); (c) Weekday 02:00 (Wd2), Weekday 08:00 (Wd8), Weekday 12:00 (Wd12), Weekend 12:00 (Wk12), Weekday 17:00 (Wd17).

3.3.3. Preliminary Test of Pedestrian Evacuation Model Results

3.3.3.1. Testing Travel Time

To test the LCD model's results, three paths representing different landscapes (up-hill and flat) were chosen to test with a real-life subject. The participant involved in the test was asked to use GPS and Google Maps from mobile phone to follow chosen paths, with participant's normal walking speed. The test was taken place on sunny, and calm wind day in Sumner (5th June, 2016). The participant was New Zealander, male, 1.91 metre height, 29 years old and belonged to *Working Adult (15-64 years old)* population group.

3.3.3.1.a. Uphill Evacuation paths

LCD model with average walking speed (1.43 m/s) have the closest time travels results (around 10 to 15 seconds faster) to the real-life test in both up-hill paths examined (Figure 3.21). Google maps results give the second nearest results to real-life test (around 30-40 seconds faster). LCD model results when used maximum walking speed (2.8 m/s) show the fastest travel time compared to all of the model and real-life test's results. Meanwhile, LCD model used minimum walking speed (0.88 m/s) show a much longer time travels, around twice time as much compared to real-life test.

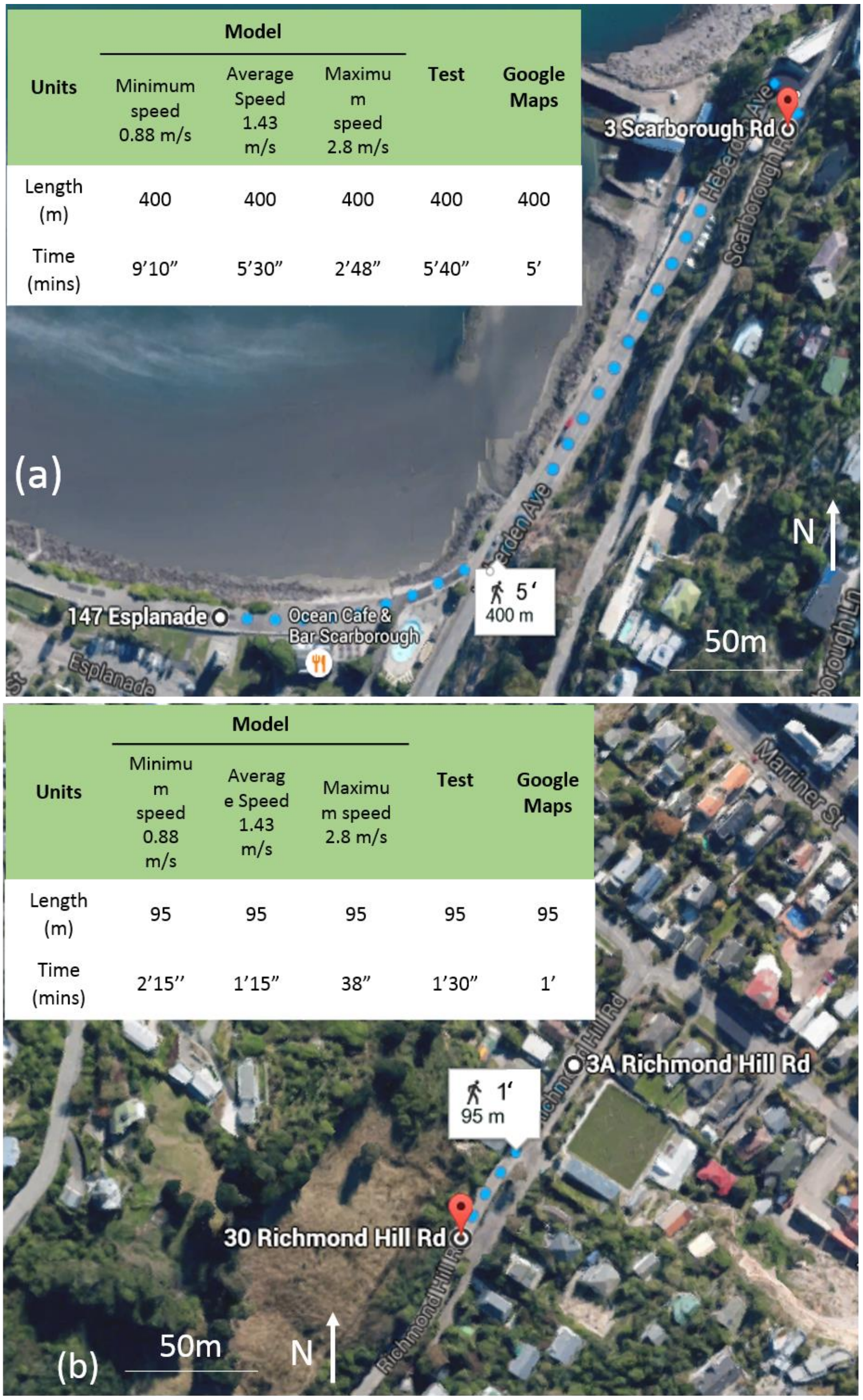

(a)

Units	Model			Test	Google Maps
	Minimum speed 0.88 m/s	Average Speed 1.43 m/s	Maximum speed 2.8 m/s		
Length (m)	400	400	400	400	400
Time (mins)	9'10"	5'30"	2'48"	5'40"	5'

(b)

Units	Model			Test	Google Maps
	Minimum speed 0.88 m/s	Average Speed 1.43 m/s	Maximum speed 2.8 m/s		
Length (m)	95	95	95	95	95
Time (mins)	2'15"	1'15"	38"	1'30"	1'

Figure 3.21. Up-hill evacuation paths; Evacuate from Esplanade to Scarborough road (a); Evacuate to up-hill on Richmond Hill Road (b), and Table compare results of distances and time travel given by LCD model (minimum, average, maximum speeds) and Google maps.

3.3.3.1.b. Evacuation through flat areas

When testing on evacuation through the flat areas, the bus stop evacuation scenario with the bus stop on Duncan street was chosen to be tested (Figure 3.27). Results of the models with three walking speeds compared to the real-life test continue to show the same patterns. The average walking speed gives the closest time travel result compared to real-life tests. However, unlike the up-hill evacuation path case, the travel time given by the model with average walking speed is 40 seconds longer than real-life test.

As Google Maps is unable to suggest routes that are not roads, hence, the paths suggested by Google Maps are different with the one suggested by model (Figure 3.22). Unlike up-hill evacuation case, travel time given by Google Maps is more than one minute longer when compared result by the test (10 min versus 8 min 53 seconds, Figure 3.22).

Units	Model			Test		Google Maps
	Minimum speed 0.88 m/s	Average Speed 1.43 m/s	Maximum speed 2.8 m/s	Model’s Path	Google Maps’ Path	
Length (m)	622	622	622	622	800	800
Time (mins)	12’30”	7’40”	4’	7’00”	8’53”	10’

Figure 3.22. The map shows results for evacuation on relatively flat landscape to bus stop on Duncan Street by LCD model and Google Maps; The table shows details results by LCD model (minimum, average, and maximum speed), real-life test on model’s Path and Google Maps’ Path, and Google Maps.

3.3.3.2. Comparison of different destinations

To test the ability of LCD model on picking up better accessible destinations as mentioned in Section 3.3.2.1, comparison of destinations located on Heberdeen Avenue hill side were implemented. Examples of suggested and declined destinations by LCD model, located closed to each other, are shown in Figure 3.23 and Figure 3.24. Results show that LCD model is able to compare and select optimal destinations for the most effective travel. In particular, the model chooses the farthest destination (located uphill Scarborough road) and declined the other 11 destinations in between (along Heberdeen Avenue) as these destinations are located on a very steep slope (Figure 3.23). Although the land cover dataset used in this research is the most detailed available resource up to date, some areas with impassable obstacles (containers, high fences and trees) are not identified, therefore they are not accounted in the model (Figure 3.24). As noted earlier, besides t-he fact that all those containers are on the process of being moved away, the main purpose for leaving all these obstacles is to test the sensitivity of the model, and also to emphasize that a detailed and updated land use dataset is crucial input for the model.

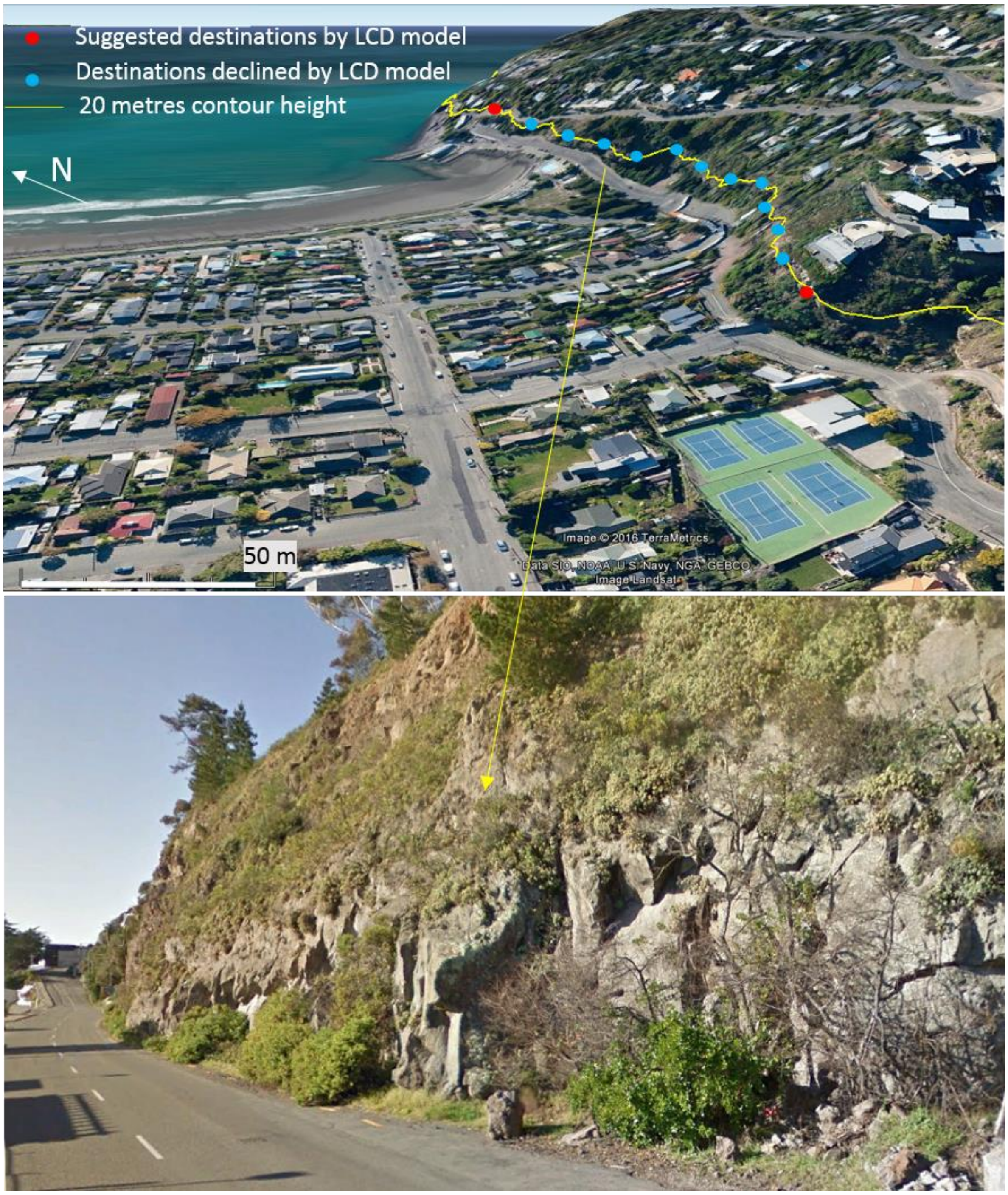

Figure 3.23. Map comparing destinations along the Heberdeen Avenue hillside suggested and declined by the LCD model, looking south-east(top); and photo shows the steepness of the slope along this parts (Google Earth, Street View, 2012) (bottom).

Figure 3.24. Map comparing destinations along the Heberdeen Avenue hillside suggested and declined by the LCD model, looking south-east (top), and photo shows the fences, containers blocking the paths which are not taken into account in the model(image taken in June, 2016) (bottom).

3.3.3.3. Discussion of pedestrian evacuation analysis

Results from real-life tests on uphill evacuation paths and evacuation through flat areas compared to results produced by LCD model with three speeds, and Google Maps give some main points below:

- In all cases, application of average walking speed (1.43 m/s) into the LCD model gives the closest time travels to results from real life testing. In the case of uphill paths, LCD model estimates longer travel time, while when tested on flat areas, it gives a shorter travel time than the test's results. It shows the underestimation on flat areas travel and overestimation on uphill area of the model. This might be explained by the higher weighting on the steepness of the slope rather than other factors when it comes to energy spending comparison in the model.
- In contrast, the Google Maps estimated travel time on uphill paths is shorter than the test; but for flat area test case, it gives a longer travel time. This shows the overestimation in this analysis of travel times by Google Maps on flat areas and underestimation on uphill travel scenarios.
- Application of maximum and minimum walking speeds into the LCD model show the underestimation and overestimation on time travel with up to two times shorter and longer, respectively, compared with the test's results.

There are several factors that might influence on the test results.

- The participant involving in the test is relatively taller than the average height of New Zealander (175.5 centimetres tall for average man) (Daley, 2013). This fact might lead to the wider walking steps; consequently, a faster walking speed although it is acknowledged that physical, mental and emotional conditions are other factors could affect the time travels of evacuees. In addition, while testing the participant only carried a phone with GPS without any backpack or heavy belongings, which is less likely to happen in real life where people tend to/might evacuate with their essential items.
- In addition, while testing the participant only carried a phone with GPS without any backpack, dependent person, or heavy belongings, which is less likely to happen in real life where people tend to/might evacuate with their essential items and/or dependents.

- Furthermore, testing paths are short distances (ranging from only 95m to less than 1km); pedestrian fatigue over time and space was not tested while the participant's speed might vary during the testing.
- When undertaking the real-life evacuation walking tests, the test walker could not start from inside the household, rather they had to start outside houses and on the streets, which means in reality people might need more time to get out of the houses (e.g. door, gate, driveway, fences) before reaching the roads. This could add up to at least 2 to 3 minutes to the time travels of the evacuee. LCD model estimates time travels based on optimal routes but not preferred routes by at-risk population. There are many paths suggested by the LCD model that run through private property, which even though it might be possible to pass through in real life, it is unlikely that evacuee will choose; in addition, the almost ubiquitous presence of fences will prevent movement. Actual travel times therefore may be longer than modelled travel times using maximum walking speed, given the perceptions and preferences of evacuees.

In summary:

- A high-resolution DEM and land use dataset are essential for the LCD model's inputs. Model limitations might be caused by the relatively low resolution (5 m DEM as opposed to 1 m or 2 m DEM, as suggested by (Wood & Schmidtlein, 2012); land cover also does not depict obstacles such as gates and fences).
- The real-life subject's travel time was best approximated by the LCD model that used average walking speed, in contrast to maximum/minimum walking speeds and the Google Maps results. However, for evacuation planning and preparation, these evacuation times based on average speeds should be combined with the delaying factors discussed above and in Section 3.3.2.2.

3.3.4. Vehicle evacuation model

This section details the method used for the vehicle evacuation model for Sumner, its inputs, and discusses the differences between it and the pedestrian models. Finally, results for evacuating by vehicles in Sumner are given. Similar to the two previous pedestrian models, after defining the cost parameters (Sections 3.3.4.1 and 3.3.4.2), Origin points are determined (which are the exposure objects, in this case is the number of vehicles distributed in hazard area (Section 3.3.4.3)). Destination points in the safe zone are then designated, where evacuees are expected to travel (Section 3.3.4.4). Results of evacuation by vehicles are given in Section 3.3.4.5. Note that effects of possible vehicle congestion are not considered, but are discussed in Chapter 4.

3.3.4.1. Cost Surface – Effects of Land Cover

Unlike the pedestrian evacuation model where landscape, demography, and physical ability/psychological factors significantly influence evacuation, almost all vehicle types have some basic standard thresholds, which hinder the movement of the vehicle, or the vehicles are not allowed to overcome for safety reasons. Especially in urban areas where transport systems are built to enable efficient travel for almost all vehicle types and where the effects of different landscapes on vehicle movement do not vary significantly. Therefore, in this study, a road constraint approach is used where all vehicles are assumed to travel to the closest road, and stay on roads to leave the hazard zone. Therefore, land cover is divided into two types: roads with no impediments to travel; and other land types with a higher impediment weighting (ten times higher). This approach forces the model to choose vehicle evacuation paths that only use roads, eliminating the possibility of impassable routes along other land surfaces.

3.3.4.2. Vertical Factor

The vertical factor describes how difficult it is for a vehicle to drive on a particular slope, with high values indicating higher difficulty. In the model, the maximum steepness for vehicles to overcome is -35 (downhill) and 35 (uphill) degrees slope. The vertical factor within this range is one (the lowest and least difficult) whereas road slopes outside this range have an infinite vertical factor (impossible to travel) (Figure 3.25). These chosen bounds are based on the research conducted by (Pingel, 2010)who drove in the foothills and mountainous terrain of Santa Barbara, California to determine the relationship between speed and slope (over a 2.5 hour, 100 km trip). Although the slope's steepness has an effect on travel speed, in most cases the legal speed limit plays a more important role (Pingel, 2010). In this study, 50 km/h, legal speed limit in most of Sumner, is applied for all vehicles in this model, although in the event of a hazard, some people might not always follow the speed limit. As a result, when vehicles are ascending or descending, the only factor that has an effect on the vehicle's travel time is the surface distance it has travelled which is actually always longer if the ground is not flat, and hence travel time would take longer. It is also acknowledged that in reality other factors could affect the movement of vehicle such as weather and road conditions, differences among vehicle types, and traffic congestion.

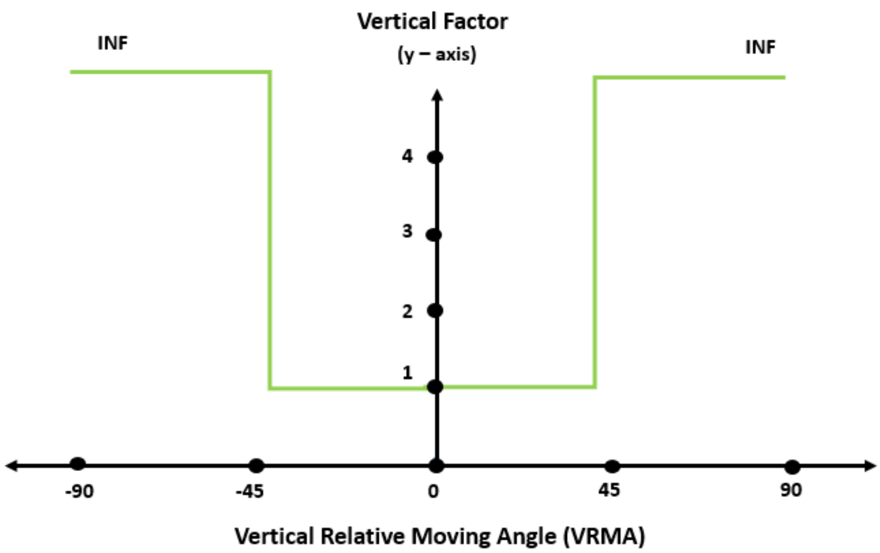

Figure 3.25. Vertical factor binary graph with high and low cutting angles are -35 and 35 degrees. Vertical factor of 1 means no hindrance to the movements while vertical factor of infinity means the vehicles cannot overcome that angle.

3.3.4.3. Origin points for the vehicle evacuation model

The origin points in the vehicle models are based on the spatial overlap of the tsunami inundation zone and vehicle distributions. As determined in (Section 2.3.2.4), vehicles are distributed in three main locations: residential locations; in car parks (for working people and visitors); and on the road for overflow cars from the two previous locations (Figure 3.22). The rules used to assign origin points locations differ:

- *Residential buildings*: each point is located at the centroid of the polygon representing the building. Each point holds a corresponding number of vehicles at that house.
- *Work places - Carpark:* each car park is represented as one point located at the centroid of the polygon representing the car park, except for the Esplanade carpark where the origin points are distributed with the interval of 100 m. Using one point to represent cars in a car park is justified because car parks in Sumner

are relatively small and the actual distance between cars has a negligible effect on overall evacuation distance and time.

- *Unspecified location - Road:* this uses the same origin points dataset as in the pedestrian models, with each point containing the number of vehicles at a given time scenario.

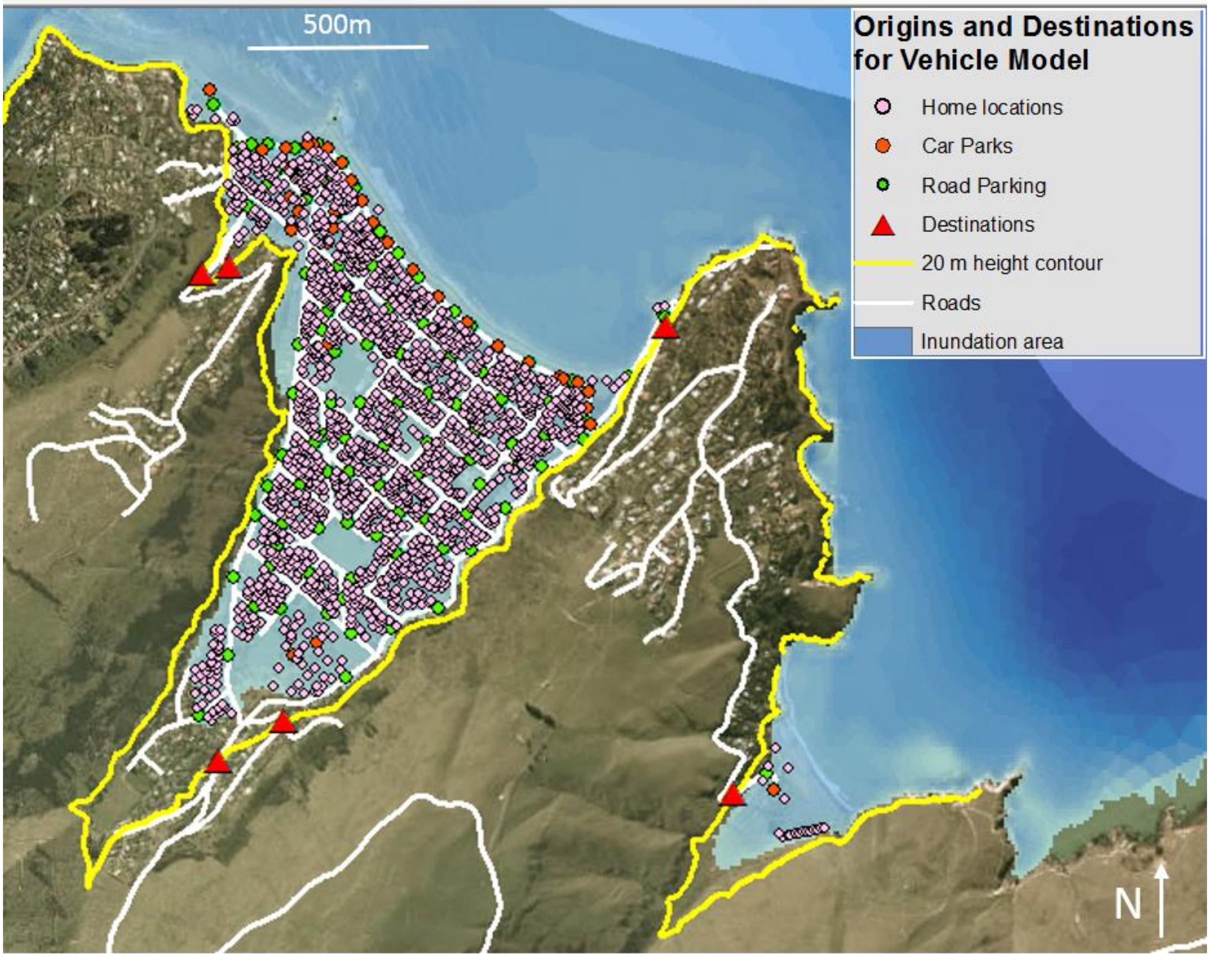

Figure 3.26. Origins and Destinations for vehicle evacuation model.

3.3.4.4. Destination points for vehicle evacuation model

The 20 m contour line from the 5m DEM is used as the boundary between safe and evacuation zones. Instead of producing a collection of destinations points like in the pedestrian models, intersections between the 20 m contour line and roads are chosen to be the destination points for the vehicle model.

3.3.4.5. Results of vehicle evacuation model

The vehicle evacuation model generates three products: (1) recommended evacuation zones and directions based on results produced from the LCD analysis; (2) evacuation time maps for different time scenarios; and (3) evacuation time curves that show the number of evacuating vehicles overtime.

Figure 3.27 shows the optimal directions for vehicles to evacuate from the hazard zone. The major vehicle evacuation zones are presented; zone boundaries were manually delineated along areas separating dominant evacuation directions.

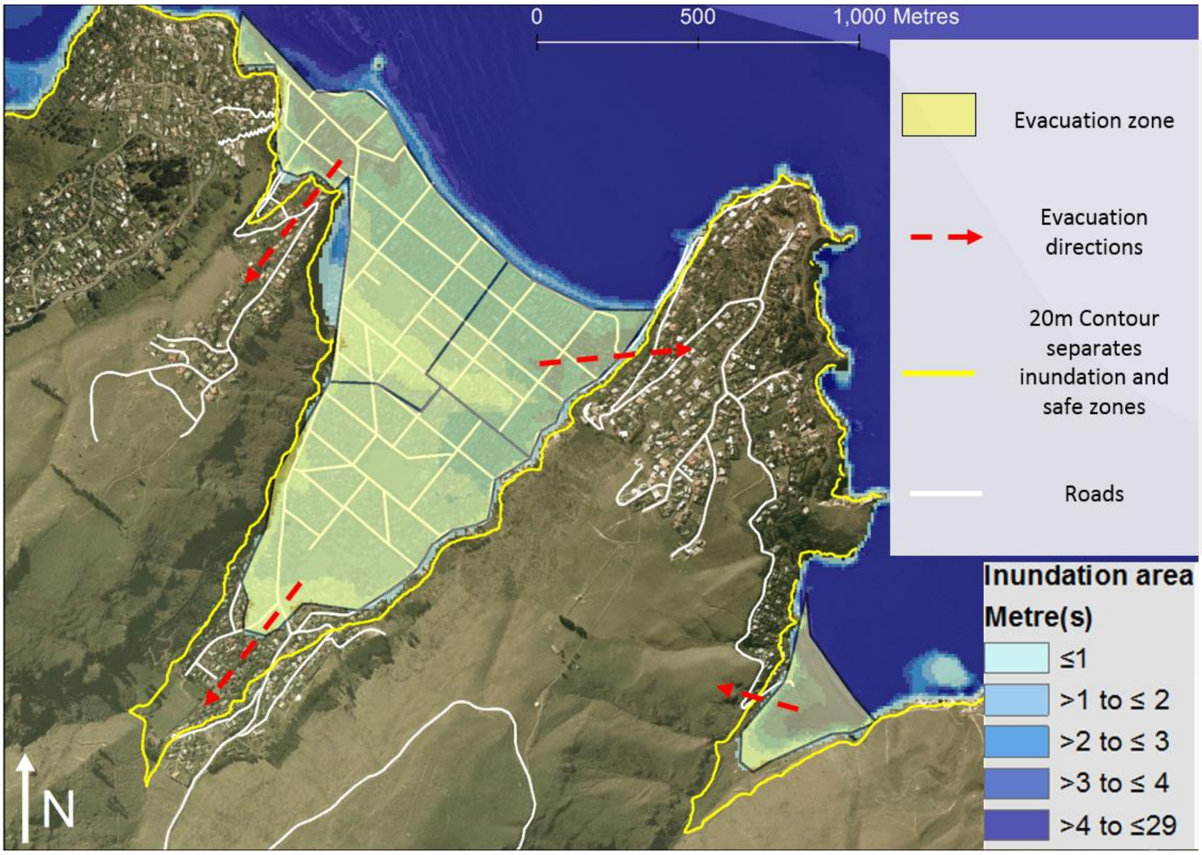

Figure 3.27. Evacuation zones and directions recommended from vehicle evacuation model.

Figure 3.28 shows an example of evacuation times for Sumner for a 12:00 weekend scenario in February. This map shows that the block bounded by Colenso Street, Menzies Street, Head Street and Nayland Street need the longest time (over 1.5 to 2 minutes) to exit the inundation zone using private vehicles.

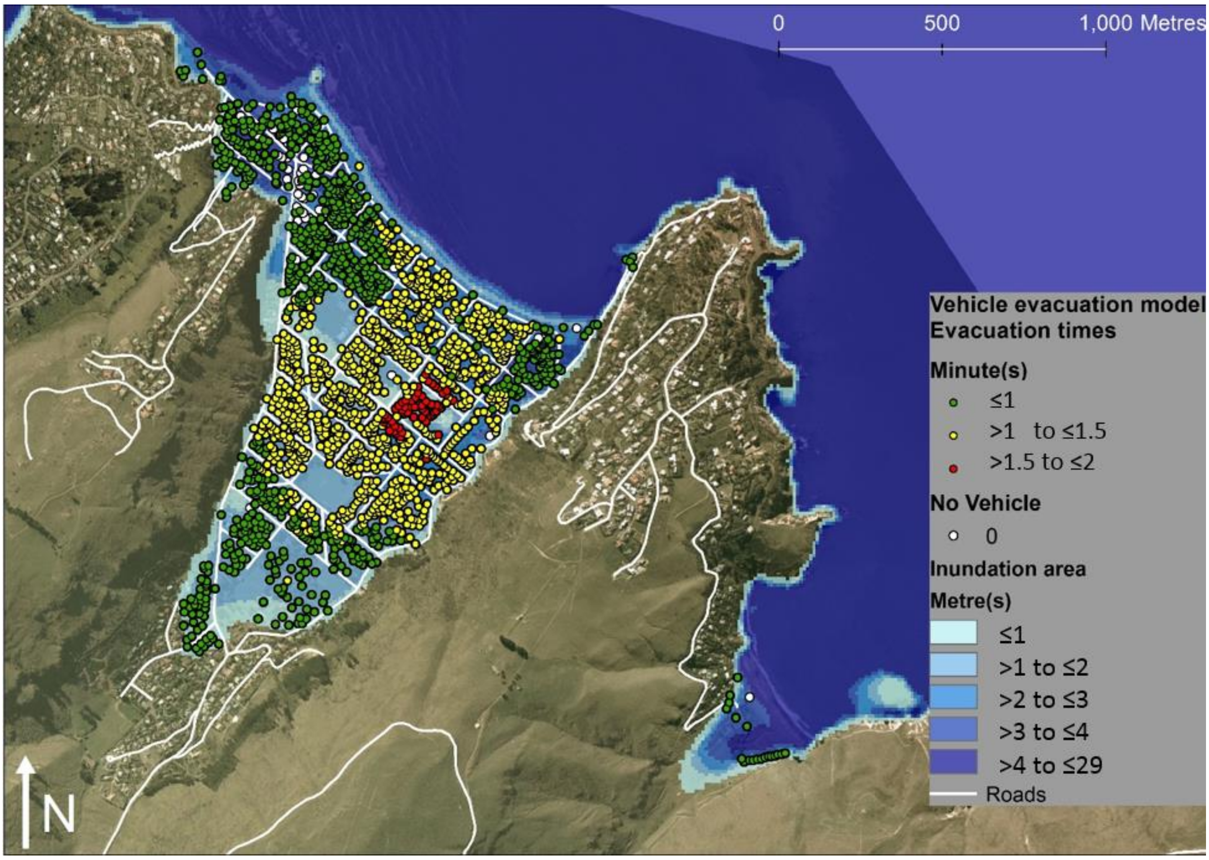

Figure 3.28. Evacuation time for the population in Sumner evacuating by private vehicles, February 12:00 weekend scenario. Time data are overlaid on tsunami inundation model indicating depth values.

Figure 3.29 presents evacuation time curves showing the number of vehicles and corresponding time to evacuate along the resultant paths in all spatio-temporal scenarios. Results for vehicle evacuation time are concentrated in a narrow range from >0 to <2 minutes to exit the hazard zone. Of the vehicles in the inundation zone, 14.5% require 1 min to evacuation; 8.5% of those require 1.5 mins; while only 0.6% of those need 2 mins. Again if all the vehicles depart at the same time, there will be nearly 60% of vehicles evacuate successfully out of hazard zone, and this number increases to 98% after 1.5 min of evacuation. In reality, this would create serious traffic congestion if 2826 cars (in the maximum case with February weekend 12:00) travelled simultaneously from Sumner using the three main exit routes. Discussion of traffic congestion will be presented in Chapter 4.

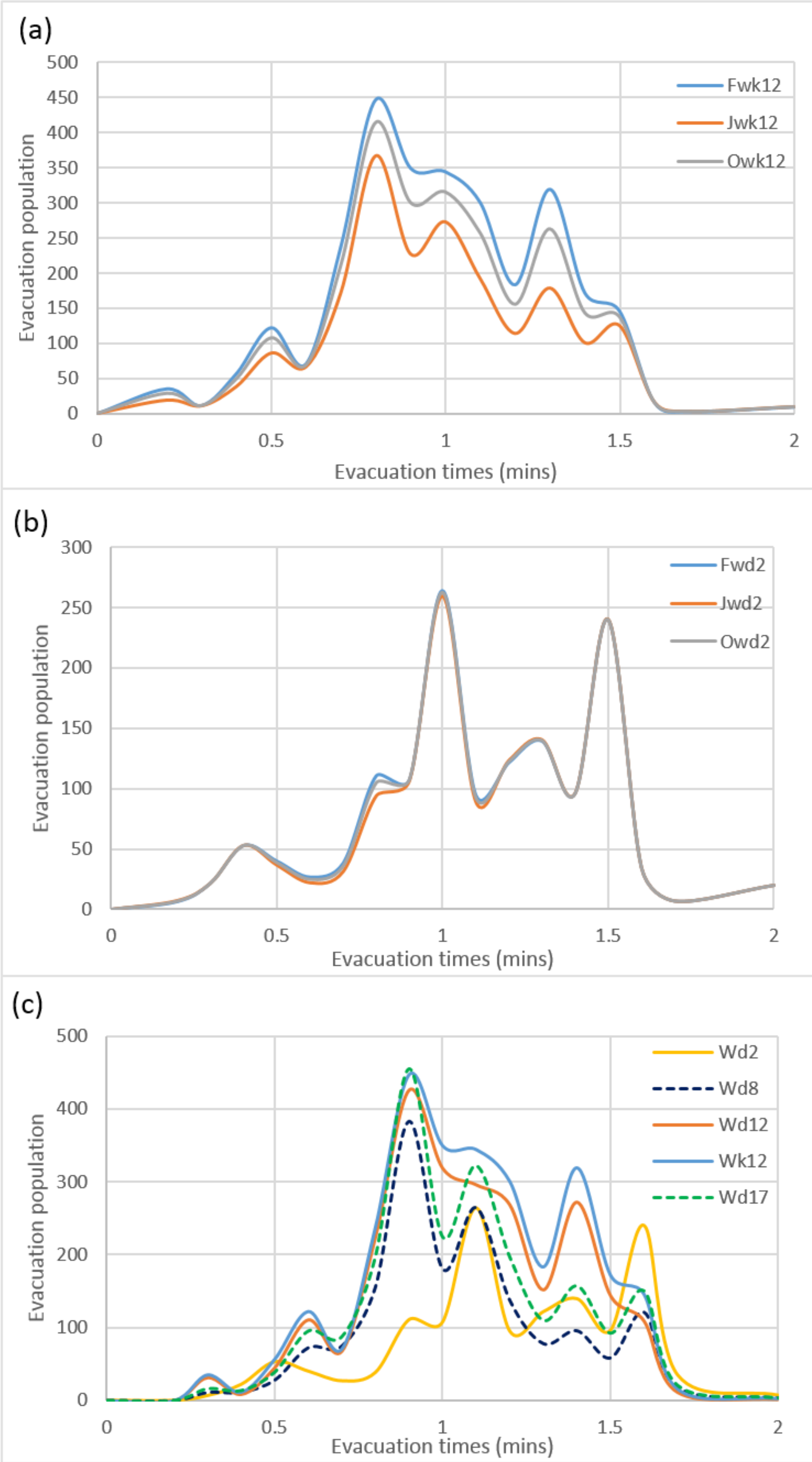

Figure 3.29. Evacuation time curves for vehicles model comparing between different time scenarios; (a) February weekend 12:00 (Fwk12), June weekend 12:00 (Jwk12); October weekend 12:00 (Owk12); (b) February weekend 02:00 (Fwk2), June weekend 02:00 (Jwk2), October weekend 02:00 (Owk2); (c) Weekday 02:00 (Wd2), Weekday 08:00 (Wd8), Weekday 12:00 (Wd12), Weekend 12:00 (Wk12), Weekday 17:00 (Wd17).

3.4. Summary and link to next chapter

This chapter presented a method for anisotropic least cost path distance evacuation modelling for pedestrians, and a similar model modified for private vehicle evacuation. The method has been used to: (1) identify the different evacuation zones with their optimal evacuation paths; and (2) generate evacuation time curves showing the numbers of people/vehicles and their corresponding evacuation times. The next chapter presents a synthesis of the work that has been presented in previous chapters. The next chapter presents a synthesis of the work that has been presented in previous chapters, and are critically discusses the results, research limitations, potential model refinements, and future work.

Chapter 4 Discussion and conclusions

Contents

4.1. Introduction

The aim of this thesis, as outlined in Chapter 1, is to enhance the methodological basis for development of tsunami evacuation plans in Sumner, Christchurch, New Zealand. To achieve this aim, a numerical simulation output of far-field tsunami impacts at Sumner (Lane et al., 2014) was used to establish the maximum likely inundation extent and flow depth. This, together with population census data and daily activity patterns specified for the study area, established the spatio-temporal basis for characterising population exposure (Chapter 2). A geospatial evacuation analysis method (Least Cost Path Distance), augmented with variable population exposure and distributed travel speeds, was used to characterise spatial variation in evacuation times and the corresponding numbers of evacuees and vehicles (Chapter 3). Three 'extreme' end-member scenarios were utilised to address possible evacuation methods; all pedestrians evacuated to 20 metre elevation, all pedestrians to bus stops, and all people evacuated using private vehicles.

This research successfully proposes a method for visualising spatial variation in evacuation times, and relevant numbers of pedestrians and vehicles, to support evacuation planning for Sumner. Implications for tsunami evacuation planning in Sumner are presented in Section 4.4. Although the tsunami inundation scenario used in this research is that of a far-field tsunami, the proposed methods of incorporating population, speed and vehicle distributions, and the evacuation model, are applicable to regional and local source tsunami scenarios. The method is also applicable to other locations, and could contribute to tsunami risk reduction in New Zealand and internationally.

A number of assumptions and limitations exist within components of the population distribution and tsunami evacuation models, which need to be appreciated for valid use of the models and for identifying directions for improvements and future research. Influences of model assumptions on the results are discussed in Section 4.2, followed by recommendations for future research in Section 4.3. Finally, conclusions of this work are presented in Section 4.5.

4.2. Assumptions and limitations of the models

This Section critically discusses the influences of assumptions within the spatio-temporal population distribution and tsunami evacuation models on the results. This critique will inform implications of research results for tsunami evacuation planning in Sumner (Section 4.4) and recommendations for future research (Section 4.3).

4.2.1. Spatio-temporal population exposure models

Due to census data not specifically categorising certain population groups of interest (numbers of children under five year of age staying at home, children aged between 13-14, home-based impaired people, and visitors), assumptions for these groups' numbers were required (Section 2.3.2.1). Although these assumptions are based upon local knowledge and reasonable estimations, without updated and detailed census data the uncertainty of these assumptions remains. The over- or under-estimation of any population group would result in the under- or over-estimations of population exposure. In this specific case study, visitor numbers are likely an important influence on the population exposure results, as this is a large population group with pronounced diurnal, weekday/weekend, and seasonal changes. Therefore, the population of each group and their commuting patterns are critical inputs to the population, speed and vehicle distribution models. This is because the latter two models are based on the results of the former model.

Regarding the time profiles of human activities, the method applied in this research integrates data on commuting patterns and work shifts, local knowledge, and other related research (Fraser et al., 2014; Glickman, 1986; Southworth, 1991). However, as mentioned above, this approach also relies on a priori assumptions and modeller judgement. Future validation of these assumptions will be important to reduce model uncertainty and provide more robust estimates of evacuation times and population movements.

Assumptions in this research for the pedestrian speed distribution model account for group evacuation, including variability in mobility relating to age and physical ability. However other factors such as gender, culture, or religion of the exposed population remain unaddressed. As discussed in Chapter 1, these factors influence evacuee travel speed and hence potentially influence model results.

As discussed in Chapter 2 when developing the vehicle distribution model, the assumption of one car per non-resident working in Sumner, and one car per four visitors, is a simplified approach. This is because people might travel to Sumner by bus, or the number of visitors using a single vehicle to visit Sumner might vary. In addition, simply assuming all private vehicles as having the areal footprint (2 × 5 metres) will contribute to inaccuracy in determining traffic flows.

4.2.2. Tsunami evacuation models

In reality, not all people evacuate in the event of a hazard, as they are unaware of the danger of the situation due to inexperience or lack of knowledge (Wood & Schmidtlein, 2012). Other factors could be physical or mental disability, or their emotional state (Fraser et al., 2014; Nishikiori et al., 2006; Post et al., 2009; Yeh, 2010). In addition, given the difference in people's preferences, their selection of evacuation means may vary. Therefore, utilising the three "extreme" end-member scenarios (on foot to higher ground, on foot to public transportation pick-up points, and using private vehicles) with a compliance rate of 100% is unrealistic. However, these separate approaches should be considered initial steps towards developing a more comprehensive mixed pedestrian-vehicle model.

In the scope of this analysis, pedestrian fatigue is assumed to be minimal and travel speeds are presumed to remain constant. In reality, people's travel speed will vary depending on physical fitness and interaction with others in crowds, particularly on the longer travel paths, as well as climatic conditions (e.g. temperature, precipitation and wind, time of day, season). As noted in the discussion of the pedestrian evacuation model results in Section 3.3.3.3, it is likely that people will travel with their essential belongings, which will further affect their travel speed. Thus the approach here is simplified, and could be improved using agent-based modelling approaches that account for individual differences in physical fitness and impacts of carrying possessions.

The assumption on using vehicles for evacuation as one vehicle per household (home locations) or five people (work and unspecified locations) is a simplified approach. In reality people might travel with their possessions or even their trailer (Lindell et al., 2005), and hence consuming greater road space. Applying a speed of 50 km/h for all vehicles in the case of far-field scenario when people have longer preparation time appears to be realistic. However, in other scenarios with very limited time to evacuate, it would be expected that people exceed the speed limit.

The LCD approaches described in this study do not account for changes in route capacity or congestion, which especially affect the Sumner area where there are limited exit routes. Research by Homburger et al. (1992) showed that with vehicle speeds of 48-74 km/hr on two-lane roads, the maximum traffic volume is 1400 passenger car per hour per lane, or 23 cars per minute per lane. Results of the vehicle evacuation model presented here indicate that if everyone in Sumner were to evacuate by car and depart at the same time, within two minutes there would be 1,400-2,800 cars heading to 4-5 locations, mostly on narrow windy dead-end roads. This means serious congestion would be expected to happen in Sumner if all the at-risk population evacuated by private vehicles, compromising rapid evacuation, especially if vehicles start to break down in traffic jams. Another issue is capacity for cars at the destination points as people might park their cars part-way up the hills and block further people from coming uphill. The vehicle evacuation model also does not account for traffic flows entering Sumner from Christchurch City using the coastal evacuation routes. These congestion and contra-flow effects need to be addressed in future modelling. Additional factors that may increase travel times are environmental conditions at the time of an evacuation (e.g. adverse weather, night-time evacuation) are also not considered in the model. Furthermore, potential impacts to evacuation routes from local-source tsunamigenic earthquakes, such as ground failure and rock fall, liquefaction and lateral spread, and rubble from damaged structures, would also have a significant impact on travel times.

Although a pedestrian speed distribution model has been developed (Chapter 2), only a single speed simulation has been used as an input for the LCD model (Chapter 3). Therefore, using average speeds from a number of simulations for speed distribution model is required to have a more reliable evacuation time.

As discussed in Chapter 3, travel time results from the tsunami evacuation model are based on the optimal evacuation routes, and not potentially preferred routes taken by at-risk people. There are many paths suggested by the LCD model that run through private property. However, the presence of fences and other obstructions needs to be accounted for. Even if travel paths through adjoining properties are easily traversed, in reality it is unlikely that most evacuees will use these routes due to lack of knowledge, or their initial instinct to evacuate using the nearest public roadway. For far-source scenarios this is unlikely to be an issue but in the case of local-source scenarios having the community be aware of the most efficient neighbourhood evacuation routes, which could be through adjoining properties, should be a focus of local planning and education initiatives.

4.3. Model refinements and areas for future research

The purpose of this section is to provide recommendations for future work to refine the present model, which would further the understanding of evacuation procedures, response challenges, and relief planning for tsunami threats. Areas suggested for continued and future research are discussed below.

4.3.1. Congestion and disruption during evacuation

Congestion and disruption during evacuation could happen due to both human and natural factors. As discussed in Section 4.2, the combination of different evacuation means should be considered in future research to develop mixed pedestrian-vehicle evacuation models. Similar studies on vehicle use rate have been conducted in the U.S.A. for hurricane hazard (Dow & Cutter, 2000; Lindell et al., 2005); in Auckland, New Zealand for volcanic hazard (Tomsen et al., 2014); and in the most recent report on tsunami evacuation route planning for Tauranga City, New Zealand (Tauranga City Council, 2015). To provide the most realistic estimates of congestion potential will require the identification of congestion hotspots or pinch points (Priest et al., 2015; Tauranga City Council, 2015), determining crowd density and crowd flow rates (Still, 2014), and determining the range of travel speeds for people and vehicles converging towards common evacuation routes.

Additional studies and compilation of dataset on potential disruptions due to other seismic hazards or adverse environmental conditions (discussed in Section 4.2) are required areas for future research. In Sumner, the most likely seismic hazards in the event of a local tsunamigenic earthquake are rock-falls and landslides, thus incorporating relevant geotechnical datasets would improve the realism of model results. In addition, Sumner and other coastal areas in New Zealand are characterised by strong coastal winds that might affect evacuation speeds; this factor could be integrated into the LCD approach as a horizontal factor.

4.3.2. Evacuation behaviour

Understand evacuation behaviour of the at-risk population would provide an insight into their decision making on whether or not to evacuate (which determines *compliance rate*); when to evacuate (*departure time*); and where to evacuate to (*preferred evacuation routes and wayfinding*).

4.3.2.1. Compliance rate

Ideally, modelled compliance rate should be based on empirical research, i.e. records of numbers of people that did evacuate in previous tsunami events. Given New Zealand has not experienced a major tsunami requiring a mass-evacuation in recent times, this number has been proposed based on the prior hazard assumptions by a group of scientists (NZEIR, 2015). However, more efforts are required to understand the factors involved in this complex process of evacuation decision making. Although there is a lack of sociological or psychological literature on evacuation behaviour during tsunami, as discussed in Wood et al. (2016), literature on evacuation decision-making for other sudden-onset hazards could be beneficial (Dash & Gladwin, 2007; Lindell et al., 2011). In the Protection Action Decision Model, a theoretical behaviour framework, variables such as environmental and social cues, receiver characteristics, and information sources are identified as deciding factors for decision making (Lindell & Perry, 2012). This framework has been used to explain evacuation behaviour in American Samoa during the 2009 Samoa Islands tsunami (Apatu et al., 2016).

4.3.2.2. Departure time

The evacuation behaviour surveys among visitors and residents in Napier conducted by Fraser et al. (2013) confirmed that people's intended actions would *delay evacuation*, although real-life disaster responses may in fact differ from those described in the survey. Wood & Schmidtlein (2012) have explained this delayed action through people attempting to fulfil caregiver roles (e.g. helping children, the elderly, or pets) or gathering items they deem to be critical to their post-disaster quality of life (e.g. emergency kits, important paperwork). Individuals will also take time to process observed natural cues (prolonged ground shaking or shoreline draw-down) or social cues (being told by people to evacuate). In addition, many will take time to validate what they experienced (follow people around them, contact trusted sources, or consult social media), which is often called "milling" in the social sciences literature (Wood & Schmidtlein, 2012).

Other evacuation research (Fraser et al., 2014) addressed this factor by applying a Rayleigh function to randomly assign a departure time. Values of 7 and 38 mins were used as lower and upper bounds, respectively, for the potential evacuation departure time curves, and each individual or group had a randomly chosen number of minutes added to their evacuation time to estimate the total required time to evacuate successfully. Thus, in the case of near-field tsunami scenario in Sumner, with less than one hour of tsunami wave travel time, people with evacuation times of more than 10 minutes might not be able to evacuate successfully from the inundation zone if these delaying factors are considered.

4.3.2.3. Preferred evacuation routes and wayfinding of at-risk population

Previous research has shown various factors affect evacuation route choice: knowledge of the local road network (Lindell & Prater, 2007); most familiar routes (Dow & Cutter, 2002; Prater et al., 2000), or evacuees taking any possible egress route (Moriarty et al., 2007). Better understanding of evacuation behaviour is still required, which could include whether people perceive the need to evacuate given the environmental cues, what additional social cues would result in quicker individual decision making, and the influence of household characteristics (e.g. caregiver status for children or pets) on evacuation decision making.

Furthermore, these understandings need to transform into factors which could be incorporated into the evacuation model. An example of evacuation choice incorporated into evacuation model is research conducted by Anh et al. (2012) using ABM, where two agent groups are developed; a fox agent and a sheep agent. A fox agent is defined as a pedestrian who has been trained on evacuation procedures or has knowledge of how get to safe place efficiently, while the sheep agent represents pedestrians evacuating randomly at junctions or following one fox agent.

Finally, a logical next step is to compare optimal routes resulting from the model to preferred routes by geospatially tracking volunteers in a local evacuation exercise. Research involving ground-truthing fieldwork could strengthen the approach by providing insights into evacuation preferences and potential congestion points. By incorporating into the model actual variations in pedestrian travel speeds over relevant land-cover types, slopes, and distances, pedestrian fatigue over time and space can be accounted for.

A mixed evacuation model that leverages LCD and network-based analytical approaches would help clarify these areas mentioned above. LCD-based approaches could model movement in less constrained areas (e.g. rural areas), whereas network-based approaches could be linked to LCD-based approaches in more constrained areas (e.g. dense urban environments with several rules relating to the network). Finally, an integration of ABM would strengthen the mixed model by incorporating individual characteristics, lending more realism to the modelling results.

4.3.3. Other areas for future research

The population time profiles developed in this research enable a comparison of different temporal cycles (diurnal changes, weekday versus weekend, seasonal changes). However, a finer temporal scale than the hourly interval will undoubtedly provide a greater insight into the spatio-temporal variability in human activities. Furthermore, as discussed in Section 4.2, validation of the underlying movement data that the time profiles are based on is necessary. In an example of recent research, Greger (2014) validated their modelled time profiles by comparing them to a real-world door count for a number of buildings within their study area. Spatio-temporal characterisation of the exposed population could also be improved beyond using the census data, which are only collected on a five-yearly basis. For example, use of appropriately anonymised postal, billing and social media data, in addition to traffic monitoring data, could provide finer-resolution population counts and movements, and could especially inform ABM approaches.

Detailed and up-to-date land cover data will also enhance the accuracy of the model. For example, a recent work by Wood et al. (2016), to better account for land cover influences on an evacuation, besides roads and buildings layers, authors created 'artificial driveways' to geospatially connect buildings to road networks.

Results of spatio-temporal population distribution models could also be applicable and beneficial when estimating number of injuries. Yeh (2010) conducted research using a simplified model of a human body to test whether a person can remain standing within tsunami flow. Incorporating findings from this research with results from the distribution models could provide a better estimation of injuries for those who do not evacuate successfully. In addition, spatial accessibility for population evacuation expressed in time can be used not only for evacuees but also for pre- and post-event rescue teams. In this case, Pingel (2010) indicated the usefulness of the analysis of time it takes for the rescue teams to get to distressed persons.

4.4. Implications for tsunami evacuation in Sumner

A primary objective of this thesis was to develop a method to characterise spatial variability in tsunami evacuation times for Sumner, and corresponding evacuee population and vehicle numbers. To support official Civil Defence and Emergency Management (CDEM) planning, further research is required to better characterise spatio-temporal population exposure, the dynamics of population movements during evacuation, and the psycho-social aspects of human behaviour that may impede or facilitate successful evacuation (as discussed in Section 4.3). However, this thesis provides the most detailed tsunami evacuation assessment to date for any part of coastal

Christchurch. The following results are of immediate use to guide CDEM thinking on tsunami evacuation for Sumner:

- Census count, schools rolls, and numbers/locations of vulnerable people in aged care; estimates of numbers/locations of private vehicles for Sumner in the maximum extent tsunami zone;
- Detailed multiple exposure scenarios facilitate visualisation of spatio-temporal distribution of evacuation demand, and better characterisation of population demographics and evacuation dynamics could provide information on:
    - Approximate numbers of people and demographic composition exposed to the tsunami hazard, and potential casualties;
    - Areas with greatest number of people and vehicles requiring longer times to evacuate, versus the likelihood of successful evacuations for any given time scenario;
    - Approximate numbers of people and vehicles, and time required to arrive at certain evacuation points (e.g. 20 metre elevation, bus stops and private vehicle evacuation locations);
    - Optimal evacuation directions for different evacuation areas.

  This information can assist emergency managers in:
    - Prioritising the locations within the evacuation zone from which people must leave, and determining the most appropriate type of tsunami risk-reduction strategies;
    - Real-time decision making in emergency response to ensure that routes and refuges have sufficient capacity in any event, to provide adequate personnel, and to prioritise resource allocation (e.g. bus drivers, New Zealand Police, coordination between emergency management and other agencies such as public health officials);
    - Using these results and maps in evacuation education and training will enable communities to work more effectively amongst themselves and in conjunction with emergency managers to receive and manage evacuees. This may motivate faster speeds than expected given the potential evacuation delays (discussed in Section 4.3).

4.5. Conclusions

This thesis has made a methodological contribution to tsunami evacuation simulation by characterising variable spatio-temporal population exposure, and incorporating terrain properties into population and vehicle movements.

Based on the dynamics of daily human activity, methods for modelling spatio-temporal distributions of different population groups, their relevant speeds, and private vehicles in Sumner were presented (Chapter 2). Results of the distribution model reflect variations in human daily activities, accounting for diurnal and seasonal variation. This helps provide a more realistic assessment of the population exposure to tsunami hazard in Sumner, and hence is an important input for the anisotropic Least Cost Path Distance evacuation model used for pedestrian and private vehicle evacuation (Chapter 3).

Results of this research show the usefulness of applying terrain effects on evacuation time estimates, and the valuable contribution of GIS for visualising variable evacuation times and evacuation demand. These results are presented in the form of three products: evacuation zones; evacuation time curves; and evacuation time maps. This set of results enables emergency managers to make a rapid assessment of the optimal evacuation directions from different evacuation zones, and the total exposed population with their evacuation times in different scenarios. Thus, emergency managers can use these results to prioritise locations and determine the most appropriate type of tsunami risk-reduction strategies. Furthermore, by focusing on three end-member scenarios (pedestrians moving to higher ground and to bus stop pickup points, and use of private vehicles), this approach provides important information on evacuation times and contributes to the initial stages of evacuation planning. It also emphasises the need, and lays the foundation for, more realistic research in future on mixed evacuation analyses.

Sumner, a coastal suburb in Christchurch city, New Zealand has been used in this research as a case study for evacuation modelling. There are site-specific aspects of this case study that may be different from other coastal sites, such as New Brighton, Christchurch, where the landscape is flat, unlike Sumner which is surrounded by hills. However, the methods introduced in this study can be generalised other areas and indeed other hazards where evacuation is considered for implementation due to the generic methods. Extending the study to include regions outside of the area assessed in this research will also help inform tsunami evacuation planning for wider Christchurch City and around New Zealand. In addition, the methods are equally applicable for post-disaster analyses, in particular evacuation of surviving people from fast-onset disaster zones impacted by, for example, earthquakes or industrial accidents.

Further work is required to satisfy the needs of real evacuation planning for Sumner with regards to the dynamics of population movements during evacuation, and the psycho-social aspects of human behaviour. This research developed an evacuation model based on one tsunami inundation model (far-field scenario). Modelling tsunami evacuation with different inundation levels would provide a test of the present research, as well as informing emergency managers and planners about the likely impacts associated with lower-magnitude events from local- and regional-source tsunami.

References

Abidin, H. Z., & Kato, T. (2009). Why Many Victims: Lessons from the July 2006 South Java Tsunami Earthquake. *Advances in Geosciences, Volume 13: Solid Earth (SE)*, *13*, 249.

Abustan, M. S. B. H. (2013). Numberical simulation of evacuation process against tsunami disaster in Malaysia by using distinct element method based multi agent model. PhD Thesis, Kyoto University. http://dx.doi.org/10.14989/doctor.k17864

Affan, M., Goto, Y., & Sabti, A. (2012). Tsunami Evacuation Simulation for Disaster Awareness Education and Mitigation Planning of Banda Aceh. In *Proceeding of the 15th World Conference on EarthquaNe Engineering, Lisbon, Portugal*.

Ahola, T., Virrantaus, K., Krisp, J. M., & Hunter, G. J. (2007). A spatio-temporal population model to support risk assessment and damage analysis for decision-making. *International Journal of Geographical Information Science*, *21*(8), 935–953.

Anguelova, Z., Stow, D. A., Kaiser, J., Dennison, P. E., & Cova, T. (2010). Integrating fire behavior and pedestrian mobility models to assess potential risk to humans from wildfires within the US–Mexico border zone∗. *The Professional Geographer*, *62*(2), 230–247.

Anh, N. N., Chevaleyre, Y., & Zucker, J. D. (2012). Optimizing sign placements for crowd evacuation on road network in case of tsunami alert. *International Journal of Computer Science and Artificial Intelligence*, *2*(4), 33.

ArcGIS. (2009a). How the path distance tool works. Retrieved from http://pro.arcgis.com/en/pro-app/tool-reference/spatial-analyst/how-the-path-distance-tools-work.htm

ArcGIS. (2009b). Understanding Cost Distance analysis. Retrieved from http://pro.arcgis.com/en/pro-app/tool-reference/spatial-analyst/understanding-cost-distance-analysis.htm

Atwater, B. F., Cisternas, M. V, Bourgeois, J., Dudley, W. C., Hendley II, J. W., & Stauffer, P. H. (1999). *Surviving a tsunami: lessons from Chile, Hawaii, and Japan*. US Dept. of the Interior, US Geological Survey;

Bernard, E. N. (2005). *Developing tsunami-resilient communities: the national tsunami hazard mitigation program*. Springer Science & Business Media.

Berryman, K. (2005). *Review of tsunami hazard and risk in New Zealand*. Institute of Geological & Nuclear Sciences.

Bhaduri, B., Bright, E., Coleman, P., & Urban, M. L. (2007). LandScan USA: a high-resolution geospatial and temporal modeling approach for population distribution and dynamics. *GeoJournal*, *69*(1-2), 103–117.

Blong, R. (2000). Volcanic hazards and risk management. *Encyclopedia of Volcanoes (E. H. Sigurdsson)*, 1215–1227.

Bonnefoy, P., & J.Lyons, P. (2015, September 17). Why Chile's lastest Big Earthquake has a smaller death toll. *New York Times*. Retrieved from http://www.nytimes.com/2015/09/18/world/americas/chile-earthquake-tsunami-impact.html?_r=0

Borrero, J. C., & Goring, D. G. (2015). South American Tsunamis in Lyttelton Harbor, New Zealand. *Pure and Applied Geophysics*, *172*(3-4), 757–772.

Bryant, E. (2014). *Tsunami: the underrated hazard*. Springer.

Budiarjo, A. (2006). Evacuation shelter building planning for tsunami prone area: a case study of Meulaboh city, Indonesia. *Enschede, ITC*.

Canterbury Geotechnical Database. (2015). LiDAR and Digital Elevation Models Map Layer CGD0500. Retrieved June 30, 2015, from https://canterburygeotechnicaldatabase.projectorbit.com/

CBRE. (2012). NZ office worker space "average", says CBRE. Retrieved from http://www.cbre.co.nz/aboutus/mediacentre/mediaarchives/Pages/042012.aspx

CDEM Bay of Plenty. (2013). Tauranga Tsunami Evacuation Zones. Retrieved from http://bopcivildefence.govt.nz/media/11308/tsunami_map_-_tauranga_mt_maunganui_papamoa_1_.pdf

Charnkol, T., & Tanaboriboon, Y. (2006a). Evacuee behaviors and factors affecting the tsunami trip generation model: A case study in phang-nga, Thailand. *Journal of Advanced Transportation*, *40*(3), 313–330.

Charnkol, T., & Tanaboriboon, Y. (2006b). Tsunami evacuation behavior analysis: One step of transportation disaster response. *IATSS Research*, *30*(2), 83–96.

Charvet, I., Ioannou, I., Rossetto, T., Suppasri, A., & Imamura, F. (2014). Empirical fragility assessment of buildings affected by the 2011 Great East Japan tsunami using improved statistical models. *Natural Hazards*, *73*(2), 951–973.

Chooramun, N., Lawrence, P. J., & Galea, E. R. (2012). An agent based evacuation model utilising hybrid space discretisation. *Safety Science*, *50*(8), 1685–1694.

Christchurch City Council. (2016a). Distant source tsunami. Retrieved from https://www.ccc.govt.nz/services/civil-defence/what-to-do-in-an-emergency/tsunami/distant-source-tsunami

Christchurch City Council. (2016b). *Getting started in Food businees. Restaurant bar/cafe*. Christchurch, New Zealand. Retrieved from http://www.ccc.govt.nz/assets/Documents/Consents-and-Licences/business-licences-and-consents/Food/RestaurantBarCafe-healthsafety.pdf

Christchurch City Council. (2016c). Tsunami Evacuation information for coastal Christchurch. Retrieved from http://resources.ccc.govt.nz/files/CCCTsunamiBrochure-informationondisastershazards.pdf

Clark, G. E., Moser, S. C., Ratick, S. J., Dow, K., Meyer, W. B., Emani, S., … Schwarz, H. E. (1998). Assessing the vulnerability of coastal communities to extreme storms: The case of reverse, MA., USA. *Mitigation and Adaptation Strategies for Global Change*, *3*(1), 59–82. http://doi.org/10.1023/A:1009609710795

Cockings, S., Martin, D., & Leung, S. (2010). Population 24/7: building space-time specific population surface models. In *The GIS Research UK 16th Annual Conference GISRUK 2008* (pp. 41–48).

Cousins, W. J. (2009). *RiskScape-Development of a Default Assets Model for Hawkes Bay*. GNS Science.

Cova, T. J. (1999). GIS in Emergency Management. *Geographical Information Systems: Principles, Techniques, Applications, and Management*, (Rejeski 1993), 845–858. Retrieved from http://citeseerx.ist.psu.edu/viewdoc/download?doi=10.1.1.134.9647&rep=rep1&type=pdf

Cova, T. J., & Church, R. L. (1997). Modelling community evacuation vulnerability using GIS. *International Journal of Geographical Information Science*, *11*(8), 763–784. http://doi.org/10.1080/136588197242077

Daley, C. (2013). Body shape and dieting - Average heights and weights. Retrieved from Te Ara - the Encyclopedia of New Zealand

Dash, N., & Gladwin, H. (2007). Evacuation decision making and behavioral responses: Individual and household. *Natural Hazards Review*, *8*(3), 69–77.

Davies, H. L., Davies, J. M., Perembo, R. C. B., & Lus, W. Y. (2003). The Aitape 1998 tsunami: Reconstructing the event from interviews and field mapping. In *Landslide Tsunamis: Recent Findings and Research Directions* (pp. 1895–1922). Springer.

Davies, W. K. D. (1984). Factorial ecology. Gower Publishing Co., Aldershot (UK). 1984.

De Lange, W. P., & Healy, T. R. (1986). New Zealand tsunamis 1840–1982. *New Zealand Journal of Geology and Geophysics*, *29*(1), 115–134.

Dewi, R. S. (2012). A-Gis Based Approach of an Evacuation Model for Tsunami Risk Reduction. *Journal of Integrated Disaster Risk Management*, *2*(2), 22. http://doi.org/10.5595/idrim.2012.0023

Dobson, J. E., Bright, E. A., Coleman, P. R., Durfee, R. C., & Worley, B. A. (2000). LandScan: a global population database for estimating populations at risk. *Photogrammetric Engineering and Remote Sensing*, *66*(7), 849–857.

Doughton, S. (2013). Grays Harbor County school to build first US vertical-tsunami refuge. *Seattle Times, October 15*.

Dow, K., & Cutter, S. L. (2000). Public orders and personal opinions: Household strategies for hurricane risk assessment. *Global Environmental Change Part B: Environmental Hazards*, *2*(4), 143–155.

Dow, K., & Cutter, S. L. (2002). Emerging hurricane evacuation issues: hurricane Floyd and South Carolina. *Natural Hazards Review*, *3*(1), 12–18.

Dunbar, P., McCullough, H., Mungov, G., Varner, J., & Stroker, K. (2011). 2011 Tohoku earthquake and tsunami data available from the National Oceanic and Atmospheric Administration/National Geophysical Data Center. *Geomatics, Natural Hazards and Risk*, *2*(4), 305–323. http://doi.org/10.1080/19475705.2011.632443

Elnashai, A. S., Gencturk, B., Kwon, O.-S., Al-Qadi, I. L., Hashash, Y., Roesler, J. R., … Valdivia, A. (2010). The Maule (Chile) earthquake of February 27, 2010: Consequence assessment and case studies. *MAE Center Report No. 10-04*.

Franzese, O., & Liu, C. (2008). Emergency evacuations, transportation networks. In *Encyclopedia of GIS* (pp. 271–274). Springer.

Fraser, S. (2014). *Informing the development of tsunami vertical evacuation strategies in New Zealand*. PhD Thesis, Massey University.

Fraser, S. A., Johnston, D. M., & Leonard, G. S. (2013). *Intended evacuation behaviour in a local earthquake and tsunami at Napier, New Zealand*.

Fraser, S. A., Matsuo, I., Leonard, G. S., & Murakami, H. (2012). Tsunami evacuation: Lessons from the Great East Japan Earthquake and tsunami of March 11th 2011. GNS Science Report.

Fraser, S. A., Wood, N. J., Johnston, D. M., Leonard, G. S., Greening, P. D., & Rossetto, T. (2014). Variable population exposure and distributed travel speeds in least-cost tsunami evacuation modelling. *Natural Hazards and Earth System Science*, *14*(11), 2975–2991.

Freire, S., Aubrecht, C., & Wegscheider, S. (2012). When the Tsunami Comes to Town – Improving Evacuation Modeling by Integrating High-resolution Population Exposure. *Proceedings of the 9th International ISCRAM Conference*, (April), 1–5.

Fritz, H. M., & Borrero, J. C. (2006). Somalia field survey after the December 2004 Indian Ocean tsunami. *Earthquake Spectra*, *22*(S3), 219–233.

Fritz, H. M., Borrero, J. C., Synolakis, C. E., & Yoo, J. (2006). 2004 Indian Ocean tsunami flow velocity measurements from survivor videos. *Geophysical Research Letters*, *33*(24).

Fritz, H. M., Papantoniou, A., Biukoto, L., Albert, G., & Wei, Y. (2014). The Solomon Islands tsunami of 6 February 2013 in the Santa Cruz Islands: field survey and modeling. In *EGU General Assembly Conference Abstracts* (Vol. 16, p. 15777).

Gatrell, A. C., Vincent, P., & Initiative, R. R. L. (1990). *Managing natural and technological hazards: the role of GIS*. Economic and Social Research Council, Regional Research Initiative.

Geohaz. (2008). *Tsunami Preparedness Guidebook*. Retrieved from http://www.geohaz.org/#!tsunami-preparedness-guidebook/n7k4w

Gisborne District Council. (2013). *Proposed Plan Change 56 - Firefighting Water Supplies Code of Practice. Combined Regional Land and District Plan Section 32 Report.*

Glickman, T. S. (1986). A Methodology for Estimating Time-of-Day Variations in the Size of a Population Exposed to Risk. *Risk Analysis*, *6*(3), 317–324.

GNS. (n.d.). New Zealand Tsunami Database: Historic and Morden Records. Retrieved January 1, 2016, from http://data.gns.cri.nz/tsunami/

Goff, J., Chagué-Goff, C., Nichol, S., Jaffe, B., & Dominey-Howes, D. (2012). Progress in palaeotsunami research. *Sedimentary Geology*, *243*, 70–88.

González Riancho, P., Aguirre Ayerbe, I., Aniel Quiroga, Í., Abad, S., González, M., Larreynaga, J., … Medina, R. (2013). Tsunami evacuation modelling as a tool for risk reduction: application to the coastal area of El Salvador. *Natural Hazards*, *13*, 3249–3270.

Goodchild, M. F., Klinkenberg, B., & Janelle, D. G. (1993). A Factorial Model of Aggregate Spatio-temporal Behavior: Application to the Diurnal Cycle. *Geographical Analysis*, *25*(4), 277–294.

Graehl, N., & Dengler, L. (2008). Using a GIS to Model Tsunami Evacuation Times for the Community of Fairhaven, California. *AGU Fall Meeting Abstracts*, D1324.

Greger, K. (2014). Spatio-Temporal Building Population Estimation for Highly Urbanized Areas Using GIS. *Transactions in GIS*.

Gregg, C. E., Houghton, B. F., Paton, D., Johnston, D. M., Swanson, D. A., & Yanagi, B. S. (2007). Tsunami warnings: understanding in Hawai ‘i. *Natural Hazards*, *40*(1), 71–87.

Hayashi, S., & Koshimura, S. (2013). The 2011 Tohoku tsunami flow velocity estimation by the aerial video analysis and numerical modeling. *J. Disaster Res*, *8*(4), 561–572.

Hollywood 3. (2015). Hollywood 3 Cinema. Retrieved from http://www.hollywoodcinema.co.nz/index.php/about-us

Horspool, N., Cousins, W. J., & Power, W. L. (2015). *Review of Tsunami Risk Facing New Zealand: A 2015 Update. GNS Science Consultancy Report 2015/38.*

Horspool, N., & Fraser, S. (2015). *Tsunami Impacts to Lifelines - Auckland Lifelines Group*. Retrieved from http://www.aelg.org.nz/publicdownload.ashx?q=yIsue%2B9vBdsNKmSGQLcvc2cdghF4MYlfIvuRl4Z22kUlcjw%2FwfYa9qC2JQzV3kvi%2BS4mhj3dniFqMGFaWXkLBGrPtClASDhoycQOtgslOOs%3D

IBC, I. C. C. (2006). International building code. *International Code Council, Inc.(formerly BOCA, ICBO and SBCCI)*, *4051*, 60478–65795.

Imamura, F., Muhari, A., Mas, E., Pradono, M. H., Post, J., & Sugimoto, M. (2012). Tsunami disaster mitigation by integrating comprehensive countermeasures in Padang city, Indonesia. *Journal of Disaster Research*, *7*(1), 48–64.

Ishida, M., & Ando, M. (2014). *Earthquake Hazard, Risk and Disasters*. *Earthquake Hazard, Risk and Disasters*. http://doi.org/10.1016/B978-0-12-394848-9.00004-3

Jobe, R. T., & White, P. S. (2009). A new cost-distance model for human accessibility and an evaluation of accessibility bias in permanent vegetation plots in Great Smoky Mountains National Park, USA. *Journal of Vegetation Science*, *20*(6), 1099–1109.

Johnston, D. M., Saunders, W. S. A., Leonard, G. S., Beban, J., Wright, K., & Fraser, S. A. (2014). History of Tsunami Planning in New Zealand: 1960 to the present. In *UHPH_14: Landscapes and ecologies of urban and planning history. Proceedings of the 12th conference of the Australasian Urban History/Planning History Group* (pp. 361–372).

Johnston, D., Tarrant, R., Tipler, K., Coomer, M., Pedersen, S., & Garside, R. (2011). Preparing schools for future earthquakes in New Zealand: Lessons from an evaluation of a Wellington school exercise. *Australian Journal of Emergency Management, The*, *26*(1), 24.

Johnston, K. M. (2013). Agent analyst: agent-based modeling in ArcGIS. Redlands, CA: Esri Press.

Jonkman, S. N., Vrijling, J. K., & Vrouwenvelder, A. (2008). Methods for the estimation of loss of life due to floods: a literature review and a proposal for a new method. *Natural Hazards*, *46*(3), 353–389. http://doi.org/http://dx.doi.org/10.1007/s11069-008-9227-5

Kawata, Y. (2001). Disaster mitigation due to next Nankai earthquake tsunamis occurring in around 2035. In *Proc. International Tsunami Symposium* (pp. 315–329).

Kietpawan, M. (2008). Simulation approach to evaluating the effectiveness of a Tsunami evacuation plan for Patong Municipality, Phuket, Thailand.

Klepeis, N. E., Nelson, W. C., Ott, W. R., Robinson, J. P., Tsang, a M., Switzer, P., … Engelmann, W. H. (2001). The National Human Activity Pattern Survey (NHAPS): a resource for assessing exposure to environmental pollutants. *Journal of Exposure Analysis and Environmental Epidemiology*, *11*(3), 231–252. http://doi.org/10.1038/sj.jea.7500165

Knoblauch, R., Pietrucha, M., & Nitzburg, M. (1996). Field studies of pedestrian walking speed and start-up time. *Transportation Research Record: Journal of the Transportation Research Board*, (1538), 27–38.

Kobayashi, T., Medina, R. M., & Cova, T. J. (2011). Visualizing diurnal population change in urban areas for emergency management. *The Professional Geographer*, *63*(1), 113–130.

Kolen, B., & Helsloot, I. (2012). Time needed to evacuate the Netherlands in the event of large-scale flooding: strategies and consequences. *Disasters*, *36*(4), 700–722.

Koshimura, S., Katada, T., Mofjeld, H. O., & Kawata, Y. (2006). A method for estimating casualties due to the tsunami inundation flow. *Handbook of Environmental Chemistry, Volume 5: Water Pollution*, *39*(2), 265–274. http://doi.org/10.1007/s11069-006-0027-5

Laghi, M., Cavalletti, A., & Polo, P. (2006). Coastal risk analysis of tsunamis and environmental remediation. *Asian Disaster Preparedness Center, Klong Luang, Thailand*.

Land Resources Information Systems. (2014). Land Cover Database - LCDB v4.0 Change. Retrieved from https://lris.scinfo.org.nz/layer/413-land-cover-database-lcdb-v40-change/metadata/

Lane, E., Arnold, J., Sykes, J., & Roulston, H. (2012). Modelling coastal inundation in Christchurch and Kaiapoi from a South American tsunami using topography from after the 2011 February earthquake. *Environment Canterbury Report*, *12*, 36.

Lane, E., Kohout, A., Chiaverini, A., Jade, A., & Canterbury, E. (2014). *Updated inundation* *modelling in Canterbury from a South American Tsunami*. Christchurch: NIWA. Retrieved from http://www.ecan.govt.nz/publications/Plans/modelling-coastal-inundation-chch-kaiapoi.pdf

Leonard, G., Evans, N., Prasetya, G., Saunders, W., Pearse, L., Monastra, D., & Fraser, S. (2011). *Scoping study for evaluating the tsunami vulnerability of New Zealand buildings for use as evacuation structures*.

Leonard, G. S., & Wright, K. C. (2011). *Evaluation of Get Ready Get Thru The Vines*. Lower Hutt, New Zealand.

Lindell, M. K., Kang, J. E., & Prater, C. S. (2011). The logistics of household hurricane evacuation. *Natural Hazards*, *58*(3), 1093–1109.

Lindell, M. K., Lu, J.-C., & Prater, C. S. (2005). Household decision making and evacuation in response to Hurricane Lili. *Natural Hazards Review*.

Lindell, M. K., & Perry, R. W. (2012). The Protective Action Decision Model: Theoretical Modifications and Additional Evidence. *Risk Analysis*, *32*(4), 616–632. http://doi.org/10.1111/j.1539-6924.2011.01647.x

Lindell, M. K., & Prater, C. S. (2007). Critical behavioral assumptions in evacuation time estimate analysis for private vehicles: Examples from hurricane research and planning. *Journal of Urban Planning and Development*.

Liu, Y., Hatayama, M., & Okada, N. (2006). Development of an adaptive evacuation route algorithm under flood disaster. *Annuals of Disaster Prevention Research Institute, Kyoto University*, *49*, 189–195.

Liu, Y., Okada, N., Shen, D., & Li, S. (2009). Agent-based flood evacuation simulation of life-threatening conditions using vitae system model. *Journal of Natural Disaster Science*, *31*(2), 69–77.

Lwin, K., & Murayama, Y. (2009). A GIS Approach to Estimation of Building Population for Micro-spatial Analysis. *Transactions in GIS*, *13*(4), 401–414.

MacDonald, R. (2005). How women were affected by the tsunami: A perspective from Oxfam. *PLoS Medicine*. http://doi.org/10.1371/journal.pmed.0020178

Manson, S. M., Sun, S., & Bonsal, D. (2012). Agent-based modeling and complexity. In *Agent-based models of geographical systems* (pp. 125–139). Springer.

Martin, D. (1996). An assessment of surface and zonal models of population. *International Journal of Geographical Information Systems*, *10*(8), 973–989.

Martin, D., Cockings, S., & Leung, S. (2009). Population 24/7: building time-specific population grid models.

Mas, E., Koshimura, S., Imamura, F., Suppasri, A., Muhari, A., & Adriano, B. (2015). Recent Advances in Agent-Based Tsunami Evacuation Simulations: Case Studies in Indonesia, Thailand, Japan and Peru. *Pure and Applied Geophysics*, 1–16.

Mas, E., Suppasri, A., Imamura, F., & Koshimura, S. (2012). Agent-based simulation of the 2011 great east japan earthquake/tsunami evacuation: An integrated model of tsunami inundation and evacuation. *Journal of Natural Disaster Science*, *34*(1), 41–57.

Mas, E., Suppasri, A., Srivihok, P., & Koshimura, S. (2013). Feasibility of evacuation at the Pakarang Cape in Thailand based on tsunami inundation model and human evacuation simulation. In *10th International Conference on Urban Earthquake Engineering* (pp. 1–6).

McBride, S., Becker, J. S., Coomer, M. A., Tipler, K., & Johnston, D. M. (2013). *New Zealand ShakeOut Observation Evaluation Report: A summary of initial findings.* Lower Hutt, New Zealand.

MCDEM. (2008a). *Mass Evacuation planning*. Wellington, N.Z.

MCDEM. (2008b). *National Tsunami Signage Technical Standard for the CDEM Sector.* Wellington, N.Z.

MCDEM. (2008c). *Tsunami Evacuation Zones. Director's Guideline for Civil Defence Emergency Management Groups*. Wellington, N.Z.

MCDEM. (2009). *MCDEM Response to the Tsunami Threat from the 30 September 2009 Samoan Earthquake, Report on internal review*.

MCDEM. (2010). *Working form the same page consistent messages for CDEM - Part B: Hazard - specific information. Tsunami*. Retrieved from http://www.civildefence.govt.nz/assets/Uploads/publications/consistent-messages-part-B-tsunami.pdf

McFadgen, B. (2008). *Hostile shores: catastrophic events in prehistoric New Zealand and* *their impact on Maori coastal communities*. Auckland University Press.

McGranahan, G., Balk, D., & Anderson, B. (2007). The rising tide: assessing the risks of climate change and human settlements in low elevation coastal zones. *Environment and Urbanization*, *19*(1), 17–37.

McPherson, T. N., & Brown, M. J. (2004). Estimating daytime and nighttime population distributions in US cities for emergency response activities. *The American Meteorological Society*.

Metroinfo. (n.d.). Network Map. Retrieved May 1, 2016, from http://www.metroinfo.co.nz/map/

Ministry of Health. (2011). *Mortality and Demographic Data 2008*. Wellington, N.Z. Retrieved from http://www.health.govt.nz/system/files/documents/publications/mortality-and-demographic-data-2008.pdf

Moriarty, K. D., Ni, D., & Collura, J. (2007). Modeling traffic flow under emergency evacuation situations: Current practice and future directions.

Munadi, K., Nurdin, Y., Dirhamsyah, M., & Muchalil, S. (2012). Multiagent based Tsunami Evacuation Simulation: A Conceptual Model. In *The Proceedings of 2nd Annual International Conference Syiah University 2012 & 8th IMT Uninet Biosciences Conference* (pp. 254–259).

National Research Council. (2011). *Tsunami Warning and Preparedness: An Assessment of the Tsunami Program and the Nation's Preparedness Efforts.* Washington, D.C.

Newman, A. V, Feng, L., Fritz, H. M., Lifton, Z. M., Kalligeris, N., & Wei, Y. (2011). The energetic 2010 MW 7.1 Solomon Islands tsunami earthquake. *Geophysical Journal International*, *186*(2), 775–781. http://doi.org/10.1111/j.1365-246X.2011.05057.x

Nishikiori, N., Abe, T., Costa, D. G. M., Dharmaratne, S. D., Kunii, O., & Moji, K. (2006). Who died as a result of the tsunami? Risk factors of mortality among internally displaced persons in Sri Lanka: a retrospective cohort analysis. *BMC Public Health*, *6*(1), 73. http://doi.org/10.1186/1471-2458-6-73

NTHMP. (2001). *Designing for Tsunamis - Seven Principles for planning and designing for Tsunami Hazards.*

NZEIR. (2015). *Tsunami risk facing New Zealand*. Retrieved from http://www.eqc.govt.nz/sites/public_files/Report on Tsunami Risk facing New Zealand Aug 2015.pdf

NZTA. (2014). *Requirements for urban buses in New Zealand*. Retrieved from http://www.nzta.govt.nz/assets/resources/requirements-for-urban-buses/docs/requirements-for-urban-buses.pdf

Oya, T., Koshimura, S., & Imamura, H. (2006). Tsunami inundation simulation due to 2004 Indian Ocean Great Tsunami and damage analysis of the city area of Banda Aceh. *Tohoku University Tsunami Engineering Technical Report*, *23*, 21–23.

Palliyaguru, R., Amaratunga, D., & Haigh, R. (2008). Economic development perspectives of post-disaster infrastructure reconstruction in Sri Lanka. In *Proceedings of the International Conference in Building Education and Research*.

Papathoma, M., & Dominey-Howes, D. (2003). Tsunami vulnerability assessment and its implications for coastal hazard analysis and disaster management planning, Gulf of Corinth, Greece. *Natural Hazards and Earth System Science*, *3*(6), 733–747.

Park, S., van de Lindt, J. W., Gupta, R., & Cox, D. (2012). Method to determine the locations of tsunami vertical evacuation shelters. *Natural Hazards*, *63*, 891–908. http://doi.org/10.1007/s11069-012-0196-3

Parrott, R., & Stutz, F. P. (1991). Urban GIS applications. *Geographical Information Systems*, *2*, 247–260.

Pedlow, D., Proffitt, C., Wren, J. ., Kumar, B. R., Buchannan, J., & Kelling, M. (2010). *Estimating Government Expenditure on Injury Prevention*. Wellington, N.Z. Retrieved from http://www.acc.co.nz/PRD_EXT_CSMP/groups/external_ip/documents/guide/wpc133828.pdf

Phillips, B. D., & Morrow, B. H. (2007). Social science research needs: Focus on vulnerable populations, forecasting, and warnings. *Natural Hazards Review*, *8*(3), 61–68.

Pingel, T. J. (2010). Modeling slope as a contributor to route selection in mountainous areas. *Cartography and Geographic Information Science*, *37*(2), 137–148.

Post, J., Wegscheider, S., Mück, M., Zosseder, K., Kiefl, R., Steinmetz, T., & Strunz, G.

(2009). Assessment of human immediate response capability related to tsunami threats in Indonesia at a sub-national scale. *Natural Hazards and Earth System Science*, *9*(4), 1075–1086. http://doi.org/10.5194/nhess-9-1075-2009

Power, W. (2013). Review of tsunami hazard in New Zealand (2013 update). *GNS Science Consultancy Report 2013*, *131*, 222.

Prater, C., Wenger, D., & Grady, K. (2000). Hurricane Bret post storm assessment: A review of the utilization of hurricane evacuation studies and information dissemination. *Texas A&M Univ. Hazard Reduction & Recovery Center, College Station, Tex*.

Rees, S., Pittaway, E., & Bartolomei, L. (2005). Waves of violence - Women in post-tsunami Sri Lanka. *Australasian Journal of Disaster and Trauma Studies*.

Reese, S., Cousins, W. J., Power, W. L., Palmer, N. G., Tejakusuma, I. G., & Nugrahadi, S. (2007). Tsunami vulnerability of buildings and people in South Java - Field observations after the July 2006 Java tsunami. *Natural Hazards and Earth System Science*, *7*(5), 573–589. http://doi.org/10.5194/nhess-7-573-2007

Revi, A., & Singh, A. K. (2007). Cyclone and storm surge, pedestrian evacuation and emergency response in India. In *Pedestrian and Evacuation Dynamics 2005* (pp. 119–130). Springer.

Rossetto, T., Peiris, N., Pomonis, A., Wilkinson, S. M., Del Re, D., Koo, R., & Gallocher, S. (2007). The Indian Ocean tsunami of December 26, 2004: observations in Sri Lanka and Thailand. *Natural Hazards*, *42*(1), 105–124.

Scheele, F. (2016). *Impact Assessment of a far-field tsunami scenario for building damage and habitality in Christchurch,*. University of Canterbury.

Scheer, S., Gardi, A., Guillande, R., Eftichidis, G., Varela, V., de Vanssay, B., & Colbeau-Justin, L. (2011). Handbook of Tsunami evacuation planning. *Retrieved March*, *3*, 2013.

Scheer, S. J., Varela, V., & Eftychidis, G. (2012). A generic framework for tsunami evacuation planning. *Physics and Chemistry of the Earth*, *49*, 79–91. http://doi.org/10.1016/j.pce.2011.12.001

Schmidtlein, M. C., & Wood, N. J. (2015). Sensitivity of tsunami evacuation modeling to direction and land cover assumptions. *Applied Geography*, *56*, 154–163.

Schmitt, R. C. (1956). Estimating daytime populations. *Journal of the American Institute of Planners*, *22*(2), 83–85.

Servicio Sismológico. (2010). Informe de simo sensible. Retrieved January 1, 2016, from http://www.sismologia.cl/events/sensibles/2010/02/27-0634-28L.S201002.html

Shuto, N. (1997). A natural warning of tsunami arrival. In *Perspectives on tsunami hazard reduction* (pp. 157–173). Springer.

Simonovic, S. P., & Ahmad, S. (2005). Computer-based model for flood evacuation emergency planning. *Natural Hazards*, *34*(1), 25–51. http://doi.org/10.1007/s11069-004-0785-x

Sinaga, T. P. T., Nugroho, A., Lee, Y.-W., & Suh, Y. (2011). GIS mapping of tsunami vulnerability: Case study of the Jembrana Regency in Bali, Indonesia. *KSCE Journal of Civil Engineering*, *15*(3), 537–543.

Sorensen, J. H. (2000). Hazard warning systems: Review of 20 years of progress. *Natural Hazards Review*, *1*(2), 119–125.

Sorensen, J., & Vogt, B. (2006). Interactive emergency evacuation guidebook. *URL: Http://emc. Ornl. gov/CSEPPweb/evac_files/files (Last Accessed 13 December 2007)*.

Soule, R. G., & Goldman, R. F. (1972). Terrain coefficients for energy cost prediction. *Journal of Applied Physiology*, *32*(5), 706–708.

Southworth, F. (1991). Regional evacuation modeling: a state-of-the-art review.

Standard New Zealand. (2009). *Risk Management - Principles and Guidlines, ISO31000*.

Statistics New Zealand. (2013). 2013 Census meshblock dataset. Retrieved from http://www.stats.govt.nz/Census/2013-census/data-tables/meshblock-dataset.aspx

Sugimoto, T., Murakami, H., Kozuki, Y., Nishikawa, K., & Shimada, T. (2003). A human damage prediction method for tsunami disasters incorporating evacuation activities. *Natural Hazards*, *29*(3), 585–600. http://doi.org/10.1023/A:1024779724065

Suppasri, A., Koshimura, S., Imai, K., Mas, E., Gokon, H., Muhari, A., & Imamura, F. (2012). Damage characteristic and field survey of the 2011 Great East Japan Tsunami in Miyagi Prefecture. *Coastal Engineering Journal*, *54*(01), 1250005.

Suppasri, A., Muhari, A., Ranasinghe, P., Mas, E., Imamura, F., & Koshimura, S. (2014). Damage and Reconstruction After the 2004 Indian Ocean Tsunami and the 2011 Tohoku Tsunami. In *Tsunami Events and Lessons Learned* (pp. 321–334). Springer.

Suppasri, A., Shuto, N., Imamura, F., Koshimura, S., Mas, E., & Yalciner, A. C. (2013). Lessons learned from the 2011 Great East Japan tsunami: performance of tsunami countermeasures, coastal buildings, and tsunami evacuation in Japan. *Pure and Applied Geophysics*, *170*(6-8), 993–1018.

Sutton, P. C., Elvidge, C., & Obremski, T. (2003). Building and evaluating models to estimate ambient population density. *Photogrammetric Engineering & Remote Sensing*, *69*(5), 545–553.

Synolakis, C., Okal, E., & Bernard, E. (2005). The megatsunami of December 26, 2004. *BRIDGE-WASHINGTON-NATIONAL ACADEMY OF ENGINEERING-*, *35*(2), 26.

Tobler, W. (1993). *Three presentations on geographical analysis and modeling*. NCGIA.

Tobler, W. R. (1979). Smooth pycnophylactic interpolation for geographical regions. *Journal of the American Statistical Association*, *74*(367), 519–530.

Tomsen, E. (2010). *GIS-Based Mass Evacuation Planning for the Auckland Volcanic Field.* University of Auckland, New Zealand.

Tomsen, E., Lindsay, J. M., Gahegan, M., Wilson, T. M., & Blake, D. M. (2014). Evacuation planning in the Auckland Volcanic Field, New Zealand: a spatio-temporal approach for emergency management and transportation network decisions. *Journal of Applied Volcanology*, *3*(1), 1–22.

Tripcevich, N. (2007). *Quarries, caravans, and routes to complexity: prehispanic obsidian in the south-central Andes*. University of California Santa Barbara.

Tripcevich, N. (2008). Llama caravan transport: A study of mobility with a contemporary Andean salt caravan.

Urbanik, T. (1979). Hurricane evacuation demand and capacity estimation. *Hurricanes and Coastal Storms: Awareness, Education and Mitigation. Tallahassee, FL: Florida State University*.

Velotti, L., Trainor, J. E., Engel, K., Torres, M., & Myamoto, T. (2013). Beyond vertical evacuation—research considerations for a comprehensive vertical protection strategy. *International Journal of Mass Emergencies and Disasters*, *31*(1), 60–77.

Whitley, T. G., & Hicks, L. M. (2003). A geographic information systems approach to understanding potential prehistoric and historic travel corridors. *Southeastern Archaeology*, 77–91.

Williams, J. (2016). *Impact Assessment of a Far-field Tsunami Scenario on Christchurch City Infrastructure*. University of Canterbury.

Wilmot, C. G., & Mei, B. (2004). Comparison of alternative trip generation models for hurricane evacuation. *Natural Hazards Review*, *5*(4), 170–178.

Wolshon, B., Urbina, E., Wilmot, C., & Levitan, M. (2005). Review of policies and practices for hurricane evacuation. I: Transportation planning, preparedness, and response. *Natural Hazards Review*, *6*(3), 129–142.

Wood, N. J., Burton, C. G., & Cutter, S. L. (2010). Community variations in social vulnerability to Cascadia-related tsunamis in the US Pacific Northwest. *Natural Hazards*, *52*(2), 369–389.

Wood, N. J., Jones, J., Schelling, J., & Schmidtlein, M. (2014). Tsunami vertical-evacuation planning in the US Pacific Northwest as a geospatial, multi-criteria decision problem. *International Journal of Disaster Risk Reduction*, *9*, 68–83.

Wood, N. J., & Peters, J. (2015). Variations in population vulnerability to tectonic and landslide-related tsunami hazards in Alaska. *Natural Hazards*, *75*(2), 1811–1831.

Wood, N. J., & Schmidtlein, M. C. (2012). Anisotropic path modeling to assess pedestrian-evacuation potential from Cascadia-related tsunamis in the US Pacific Northwest. *Natural Hazards*, *62*(2), 275–300.

Wood, N. J., & Schmidtlein, M. C. (2013). Community variations in population exposure to near-field tsunami hazards as a function of pedestrian travel time to safety. *Natural Hazards*, *65*(3), 1603–1628.

Wood, N. J., Schmidtlein, M. C., & Peters, J. (2014). Changes in population evacuation potential for tsunami hazards in Seward, Alaska, since the 1964 Good Friday earthquake. *Natural Hazards*, *70*(2), 1031–1053.

Wood, N., Jones, J., Schmidtlein, M., Schelling, J., & Frazier, T. (2016). Pedestrian flow-path modeling to support tsunami evacuation and disaster relief planning in the US

Pacific Northwest. *International Journal of Disaster Risk Reduction*.

Wu, Y.-M., & Kanamori, H. (2005). Rapid assessment of damage potential of earthquakes in Taiwan from the beginning of P waves. *Bulletin of the Seismological Society of America*, *95*(3), 1181–1185.

Yeh, H. (2010). Gender and Age Factors in Tsunami Casualties. *Natural Hazards Review*, *11*(1), 29–34. http://doi.org/10.1061/ASCE1527-6988201011:129

Yeh, H. (2014). Tsunami Hazard and casualty estimation model. 10th U.S. National Conference on Earthquake Engineering - Frontiers of Earthquake Engineering; July 21-25, 2014.

Yun, N.-Y., & Hamada, M. (2012). Evacuation behaviors in the 2011 Great East Japan earthquake. *Journal of Disaster Research*, *7*(7), 458–467.

Yun, N.-Y., & Hamada, M. (2014). Evacuation behavior and fatality rate of residents during the 2011 Great East Japan earthquake and tsunami. *Earthquake Spectra*.

Appendices

Appendix A: Chapter 1 Appendix

A.1: Christchurch Tsunami Hazard Models

Lane et al. (2014) have modelled the tsunami hazard for Christchurch city using a mathematical equation of fluid motion, based on a Mw 9.485 Peru subduction zone event. It represents the hazard at a 2,500 year return period. This updated tsunami model represents the best estimate of far-field tsunami inundation of the Christchurch coast to date and indicates that Christchurch city and Lyttelton Harbour would experience the worst of the inundation in Canterbury. The largest wave arrival is assumed to coincide with mean high water spring tide (MHWS) in this model. Areas which experience the highest levels of inundation (>2.5m) include New Brighton, South Shore, Redcliffs, Sumner, Taylors Mistake and low lying areas of Lyttelton Port. The highest flow velocities are concentrated around the Avon-Heathcote mouth, including South Shore, Ferrymead and Sumner, with velocities greater than 5.1m/s, which are also seen at the entrance of the Lyttelton Port. New Brighton sees velocities of up to 4m/s, but most of the other inundated areas experience velocities below 2 m/s.

The research presented in this thesis uses what has been considered a credible worst case scenario for Christchurch city from 4 possible source event variations. The technical details of the chosen scenario model are presented below (GNS & NIWA 2015).

Model name: Canterbury Tsunami Model 1 in 2,500 year return period from South Peru – North Canterbury (Scenario 2)

Author: Dr Emily Lane

Organisation: National Institute of Water and Atmospheric Research

Date: August 2014

Description: Inundation model of coastal locations in Canterbury by a tsunami generated from an earthquake off-shore of South Peru with a magnitude Mw 9.485. This comes from the de-aggregation of tsunami hazard with a return period of 1:2,500 years for Christchurch city as calculated in Power (2013).

Model: Far-field modelling:

Gerris: Gerris is based on a quad-tree grid and is able to adaptively refine specified areas to ensure error is kept below a given level. Gerris was used to model the wave from source to approximately 197 E, the boundary with the RiCOM inundation grids.

RiCOM: The RiCOM hydrodynamics model uses an irregular, unstructured, finite element grid which allows high resolution and refinement in areas of inundation around the coast, and improves numerical accuracy by controlling grid size relative to water depth. The grids used were originally made for several earlier inundation studies for ECAN.

Input Data: LIDAR supplied by ECAN (post February 2011 earthquake for Christchurch and Kaiapoi), digitised charts, NIWA bathymetry. Post-earthquake bathymetry of the Avon-Heathcote Estuary. Avon stop banks, Waimakariri stop banks and Sumner sea wall design heights and positions.

Model Area: The grid extends from the east coast of New Zealand to 197 E. Areas of interest for inundation modelling have increased resolution such as Christchurch and Banks Peninsula, which includes Christchurch city, Lyttelton Harbour coastal margin and Akaroa Harbour coastal margin.

Additional Source Event Information: Scenario 2 (40 m slip; 1,500 km by 150 km):

- Location: x = 286.608056°E y = -17.418918°N
- Depth = 25000m
- Strike = 307° dip = 10° rake = 90°
- Length = 600e3m width = 150e3m U = 40m

Coordinate System: New Zealand Transverse Mercator

Output Format: Ascii raster grid (regular), GIS Maps

Model Limitations: Spatial resolution is variable but in the regions of interest for inundation is around 10-15 m. Open ocean at the edges of the grid have resolution as coarse as several kilometres and resolution grades smoothly between these. Variable, finest resolution of modelling around 10 m. Ascii raster files should be used at a scale of 1:25,000 at most. Tide not accounted for except as static level, erosion/accretion of land not considered, bare earth LiDAR used, constant land friction assumed, uncertainties in incoming wave train source. Climate change not considered.

A2: Types of Evacuation (MCDEM, 2008a)

Types of evacuation

Introduction

Evacuation may be pre or post event. The physical act of evacuation can be further classified into two types: voluntary-evacuation, or mandatory-evacuation.

Mandatory-evacuation

Mandatory-evacuation is directed when it is believed that the risk to residents is too great to allow them to remain where they are.

Mandatory-evacuation places a great burden on the resources of the emergency services and places a duty of responsibility on authorities to ensure that people who are evacuated are cared for.

Voluntary-evacuation

Voluntary-evacuees are those that leave their current location because of actual or perceived risk without being directed to do so. This has benefits for those that are actually threatened by an event and can make the task of emergency services easier as there may be significantly fewer people to warn and assist.

Occupants of areas outside of the evacuation zone that leave despite the fact they are not threatened by the hazard are also referred to as 'shadow evacuees'. This situation can pose significant disadvantages, as these actions can congest transport corridors. In the case of severe weather, those who voluntarily evacuate can put themselves in greater danger than if they remain in their homes or place of business.

The potentially negative consequences of people voluntarily evacuating can be minimised by effective public information management. For more information on public information management refer to Section 3 of this guideline and *Public Information Management, Information for the CDEM Sector [IS9/07]*.

A3: Phases of Evacuation ((MCDEM, 2008a)

Phases of evacuation

Introduction

Evacuations move through five distinct phases:
- Decision (to order an evacuation);
- Warning;
- Evacuation;
- Shelter; and
- Return.

The demands on emergency managers and resources will change as the evacuation progresses through each phase. This guideline covers planning considerations for each phase. Evacuation plans should also cover all phases.

Evacuation phases diagram

The diagram below shows the generic evacuation phase sequence for a mass evacuation, including the 'shelter-in-place' option and 'shadow' voluntary-evacuees:

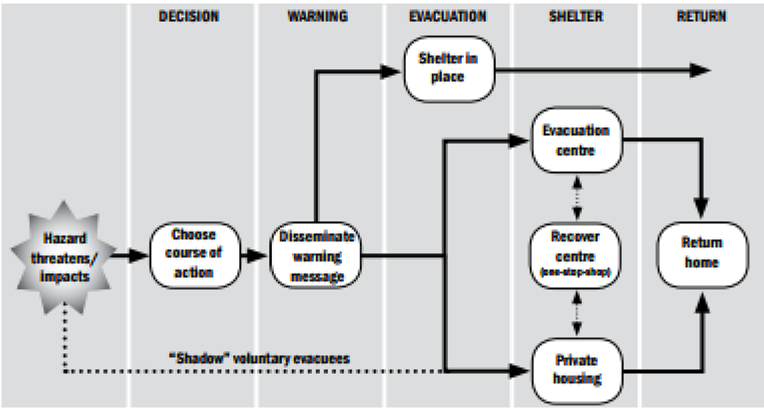

Decision

The decision phase constitutes the period when intelligence from the field is measured and a choice is made whether to order an evacuation or advise people to 'shelter-in-place'.

Warning

This phase occurs when notifications are issued to the public advising them of the situation and what action they should take.

Note: In this guideline 'warning' is used to describe any message/system used for notifying the public, regardless of whether the notification comes from local, Group or national level.

continued on next page

Evacuation

This phase describes the actual physical evacuation of occupants from an area.

Shelter

The 'shelter' phase incorporates:

- the registration process;
- accommodating evacuees; and
- the assessing and provision of welfare and recovery requirements.

Return

The 'return' phase involves:

- an assessment of the evacuated area;
- issuing an 'all-clear';
- coordinating the physical return of evacuees; and
- the continuation of recovery provisions.

Appendix B: Chapter 2 Appendix

B.1: Weekday working shift patterns calculation process

Full-time 0.98*0.7 (day)													
Occupation	Number of people based on		Commute			work hours		resident_stay_unspecified		resident_out_unspecified		non_resident_in_unspecified	
	work place address	usually ressidential	Stay	out	in	start	end	leave home	leave work	leave home	back Sumner	moving in	leave work
Legislators, Administrators and Managers	86.436	253.134	86.436	166.698	0	9	16	8	17	7	18	-	-
Professionals	129.654	329.28	129.654	199.626	0	9	16	8	17	7	18	-	-
Technicians and Associate Professionals	123.48	205.8	123.48	82.32	0	9	16	8	17	7	18	-	-
Clerks	88.494	98.784	88.494	10.29	0	9	16	8	17	7	18	-	-
Service and Sales Workers 1	251.076	129.654	129.654	0	121.42	8	16	7	17	-	-	7	17
Agriculture and Fishery Workers	16.464	10.29	10.29	0	6.174	7	16	6	17	-	-	6	17
Trades Workers	30.87	98.784	30.87	67.914	0	7	17	6	18	5	19	-	-
Plant and Machine Operators and Assemblers	22.638	16.464	16.464	0	6.174	7	17	6	18	-	-	6	18
Elementary Occupations (incl Residuals)	41.16	92.61	41.16	51.45	0	7	17	6	18	5	19	-	-
Full-time 0.02*0.7 (over-night)													
Occupation	Number of people based on		Commute			work hours		resident_stay_unspecified		resident_out_unspecified		non_resident_in_unspecified	
	work place address	usually ressidential	Stay	out	in	start	end	leave home	leave work	leave home	back Sumner	moving in	leave work
Professionals, Technicians and Associate Professionals	3.543876	7.49112	3.54388	3.94724	0	23	7	22	8	21	9	-	-
Service and Sales Workers 1	5.124	2.646	2.646	0	2.478	23	7	22	8	-	-	22	8
Part-time 0.3*0.08 (night) and 0.3*0.92(day)													
Occupation	Number of people based on		Commute			work hours		resident_stay_unspecified		resident_out_unspecified		non_resident_in_unspecified	
	work place address	usually ressidential	Stay	out	in	start	end	leave home	leave work	leave home	back Sumner	moving in	leave work
Clerks	35.604	39.744	35.604	4.14	0	9	13	8	14	7	15	-	-
Service and Sales Workers *0.4	40.4064	20.8656	20.8656	0	19.541	10	14	9	15	-	-	9	15
Service and Sales Workers *0.2	20.2032	10.4328	10.4328	0	9.7704	10	16	9	17	-	-	9	17
Service and Sales Workers *0.4	3.5136	1.8144	1.8144	0	1.6992	17	22	16	23	-	-	16	23
Professionals, Technicians and Associate Professionals*0.4	40.7376	86.112	40.7376	45.3744	0	9	13	8	14	7	15	-	-
Professionals, Technicians and Associate Professionals*0.4	40.7376	86.112	40.7376	45.3744	0	14	19	13	20	12	21	-	-
Professionals, Technicians and Associate Professionals*0.2	1.7712	3.744	1.7712	1.9728	0	19	22	18	23	17	24	-	-

B.3: Weekend working shift patterns calculation process

Day - full time 0.98*0.7													
	Number of people based		Commute			work hours		resident_stay_unspecified		resident_out_unspecified		ion_resident_in_unspecified	
	work place address	usually ressidential	Stay	out	in	start	end	leave home	leave work	leave home	back Sumner	moving in	leave work
Professionals	129.654	329.28	105.84	162.96	0	9	16	8	17	7	18	-	-
Technicians and Associate Professionals	123.48	205.8	100.8	67.2	0	9	16	8	17	7	18	-	-
Service and Sales Workers 1	251.076	129.654	105.84	0	99.12	10	16	9	17	-	-	9	17
Night - full time 0.02*0.7													
	Number of people based		Commute			work hours		resident_stay_unspecified		resident_out_unspecified		ion_resident_in_unspecified	
Occupation	work place address	usually ressidential	Stay	out	in	start	end	leave home	leave work	leave home	back Sumner	moving in	leave work
Professionals, Technicians and Associate Professionals	5.166	10.92	5.166	5.754	0	23	7	22	8	21	9	-	-
Service and Sales Workers 1	3.515064	1.815156	1.815156	0	1.699908	23	7	22	8	-	-	22	8
Part- time 0.3*0.08 (night) and 0.3*0.92(day)													
	Number of people based		Commute			work hours		resident_stay_unspecified		resident_out_unspecified		ion_resident_in_unspecified	
Occupation	work place address	usually ressidential	Stay	out	in	start	end	leave home	leave work	leave home	back Sumner	moving in	leave work
Service and Sales Workers *0.4	40.4064	20.8656	20.8656	0	19.5408	10	14	9	15	-	-	9	15
Service and Sales Workers *0.2	20.2032	10.4328	10.4328	0	9.7704	10	16	9	17	-	-	9	17
Service and Sales Workers *0.4	3.5136	1.8144	1.8144	0	1.6992	17	22	16	23	-	-	16	23
Professionals, Technicians and Associate	61.272	73.8576	73.8576	12.5856	0	9	13	8	14	7	15	-	-
Professionals, Technicians and Associate	61.272	73.8576	73.8576	12.5856	0	14	18	13	19	12	20	-	-
Professionals, Technicians and Associate	2.664	3.2112	3.2112	0.5472	0	19	22	18	23	17	0	-	-

B.4: Summary of all time profile scenarios

Time	under5			5to14			15to64			Independent Elderly		Impaired group		Visitors		
	Home	School	Unspecified	Home	School	Unspecified	Home	Work	Unspecified	Home	Unspecified	Home/Rest_home/School	Unspecified	Accommodation	Business	Unspecified
Weekday 2AM	100	0	0	71	0	0	97	1	1	100	0	100	0	34	0	1
Weekday 8 AM	75	25	0	0	0	87	40	20	25	70	30	100	0	25	5	5
Weekday 12 PM	75	25	0	0	87	0	20	40	15	60	40	80	20	10	40	50
Weekday 17 AM	75	25	0	53	0	13	45	10	35	90	10	90	10	20	30	30
Weekend 12 PM	50	0	50	50	0	50	38	25	25	60	40	80	20	10	40	50

Appendix C: Chapter 3 appendix

C.1: Map showing roads in Sumner (Google Maps)

https://www.google.co.nz/maps/@-43.5750603,172.7599348,15z

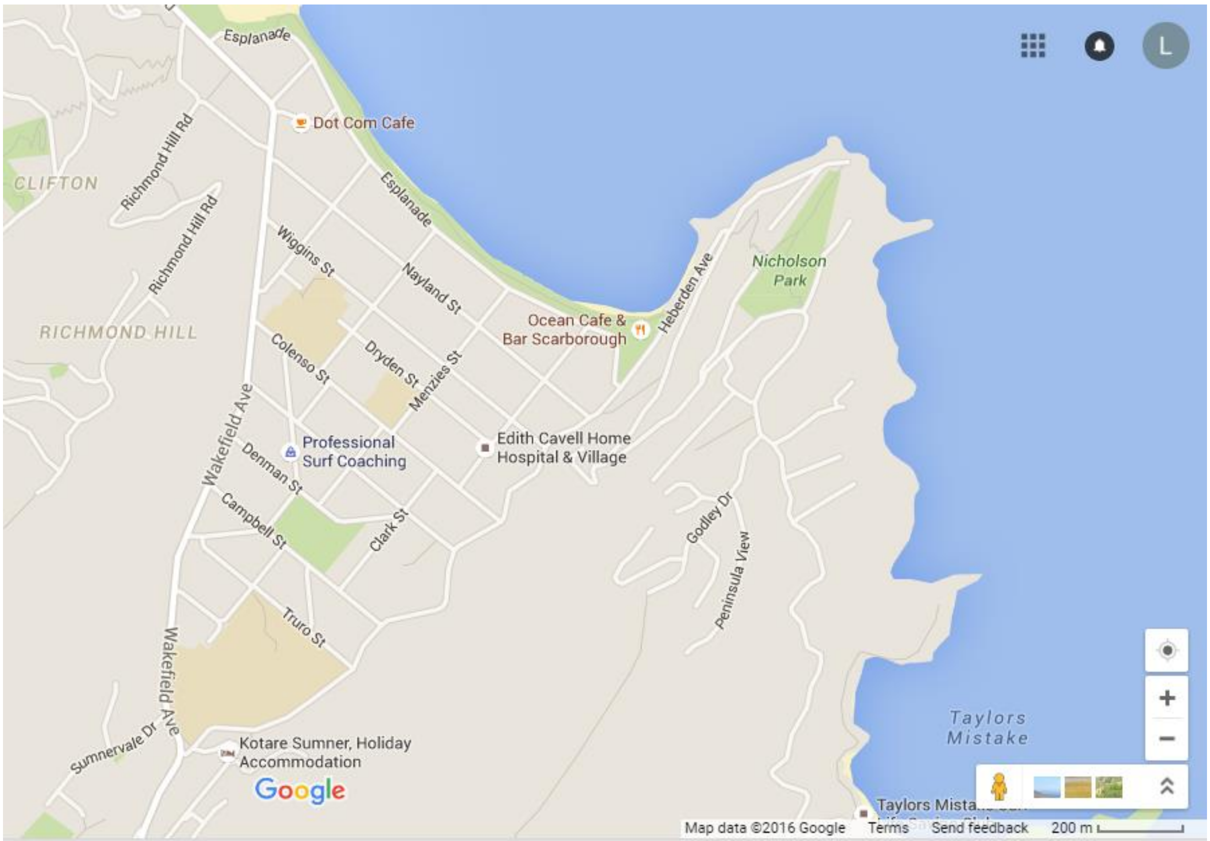

C.2: Example of five Origins travel to their best pair of Destinations

Pedestrian evacuate to higher elevation model

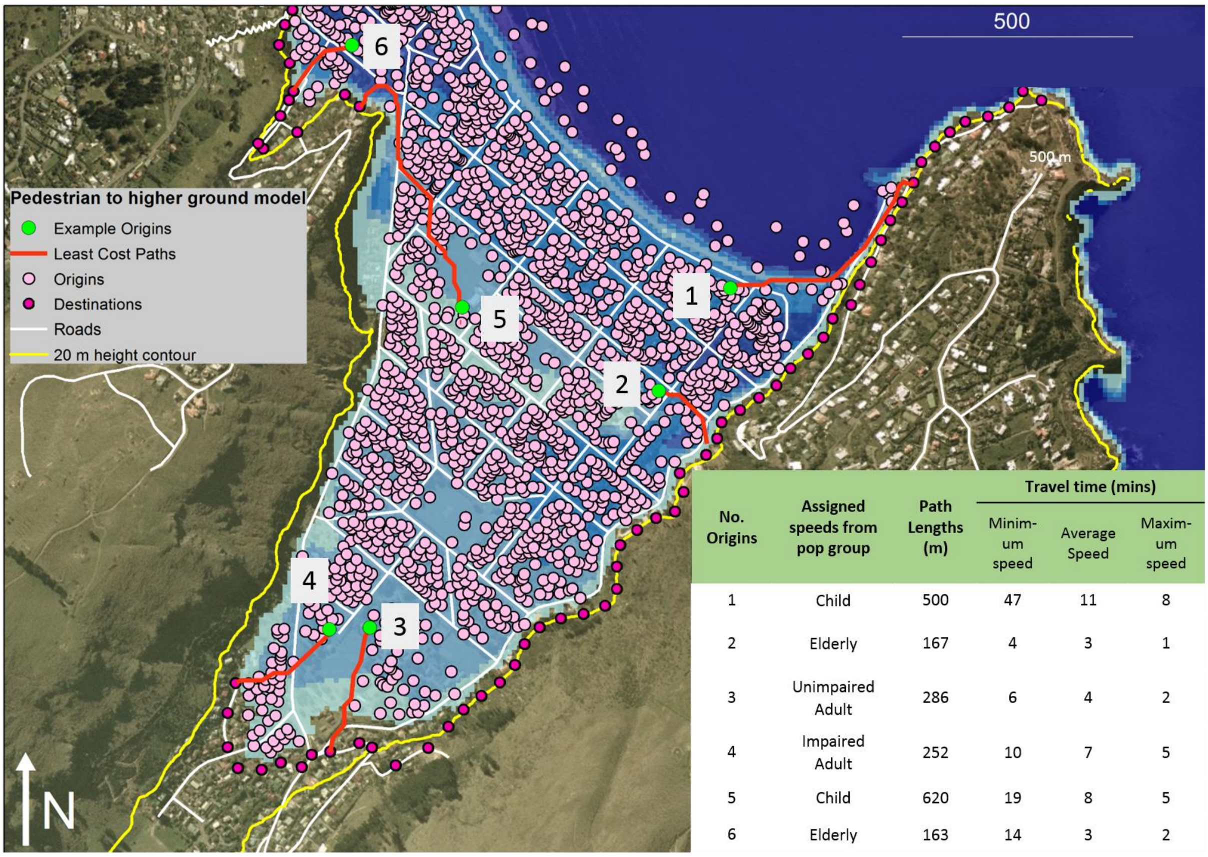

No. Origins	Assigned speeds from pop group	Path Lengths (m)	Travel time (mins)		
			Minimum speed	Average Speed	Maximum speed
1	Child	500	47	11	8
2	Elderly	167	4	3	1
3	Unimpaired Adult	286	6	4	2
4	Impaired Adult	252	10	7	5
5	Child	620	19	8	5
6	Elderly	163	14	3	2

C.3: The number of pedestrian evacuation to higher ground model results (Evacuation time vs number of people in nine time scenarios)

Minute(s)	Fwk12	Jwk12	Owk12	Fwd2	Jwd2	Owd2	Wd8	wd12	wd17
1	319	201	272	35	31	33	113	204	166
1.5	506	262	423	88	81	85	161	330	278
2	661	484	551	95	87	92	221	428	351
2.5	429	333	421	241	234	238	343	334	337
3	955	612	789	158	145	153	323	656	539
3.5	829	489	737	193	180	187	336	836	553
4	985	596	734	358	343	352	349	756	491
4.5	1195	860	1081	220	191	208	595	849	820
5	1304	828	1083	389	330	365	629	1003	842
5.5	925	730	905	269	238	257	516	712	618
6	2304	1382	1889	206	193	201	629	1637	1161
6.5	722	477	705	140	130	136	294	560	466
7	490	342	430	146	137	143	295	338	322
7.5	480	242	379	259	249	255	254	433	310
8	675	510	585	104	96	101	155	592	264
8.5	353	330	368	145	136	141	433	355	399
9	781	528	664	80	74	78	158	657	380
9.5	945	492	765	91	86	89	324	715	508
10	118	149	137	91	78	86	159	98	150
10.5	127	68	111	37	35	36	39	84	66
11	158	106	82	32	31	32	54	103	61
11.5	28	28	83	36	35	36	48	24	79
12	285	179	243	87	52	73	223	250	235
12.5	122	73	102	14	14	14	43	89	65
13	16	16	16	16	16	16	10	9	16
13.5	16	16	16	16	16	16	14	14	17
14	50	35	44	18	17	17	24	42	35
14.5	2	2	2	2	2	2	1	1	2
15	5	5	5	6	6	6	5	4	6
15.5	1	1	1	1	1	1	1	1	1
16.5	21	21	21	0	0	0	6	23	19
17	58	33	48	2	2	2	10	44	29
20.5	34	19	28	0	0	0	5	25	16
17.5	185	134	159	111	104	109	142	138	164
18	435	239	314	110	102	107	143	303	235
18.5	188	199	242	100	94	97	97	133	183
19	76	65	70	47	44	46	185	119	144
19.5	107	91	101	87	81	84	113	86	102
20	118	82	79	48	45	47	39	78	58
20.5	77	94	103	77	72	75	76	61	115
21	123	50	101	30	28	29	40	83	52
21.5	77	94	77	42	40	41	52	58	82

Minute(s)	Fwk12	Jwk12	Owk12	Fwd2	Jwd2	Owd2	Wd8	wd12	wd17
22	62	33	56	36	34	35	58	47	39
22.5	18	18	18	22	21	22	31	15	37
23	17	17	17	19	18	18	28	17	20
23.5	55	31	51	36	36	36	77	263	80
24	37	51	37	41	39	40	34	29	53
24.5	43	43	43	51	50	51	48	101	50
25	31	31	31	35	34	35	29	25	36
25.5	33	33	33	35	34	34	29	27	36
26	31	31	31	36	35	35	27	24	35
26.5	9	9	9	11	10	11	11	9	11
27	21	21	21	25	24	25	22	19	24
27.5	90	90	90	93	92	93	100	90	97
28	13	13	13	14	13	14	13	12	14
28.5	18	17	18	19	19	19	15	13	19
29	22	22	22	23	23	23	22	20	24
29.5	30	30	30	32	31	31	28	25	33
30	13	13	13	14	13	13	13	12	14
30.5	6	5	6	6	6	6	5	4	6
31	9	9	9	10	10	10	7	7	10
31.5	12	12	12	13	13	13	9	8	13
32	4	4	4	4	4	4	2	2	4
32.5	2	2	2	2	2	2	2	2	2
33	9	9	9	10	9	10	9	8	10
33.5	6	6	6	7	6	6	7	6	7
34.5	6	6	6	7	6	6	6	5	7
35	4	4	4	4	4	4	4	4	4
35.5	1	1	1	2	2	2	1	1	2
36.5	3	3	3	3	3	3	2	2	3

C.4: The number of pedestrian evacuation to one bus stop model results (Evacuation time vs number of people in nine time scenarios)

Minute(s)	Fwk12	Jwk12	Owk12	Fwd2	Jwd2	Owd2	wd8	wd12	wd17
0.5	9	5	7	0	0	0	2	5	4
1	34	21	29	2	2	2	11	22	17
1.5	104	65	88	9	9	9	16	66	53
2	177	109	150	10	9	9	55	110	86
2.5	245	172	216	76	76	76	122	188	155
3	106	69	91	33	22	29	70	84	68
3.5	147	159	136	103	93	99	152	140	153
4	571	291	476	36	33	35	96	392	286
4.5	401	267	338	62	46	56	199	307	250
5	516	320	410	123	76	104	295	419	363
5.5	670	333	554	7	7	7	137	475	320
6	1054	638	896	22	21	22	189	769	529
6.5	352	224	293	25	23	24	82	249	180
7	302	146	259	36	33	35	100	228	155
7.5	121	107	104	30	28	29	58	85	96
8	109	56	96	41	38	39	55	73	59
8.5	328	152	277	31	28	30	50	217	118
9	130	139	87	90	87	89	101	86	137
9.5	236	190	210	37	33	35	63	175	108
10	180	100	185	56	52	54	142	122	127
10.5	249	158	211	41	39	40	88	175	143
11	155	53	74	36	34	35	61	176	40
11.5	108	164	155	86	84	85	47	73	109
12	360	200	291	66	62	64	103	317	169
12.5	79	88	104	51	47	49	172	228	110
13	366	145	262	86	71	80	130	284	171
13.5	129	197	170	70	65	68	90	258	161
14	246	119	134	86	79	83	136	197	127
14.5	390	256	407	95	88	92	132	277	280
15	228	166	214	102	95	99	135	162	176
15.5	225	182	75	98	90	95	135	164	98
16	596	173	341	103	91	98	137	472	213
16.5	341	460	578	167	129	152	297	286	486
17	891	558	766	109	102	106	351	650	469
17.5	185	134	159	111	104	109	142	138	164
18	435	239	314	110	102	107	143	303	235
18.5	188	199	242	100	94	97	97	133	183
19	76	65	70	47	44	46	185	119	144
19.5	107	91	101	87	81	84	113	86	102
20	118	82	79	48	45	47	39	78	58
20.5	77	94	103	77	72	75	76	61	115

Minute(s)	Fwk12	Jwk12	Owk12	Fwd2	Jwd2	Owd2	wd8	wd12	wd17
21	123	50	101	30	28	29	40	83	52
21.5	77	94	77	42	40	41	52	58	82
22	62	33	56	36	34	35	58	47	39
22.5	18	18	18	22	21	22	31	15	37
23	17	17	17	19	18	18	28	17	20
23.5	55	31	51	36	36	36	77	263	80
24	37	51	37	41	39	40	34	29	53
24.5	43	43	43	51	50	51	48	101	50
25	31	31	31	35	34	35	29	25	36
25.5	33	33	33	35	34	34	29	27	36
26	31	31	31	36	35	35	27	24	35
26.5	9	9	9	11	10	11	11	9	11
27	21	21	21	25	24	25	22	19	24
27.5	90	90	90	93	92	93	100	90	97
28	13	13	13	14	13	14	13	12	14
28.5	18	17	18	19	19	19	15	13	19
29	22	22	22	23	23	23	22	20	24
29.5	30	30	30	32	31	31	28	25	33
30	13	13	13	14	13	13	13	12	14
30.5	6	5	6	6	6	6	5	4	6
31	9	9	9	10	10	10	7	7	10
31.5	12	12	12	13	13	13	9	8	13
32	4	4	4	4	4	4	2	2	4
32.5	2	2	2	2	2	2	2	2	2
33	9	9	9	10	9	10	9	8	10
33.5	6	6	6	7	6	6	7	6	7
34.5	6	6	6	7	6	6	6	5	7
35	4	4	4	4	4	4	4	4	4
35.5	1	1	1	2	2	2	1	1	2
36.5	3	3	3	3	3	3	2	2	3

C.4. The number of pedestrian evacuation to two bus stops model results (Evacuation time vs number of people in nine time scenarios)

Minute(s)	Fwk12	Jwk12	Owk12	Fwd2	Jwd2	Owd2	wd8	wd12	wd17
0.5	27	18	23	4	3	4	11	18	15
1	92	72	84	52	48	51	65	71	77
1.5	301	210	264	114	106	111	130	225	212
2	477	372	435	255	244	250	367	459	334
2.5	563	425	508	284	269	278	359	509	432
3	710	504	628	278	241	263	419	553	525
3.5	568	439	521	343	317	333	406	554	450
4	1291	823	1108	281	260	272	418	1126	816
4.5	992	677	861	299	266	286	536	822	669
5	1372	897	1143	306	248	282	570	1137	908
5.5	1825	1024	1518	176	164	171	464	1300	940
6	435	374	423	128	119	124	215	330	313
6.5	572	409	493	131	124	128	242	525	345
7	613	397	535	204	163	188	478	557	470
7.5	251	150	191	69	64	67	95	170	145
8	934	568	809	139	136	138	292	692	538
8.5	305	253	275	72	68	70	83	203	142
9	234	110	202	41	39	40	127	151	173
9.5	155	63	136	43	41	42	57	101	78
10	71	66	61	15	14	15	45	46	63
10.5	76	60	39	15	14	15	28	49	28
11	35	19	58	11	10	11	19	25	33
11.5	119	63	92	17	16	16	32	78	39
12	45	48	49	5	5	5	33	30	53
12.5	35	22	30	3	3	3	18	23	18
13	11	4	10	4	4	4	14	8	8
14	1	1	1	1	1	1	4	1	1
14.5	2	2	2	2	2	2	1	1	2
13.5	13	12	11	0	0	0	2	8	6
15.5	0	0	0	0	0	0	0	0	0
16	24	0	20	0	0	0	0	15	11
16.5	0	15	0	0	0	0	7	0	0

C.5. The number of pedestrian evacuation to three bus stops model results (Evacuation time vs number of people in nine time scenarios)

Minute(s)	Fwk12	Jwk12	Owk12	Fwd2	Jwd2	Owd2	wd8	wd12	wd17
0.5	662	368	545	6	5	5	105	486	319
1	204	139	178	53	49	51	97	140	128
1.5	299	215	265	132	115	125	176	232	234
2	880	601	769	257	245	252	438	741	524
2.5	847	569	742	286	270	279	408	710	554
3	875	606	761	240	222	233	370	642	564
3.5	1030	701	905	399	345	378	611	922	738
4	1381	889	1190	298	269	287	480	1192	881
4.5	1507	947	1276	273	254	265	551	1165	873
5	974	694	822	332	261	303	588	852	747
5.5	560	342	491	171	161	167	277	384	346
6	485	400	452	128	119	124	223	367	333
6.5	509	359	441	130	124	128	231	481	316
7	532	339	462	133	127	131	299	449	340
7.5	131	90	117	67	64	66	85	96	108
8	354	241	314	158	145	152	226	293	277
8.5	325	231	280	71	68	70	90	231	149
9	206	114	177	41	39	40	89	142	165
9.5	93	50	84	42	40	41	45	63	68
10	44	31	38	15	14	14	27	30	28
10.5	76	50	39	15	14	15	21	49	28
11	8	8	35	11	10	10	19	8	24
11.5	90	52	77	16	15	16	24	60	31
12	37	31	32	5	5	5	28	25	41
12.5	35	22	30	3	2	3	12	23	18
13	4	4	4	4	4	4	14	4	4
14	1	1	1	1	1	1	1	1	1
14.5	2	2	2	2	2	2	1	1	2

C.6. Vehicle model results (Evacuation time vs number of vehicles nine time scenarios)

Minutes	Fwk12	Jwk12	Owk12	Fwd2	Jwd2	Owd2	wd8	wd12	wd17
0.0	0	0	0	0	0	0	0	0	0
0.2	35	19	29	7	7	7	11	32	16
0.3	12	11	11	22	22	22	11	9	14
0.4	57	38	49	53	53	53	28	45	39
0.5	122	86	108	40	37	39	72	111	95
0.6	71	66	69	27	22	25	75	68	88
0.7	238	172	212	38	31	36	156	224	198
0.8	447	366	415	111	94	105	383	425	455
0.9	350	227	300	108	107	108	181	318	224
1	344	272	316	264	259	263	264	296	322
1.1	301	192	257	95	89	93	137	268	197
1.2	184	114	156	122	123	122	78	152	110
1.3	319	178	263	139	140	140	96	272	157
1.4	172	101	144	96	96	96	58	144	92
1.5	146	125	138	240	240	240	121	109	150
1.6	16	16	16	35	35	35	17	11	21
1.7	3	3	3	7	7	7	3	2	4
2	9	9	9	20	20	20	10	7	13